Master Thesis

submitted within the UNIGIS Master's program
"Geographical Information Science & Systems – (UNIGIS MSc)"
to the Department of Geoinformatics - Z_GIS,
Paris-Lodron University of Salzburg

Exploring Fine-Scale Spawning Synchronisation in Corals through Communication: An Agent-Based Model

by

Ramona Graziella Allemann

u107163

Supervisor:
Assoc. Prof. Dr. Gudrun Wallentin

In partial fulfilment of the requirements for
the Degree of
"Master of Science", abbreviated "MSc"

Welschenrohr, December 2024

Acknowledgements

Foremost, I would like to thank my supervisor, Assoc. Prof. Dr. Gudrun Wallentin, for her invaluable guidance and expertise throughout the stages of this research. Her enthusiasm and vast knowledge have been instrumental in helping me stay focused and motivated, pushing me to develop the coral spawning simulation with both rigour and curiosity. Thank you for your constant support, insights, and willingness to engage in thoughtful discussions.

I must express my profound gratitude to Prof. Don Levitan from the Department of Biological Science at Florida State University for providing the baseline dataset that has been foundational for this thesis. His contribution has profoundly shaped this work, and I extend my heartfelt thanks for his generosity in sharing this invaluable resource.

I would also like to acknowledge my proofreaders, Kim Ferguson and Sue Ingham, for their patience and meticulous feedback. Their determination and constructive criticism gave me the motivation to refine my work in its final stages.

Finally, I am deeply thankful to my family and friends for their unwavering support and constant encouragement. With you by my side, I may have struggled, but I never faltered through the highs and lows of this journey.

Abstract

Many reef-building corals reproduce through synchronised broadcast-spawning events, maximising fertilisation success and larval dispersal. The mechanisms behind this remarkably precise synchronisation remain largely unknown, yet understanding them is vital for effective reef conservation in a changing climate. This study investigates if theoretical coral communication explains these fine-scale spawning patterns of the species *Orbicella franksi*. A reef in Bocas del Toro, Panama, is set in a spatial simulation including a framework combining an agent-based model with a discrete-event simulation to create spawning synchrony as an emergent phenomenon of the years 2002 to 2009. Alongside inter-coral communication mechanisms the model incorporates seasonal changes of key environmental cues: photoperiod, sea water temperature, lunar illumination, and periods of darkness. The emerging spatial and temporal patterns of spawning are simulated and their clustering compared to the real-world. The results suggest that while broad environmental factors set the general timing for spawning events, local communication between corals help to achieve real-world clustering patterns. Sensitivity analyses indicate that the strength and spatial decay of communication signals significantly influence the degree of clustering, supporting diffusion-based chemical signalling as a synchronising mechanism. These findings emphasise that spatial simulations provide a strategic framework to guide the investigation of complex ecological processes by identifying gaps in knowledge. Focused research efforts will ultimately solve the puzzle of coral spawning synchrony and coral communication.

Contents

1 Introduction **1**

1.1 Coral biology . . . 1

1.2 Coral reproduction . . . 2

1.2.1 Spawning process of broadcast spawners . . . 3

1.2.2 Gametogenesis . . . 3

1.2.3 Spawning synchrony . . . 4

1.2.4 Theories of coral communication . . . 5

1.3 Study species *Orbicella franksi* . . . 6

1.4 Study aim . . . 7

2 Materials and methods **8**

2.1 Study location . . . 8

2.2 Model development . . . 8

2.2.1 Agent Based Model (ABM) . . . 9

2.2.2 Discrete-Event Simulation (DES) . . . 9

2.3 Analysis plan . . . 9

2.3.1 Simulation and analysis software . . . 10

2.4 Overview, Design concepts, and Details (ODD) . . . 11

2.4.1 Purpose . . . 11

2.4.2 Entities, state variables and scales . . . 11

2.4.3 Process overview and scheduling . . . 15

2.4.4 Design concepts . . . 17

2.4.5 Initialisation . . . 20

2.4.6 Input data . . . 22

2.4.7 Submodels . . . 23

3 Calibration and validation **40**

3.1 Baseline: the real world . . . 41

3.2 Large-scale calibration . . . 42

3.3 Large-scale validation . . . 44

3.4 Fine-scale calibration: communication scenarios . . . 45

3.4.1 Scenario 1: no-communication (null hypothesis) . . . 45

3.4.2 Scenario 2: communication with varying distance decay factor . . . 45

4 Results **47**

4.1 Scenario 1: no-communication (null hypothesis) 47

4.2 Scenario 2: communication between agents 48

4.2.1 Sensitivity analysis of wC and k 48

4.2.2 Sensitivity Analysis of k 49

5 Discussion **54**

5.1 Ancillary finding: predictive accuracy 54

5.2 Scenario 1: no-communication (null hypothesis) 54

5.3 Scenario 2: communication between agents 55

5.4 Model limitations and uncertainties 55

5.4.1 Calculation of environmental factors 56

5.4.2 Modelling of a coral agent 57

5.4.3 Communication implementation versus null hypothesis 58

5.4.4 Missing communication definition 58

6 Conclusion **60**

6.1 Implications for future research 60

7 AI statement **61**

7.0.1 Text review 61

7.0.2 GAML coding 61

7.0.3 Graphs 61

7.0.4 QGIS and spatial analysis 61

References **62**

Appendices **I**

Appendix A: GUI setup of GAMA experiment I

Appendix B: lunar ephemeris data IV

1 Introduction

Coral reefs only cover an area of 0.1 % to 0.5 % of the world's oceans (Spalding and Grenfell, 1997) but are nevertheless of immense importance to marine life, economy and human society. Reef-building corals, commonly known as stony corals, are the foundational species of these ecosystems (Brusca et al., 2016). Their growth form provide the physical structure of the reef, which serves as a habitat for thousands of marine organisms. Over 30 % of the diversity of marine fish live in coral reefs and they are the nursery grounds for even more fish species. The economic goods and ecosystem services that coral reefs provide range from food security to fisheries, coastal protection, and driving tourism and recreation industries (Moberg and Folke, 1999; Woodhead et al., 2019; Spalding et al., 2017). However, in recent times coral reefs have been degrading rapidly due to numerous anthropogenic drivers (Hughes et al., 2017a) such as global warming (Hughes et al., 2017b), eutrophication (D'Angelo and Wiedenmann, 2014) and ocean acidification (Hoegh-Guldberg et al., 2017). Understanding coral reproductive processes, such as broadcast spawning, is critical for preserving these ecosystems in the face of such challenges (Shlesinger and Loya, 2019; Davies et al., 2023). Coral spawning is essential for the maintenance of coral populations, as it is the primary means by which corals reproduce and establish new colonies (Harrison, 2011). By studying the mechanisms and conditions that influence successful spawning events, we can better inform conservation efforts and restoration strategies to safeguard the future of coral reefs.

1.1 Coral biology

"It is a remarkable fact, that widely extended reefs should be developed in the midst of seas, where no land exists, and where the water is generally clear, and pure" – Darwin.

This observation is part of what Darwin termed the "coral paradox," made during his journey aboard the HMS Beagle in 1831. Darwin was intrigued by how such a thriving ecosystem could exist in nutrient-poor waters (Darwin, 1842). Coral scientists later resolved this paradox by discovering the symbiotic relationship between corals and the algae living in their tissues, which allows coral reefs to flourish in these conditions (Muscatine, 1990).

Reef-building corals, classified within the phylum Cnidaria (class Anthozoa, order Scleractinia), are related to jellyfish, similarly possessing stinging cells known as nematocysts. They exist as either solitary polyps or, more commonly, as colonies composed of genetically identical polyps (see Figure 1). Even though each polyp can feed by catching and digesting particulate matter with their tentacles (Houlbrèque and Ferrier-Pagès, 2009), they meet up to 95 % of their energy demand by hosting symbiotic algae, dinoflagellates from the family Symbiodiniaceae, commonly referred to as zooxanthellae (Muscatine, 1990; LaJeunesse et al., 2018). These symbionts are integrated within their endodermal tissue and assimilate nutrients via photosynthesis (Rädecker et al., 2015). In return, zooxanthellae have a secured and sunlit habitat to flourish. This symbiosis provides reef-building corals with enough energy for growth and the secretion of their calcium carbonate skeleton. The coral life cycle alternates between a long sessile stage, during which the colony grows, and a short planktonic stage when a larva colonises a new area (Harrison et al., 1984).

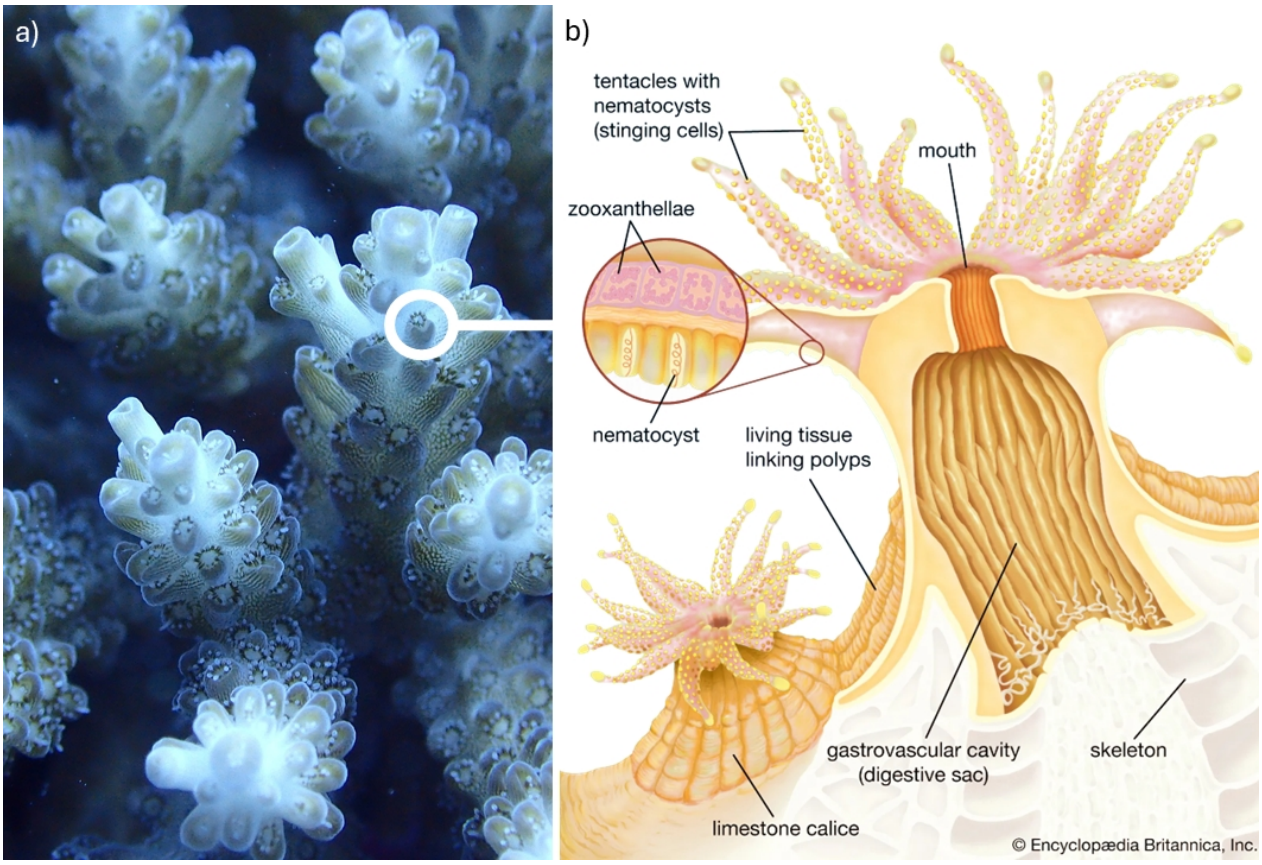

Figure 1: Acroporid coral colony (a) showing extended polyps and (b) the depiction of coral anatomy indicating the main features (Encyclopædia Britannica Inc., 2024).

1.2 Coral reproduction

Coral reproduction can be broadly categorised into asexual and sexual reproduction. Asexual reproduction involves the budding of a coral polyp to produce genetically identical offspring, which is a key mechanism for sustaining and growing colonies (Yeemin et al., 2022). Additionally, if a coral fragment breaks off due to mechanical stress the fragment can grow, under favourable conditions, into a new coral colony. This process, known as fragmentation, is widely employed in modern coral restoration techniques (Hein et al., 2021). On the other hand, sexual reproduction in corals occurs through two primary modes: broadcast spawning and brooding (Harrison, 2011). Broadcast spawners, which will be discussed in detail later, release their eggs and sperm into the water where fertilisation occurs externally.

In brooding corals, fertilisation occurs internally within the coral polyps (Harrison, 2011). The fertilised eggs are retained inside the parent coral, where they develop into planula larvae, called planulae. Planulae are capable of swimming and settling to a new location shortly after being expelled by the parent (Rougée et al., 2015). Compared to broadcast spawners, this method shortens the time planulae spend in the planktonic phase, decreasing the risk of predation, however, also decreasing the range of settlement area.

Corals exhibit a variety of sexual systems, with the majority being hermaphroditic, meaning that individual corals produce both male and female gametes, meaning sperm and eggs respectively (Harrison, 2011). Some coral species are gonochoric, meaning that individual corals are either

male or female. In these species, successful reproduction depends on the proximity of male and female individuals. There are also species that exhibit mixed sexual systems, where individuals may function as one sex in one breeding season and switch to another in subsequent seasons, or where some colonies within a species are hermaphroditic while others are gonochoric (Yeemin et al., 2022). This diversity in reproductive strategies allows corals to adapt to a wide range of environmental conditions.

1.2.1 Spawning process of broadcast spawners

The broadcast spawning process was discovered in the late 1970s when researchers observed that many stony corals did not contain planulae (Stimson, 1978; Kojis and Quinn, 1981). Over the next decade, coral mass spawning events were documented and further investigated (Babcock et al., 1986; Harrison et al., 1984). Today, it is known that broadcast spawning is the dominant reproductive strategy among stony corals. In this process, corals release vast quantities of buoyant gamete bundles, containing both eggs and sperm, into the surrounding water during synchronised mass spawning events (see Figure 2). The success of this external fertilisation depends heavily on accurate synchronisation and the proximity of other corals, as sperm must encounter eggs at the water's surface. The fertilised egg (zygote) develops into a free-swimming planula, which eventually settles on hard substrates to establish a new coral colony. This reproductive method enhances genetic diversity, enables corals to spread across larger areas, and helps maintain population resilience (Harrison, 2011).

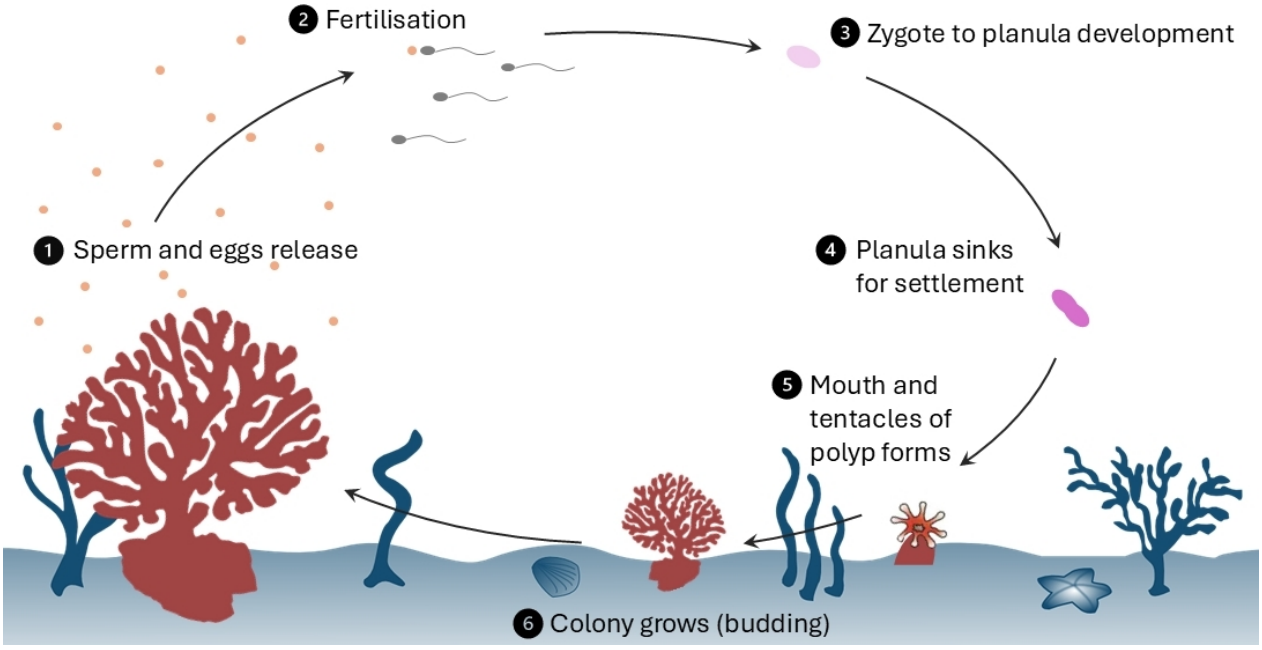

Figure 2: Infographic visualising the life and reproduction cycle of a broadcast spawning coral.

1.2.2 Gametogenesis

Corals, like many other marine organisms, produce steroid hormones that play critical roles in their reproductive cycles, particularly in the process of gametogenesis which is the development and maturation of gametes (Tarrant, 2015). The three primary sex steroids identified in corals are progesterone, testosterone, and estradiol-17β, all of which influence various stages of coral reproduction (Tan et al., 2021). Before corals can undergo spawning, as depicted in number 1 of Figure 2,

gametogenesis must be completed. This process typically spans several months and begins after the previous spawning event, often during winter when water temperatures are lower (Harrison, 2011). Various studies have tracked egg development over time, offering detailed measurements for specific coral species (Mendes, 2002; Chui et al., 2014; Tan et al., 2020). Gametogenesis is broadly categorised into six stages, beginning with Stage I, the resting phase that occurs right after spawning (Stage VI), and progressing through the maturation and development of gametes (see Figure 3).

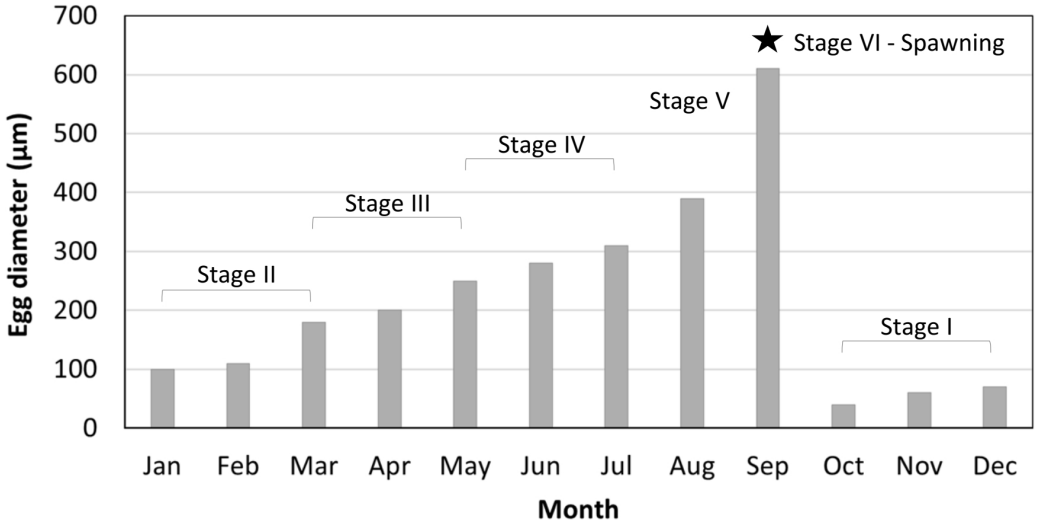

Figure 3: Yearly cycle of the gametogenesis of a broadcast spawning coral showing the process through various development stages in regard to the egg size. This generalisation is a summary from multiple studies (Mendes, 2002; Chui et al., 2014; Tan et al., 2020) and is representative for the coral species in this study.

1.2.3 Spawning synchrony

Chronobiology is the study of the internal rythm and clocks of living organisms which fundamental importance for marine organisms has been explored and summarised by Naylor (2010). Accordingly, the most remarkable aspect of coral broadcast spawning is the precise synchronisation of individuals. This mass spawning usually happens at a specific time on one or two nights, primarily after full moon periods (Sorek and Levy, 2014). The exact timing of spawning varies strongly across coral species where they spawn at a specific day around the full moon and release gametes at specific hours after sunset (Baird et al., 2009), emphasising the role of chronobiology in reproductive timing.

1.2.3.1 Large-scale synchrony

The synchronous spawning across reef systems, sometimes covering entire regions is driven by environmental cues. In this study, large-scale refers not only to the spatial extent but also to its temporal precision, specifically the alignment of spawning on particular days.

- **Water Temperature.** Water temperature influences coral reproduction where rising seawater temperature after winter induces gamete development and maturation (Gouezo et al., 2020). The molecular analysis by Tan et al. (2020) found that the expression of key reproductive genes, are synchronised with these temperature fluctuations. These genes regulate egg development and ensure the coral's reproductive readiness by promoting the incorporation of yolk protein.

- **Photoperiod.** Gene regulation in corals is influenced by the solar cycle (Brady et al., 2011) and therefore the photoperiod, the length of daylight, was chosen as an environmental influence. Furthermore, Penland et al. (2004) proposed that the increase in solar insolation in January/February, which corresponds to increasing photoperiod, triggers the onset of gametogenesis.

- **Moonlight.** The lunar cycle is a fundamental driver of biological rhythms in marine organisms, synchronising critical behaviours such as reproduction, spawning, and migration (Naylor, 2010; Andreatta and Tessmar-Raible, 2020). Corals possess photoreceptors sensitive to blue light, enabling them to detect changes in moonlight intensity (Gornik et al., 2021; Levy et al., 2007; Gorbunov and Falkowski, 2002). Moonlight, particularly during full moon, is known to be a key environmental influence for coral mass spawning events (Kaniewska et al., 2015; Komoto et al., 2023; Sorek and Levy, 2014).

- **Dark Time.** The period of darkness between sunset and moonrise is another environmental factor that influences the timing of coral spawning (Brady et al., 2009). This window of relative darkness before the rising moon is believed to be decisive trigger for the onset of the spawning event (Lin et al., 2021; Fogarty and Marhaver, 2019).

1.2.3.2 Fine-scale synchrony

The precise coordination of spawning within local populations is synchronised to an accuracy of minutes to a couple of hours. While it is hypothesised that local factors such as minor variations in temperature, current patterns may influence fine-scale timing, conclusive evidence for this process is lacking (Sorek and Levy, 2014). However, communication pathways in corals have been described to take place within coral colonies and between neighbouring corals (Witzany, 2010; Tarrant, 2015). These communication mechanisms may help in achieving spawning synchrony.

1.2.4 Theories of coral communication

1.2.4.1 Chemical signalling

The first evidence of estrogen in and around corals dates back to the early 1990s, when measurements revealed the presence of estradiol during a spawning event (Atkinson and Atkinson, 1992). Subsequent research has revealed the presence of various sex steroids, including estrogens, androgens, and progestogens discussing their potential roles in coral reproduction and early developmental processes (Tarrant, 2015; Rougée et al., 2015). Recent work by (Tan et al., 2021) suggests that while most known steroidogenic enzymes were identified in the coral genome, the pathways for steroid production and their exact regulatory functions in coral reproduction remains unclear.

Nevertheless, chemical signalling is the strongest theory explaining how fine-scale coral spawning synchrony may be induced by releasing hormones or hormone-like compounds into the water (Twan et al., 2003, 2006b). Hormones such as estradiol and gonadotropin-releasing hormone (GnRH) are known to regulate gametogenesis and spawning in corals (Twan et al., 2006a), making them plausible candidates for facilitating inter-colony communication. For example, peaks in estradiol levels prior to

spawning have been observed in several coral species, suggesting a role in triggering gamete release within colonies (Slattery et al., 1999; Tarrant et al., 1999; Atkinson and Atkinson, 1992).

While direct evidence for chemical communication transmission in corals is missing (Tarrant, 2015), other marine invertebrates have been studied more thoroughly. Research on sea urchin populations found that spawning synchrony may be initiated by the release of a chemical signal, potentially a pheromone, into the water promoting spawning of nearby individuals (Watts and Wasson, 2020; Reuter and Levitan, 2010).

1.2.4.2 Acoustic signalling

An experimental study by Ibanez and Hawker (2021) showed that certain corals produce ultrasonic emissions at night. Furthermore, reef soundscapes can guide larval settlement of corals (Aoki et al., 2024). Both studies suggest a role for acoustic signalling in reproductive behaviour. Additionally, moonlight-driven biological choruses imply a link between lunar illumination and reef acoustics (Duane et al., 2024). This is a newly emerging field with experimental theories suggesting that acoustic cues may influence biological processes in coral reef ecosystems, including spawning synchronization.

1.3 Study species *Orbicella franksi*

Orbicella franksi (Gregory, 1895) is a key reef-building coral species in the Caribbean and adjacent regions, ranging from Brazil to Bermuda (Budd et al., 2012). They belong to the *Orbicella 'annularis'* species complex which consists of three closely related taxa: *O. annularis*, *O. faveolata*, and *O. franksi* (Pandolfi and Budd, 2008). Colony size ranges from 30 cm to over 60 cm depending on location (Moulding and Ladd, 2022).

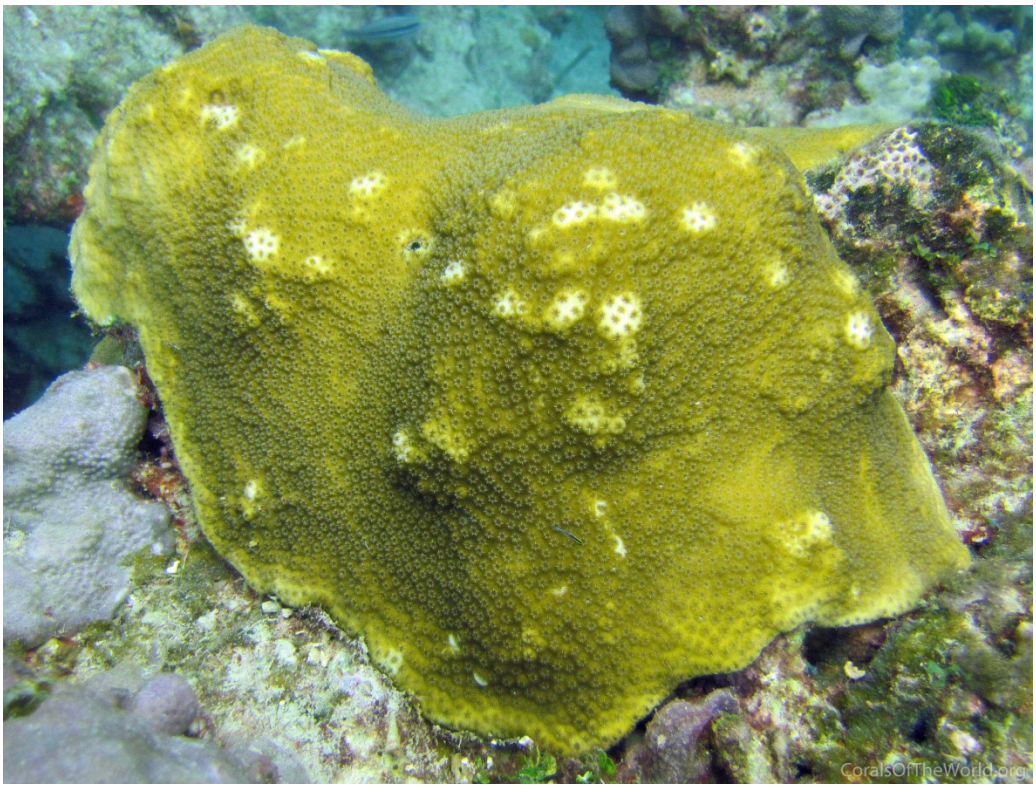

Figure 4: *Orbicella franksi* colony exhibiting a flat plate morphology, characteristic of this species in Caribbean reef environments. Photo credit: Ernesto Weil.

O. franksi is a hermaphroditic coral that reproduces through external fertilisation during annual mass spawning events as described in previous chapters. They release buoyant gamete bundles into the water column (Szmant, 1991; Van Veghel, 1994). Each gamete bundle, produced by individual polyps, contains both sperm and eggs and becomes visible on the coral surface approximately 30 minutes before spawning in a process referred to as 'setting.' Upon release, these bundles ascend to the water surface, where they break apart, facilitating cross-fertilisation with gametes from other *O. franksi* colonies (Harrison, 2011; Levitan et al., 2004).

1.4 Study aim

Environmental factors of coral spawning fail to explain the observed fine-scale synchrony, where individuals of one coral species spawn within minutes of each other. This study aimed to further deepen the understanding of the spatio-temporal patterns of spawning events and how coral communication may influence them. The hypothesis is based on the theory that coral communication signals could induce fine-scale spawning synchronisation of corals as an emergent phenomenon.

Hypothesis: Coral communication explains fine-scale spawning patterns.

Objectives:

1. Simulation model development: Create an agent-based model (ABM) that integrates environmental factors (solar cycle, lunar cycle, sea water temperature) and communication scenarios to trigger spawning of coral agents.
2. Baseline establishment: Investigate the fine-scale spawning patterns of the validation data set.
3. Predictive validation: Compare the predicted outcomes of the simulation with empirical data of coral spawning.
4. Testing communication hypotheses: Define measurables and indicators in terms of timing and spatial patterns that allow for comparison to real-life spawning on the reef. Implement a test procedure for each communication mode.

2 Materials and methods

2.1 Study location

This study focuses on a coral reef site (coordinates: 9.3273, -82.2039) near Bocas del Toro, located on the Caribbean coast of Panama (see Figure 5). The real-world validation data, kindly provided by Professor Don R. Levitan was collected at this location during the research on *O. franksi* spawning synchrony, as detailed in Levitan et al. (2011) "Genetic, Spatial, and Temporal Components of Precise Spawning Synchrony in Reef Building Corals". The calculation for the relevant large-scale environmental influences regarding solar and solar cycles and water temperature were tailored to this location.

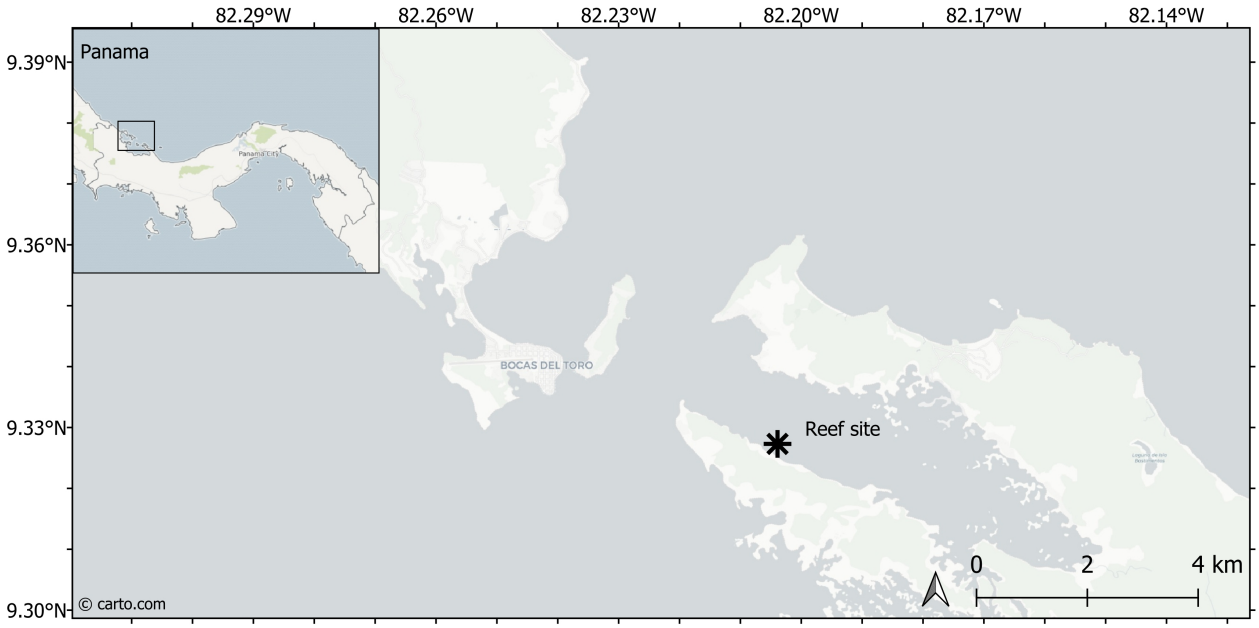

Figure 5: Location of the reef site studied by Levitan et al. (2011) in Bocas del Toro, Panama. The marker indicates the reef's coordinates (9.3273°N, 82.2039°W), and the inset map provides the geographical context of Bocas del Toro within Panama.

2.2 Model development

The applied modelling approach is grounded in systems theory, which views systems as interconnected sets of components interacting over time (von Bertalanffy, 2003). A complex system allows for interactions between individuals (agents) leading to behaviours and patterns that are neither predictable nor planned solely by the attributes of the individuals themselves (Waldrop, 1992; Grimm and Railsback, 2005).

Systems often exhibit emergence, where the interactions of numerous autonomous agents, each following relatively simple rules, yet leading to complex, system-wide phenomena (Railsback and Grimm, 2019). Additionally, they may display self-organisation, as order and patterns emerge without centralised control (Camazine et al., 2001).

The simulation model developed in this thesis adopts a hybrid approach integrating Agent-Based Modelling (ABM) with Discrete-Event Simulation (DES). By combining ABM and DES, the model captures both the micro-level behaviours of individual corals preparing and communicating prior to spawning, and the macro-level, event-driven triggering of the spawning event.

2.2.1 Agent Based Model (ABM)

ABM is a simulation method that models the actions and interactions of autonomous agents within an environment (Gooding, 2019). Each agent can have individual attributes, follows simple rules but can interact with other agents and the environment, leading to the emergence of complex system-level behaviours. According to Railsback and Grimm (2019), ABM is used for modelling systems where individual behaviours and interactions result in emergent properties, for example to simulate social or ecological models.

2.2.2 Discrete-Event Simulation (DES)

DES models a system as a series of discrete events that occur at specific points in time. Each event triggers a change in the system's state, and the simulation progresses by moving from one event to the next. Law (2014) defines DES as an effective approach for simulating systems with distinct operational processes, such as manufacturing, queuing networks, or logistics systems.

2.3 Analysis plan

The research focus was on the fine-scale spatio-temporal spawning pattern of corals. This pattern was examined using the global Moran's I cluster analysis on spawning time of individual coral agents.

Resulting from each cluster analysis were two values, the Moran's I and the Z-score. The Moran's I is a measure of spatial autocorrelation (Moran, 1950), indicating how similar or dissimilar values are distributed across space. A positive value indicates a positive spatial correlation, where similar values are clustered together, while values near 0 suggest a random spatial distribution, and negative values indicate negative spatial correlation, where dissimilar values are adjacent. The Z-score (Anselin, 1995) indicates whether the observed clustering is likely due to random variation or is statistically significant. High positive or negative Z-scores (above or below 1.96) denote the significance of either clustering or dispersion, respectively.

2.3.0.1 Baseline analysis: the real-world data

Real-world datasets by Levitan et al. (2011) documented spawning events of *O. franksi* between 2002 and 2009. To establish the baseline for comparison between communication scenarios, the spawning times of individual corals were analysed for clustering on each spawning day.

The the real-world spawning events with significant clustering (Z-score above 1.96) were selected for model comparison.

2.3.0.2 Communication scenarios: data collection

Simulation procedure:

- Spawning duration calibration: To effectively compare the baseline with the communication scenarios, the real-world spawning durations were the baseline to which the communication scenarios were calibrated to. Details to the calibration procedure is found in the corresponding Chapter 3.
- 30 simulation runs per scenario and spawning day were executed to ensure statistical robustness.
- The attributes and spawning time (in minutes) of each coral agent were logged to a CSV file during each run for further analysis.

2.3.0.3 Spatio-temporal analysis

- Each CSV file was loaded into a GIS software and analysed for clustering using the QGIS Hotspot Analysis plugin (Oxoli and Prestifilippo, 2017) was used, employing the K-nearest neighbors (KNN) approach with K set to 5. The results include the Global Moran's I value and corresponding Z-score.
- The cluster analysis results were collected and descriptive statistics and graphical interpretation was performed in R (R Core Team, 2024).

2.3.1 Simulation and analysis software

- GAMA, Version 1.9.3 (Taillandier et al., 2019)
- QGIS, Version 3.38.3 "Grenoble" (QGIS Development Team, 2024)
  - Plugin *Hotspot Analysis*, Version 2.0.0 (Oxoli and Prestifilippo, 2017)
- R, Version 4.4.1 (2024-06-14 ucrt) "Race for Your Life" (R Core Team, 2024)
  - RStudio, Version 2024.9.0.375 "Cranberry Hibiscus" (Posit-team, 2024)
  - R Package *ggplot2*, Version 3.5.1 (Wickham, 2016)
  - R Package *dplyr*, Version 1.1.4 (Wickham et al., 2023)
  - R Package *patchwork*, Version 1.3.0 (Pedersen, 2024)

2.4 Overview, Design concepts, and Details (ODD)

This ODD protocol was created using the guidelines and template by Grimm et al. (2010). According to these guidelines, the ODD protocol must be written to act as a stand-alone section. Thus, certain elements of the thesis, e.g. the purpose and study aim, will be repeated.

2.4.1 Purpose

This model simulates the spawning behaviour of corals within a defined coral reef at Bocas del Toro, Panama. This phenomenon, known as broadcast spawning where corals release their gametes almost simultaneously, is critical for successful fertilisation and subsequent coral recruitment (Harrison, 2011). While large-scale environmental factors such as water temperature, the lunar cycle, and the solar cycle are known to influence the timing of coral spawning events (Sorek and Levy, 2014), the precise mechanisms by which corals synchronise their spawning within a narrow time window remain poorly understood.

Potential communication scenarios between corals were explored without defining specific communication types. The reason is that research on whether and how coral individuals may influence each other is still in progress and evidence is in insufficient to define specific mechanisms (Witzany, 2010). The following objectives outline the development of the model and subsequent simulation procedure:

1. Develop a coral reef model at the specific location which includes all large-scale environmental factors influencing the corals. The simulation runs through the year, starting on January 1st, until the coral reef spawns. The chosen environmental factors are: water temperature, solar cycle, lunar cycle, and dark time.
2. Calibrate and validate the environmental factors.
3. Define measurable outputs: Analyse the clustering pattern concerning spawning time for different communication scenarios.
4. Establish a baseline: Investigate the clustering pattern of the real-world dataset to provide the baseline.
5. Load the coral individuals into the model as agents, each with their individual characteristics at their respective real-world location on the simulated reef.
6. Simulate communication and non-communication scenarios and record the resulting spawning times.

Hypothesis: Coral communication explains fine-scale spawning patterns.

2.4.2 Entities, state variables and scales

2.4.2.1 Entity: environmental condition

The environmental condition defines key factors such as date, water temperature, solar, and lunar cycles. Its state variables (see Table 1) vary temporally but are spatially independent, meaning they are valid for all agents within the simulation. Note that the state variables of submodels are listed in the respective chapters.

Table 1: State variables for the environmental condition.

State Variable	Identifier	Data Type	Unit
Spawning year: User input parameter between 2002 and 2009.	`spawningYear`	int	year (yyyy)
Spawning day: User input parameter to chose between day 1 or 2 of spawning.	`spawningDay`	int	1 or 2
Spawning Recording: User input if spawning times should be recorded.	`recordSpawning`	bool	true/false
Cycle step duration: changes from days to minutes when first coral spawns.	`step`	float	days or minutes
Solar variables			
Sunrise time	`sunrise`	float	hours (decimal)
Sunset time	`sunset`	float	hours (decimal)
Normalised photoperiod: day duration.	`normPhotoperiod`	float	-
Lunar variables			
Lunar Ephemeris data 2002-2029	`LunarEphemeris`	file	.csv
Moonrise time	`moonrise`	float	hours (decimal)
Moonset time	`moonset`	float	hours (decimal)
Moonlight dose	`moonlightDose`	float	-
Dark time	`darktime`	float	hours (decimal)
Sea water temperature variables			
Mean annual water temperature by Kaufmann and Thompson (2005)	`TEMP_MEAN`	float	°C
Min annual water temperature by Kaufmann and Thompson (2005)	`TEMP_MIN`	float	°C
Max annual water temperature by Kaufmann and Thompson (2005)	`TEMP_MAX`	float	°C
Summer amplitude	`amplitudeSummer`	float	°C
Winter amplitude	`amplitudeWinter`	float	°C
Normalised sea Water temperature	`normWaterTemp`	float	-
Spawning variables			
Spawning event has started.	`isReefSpawning`	bool	true/false

2.4.2.2 Entity: coral reef grid

A rectangle grid representing the reef and used to define the physical location of coral agents when they are initiated (see Table 2).

Table 2: State variables of the reef grid.

State Variable	Identifier	Data Type	Unit
Reduces the ordinary 100x100 grid of GAMA to the size of the reef: rectangle (37 x 80).	`shape`	geometry	meters

2.4.2.3 Entity: coral colony species

Coral colonies are represented as agents with individual attributes (see Table 3).

Table 3: State variables of the coral species.

State Variable	Identifier	Data Type	Unit
Coral identification number. (Levitan et al., 2011)	`coralID`	int	-
Spatial location on the reef. (Levitan et al., 2011)	`coralX`, `coralY`, `coralDepth`	float	meters
Coral size: average cross section. (Levitan et al., 2011)	`coralSize`	int	cm
Spawning readiness: measure of the coral's readiness to spawn.	`spawnReadiness`	float	-
The coral colony decides to spawn.	`isSpawning`	bool	true/false
Reproductive variability (random).	`reproductiveVar`	float	-
Total influence of neighbouring corals ot the self-readiness for spawning.	`influenceSum`	float	-
Spawning time: difference to reef spawning start.	`spawningStart`	int	cycles (minutes)

2.4.2.4 Scales

- Spatial Scale
  - Extent: The model covers a reef area of 80 to 37 meters.
  - Resolution: Corals are positioned on a metered grid with a resolution defined by coordinates, such as (19.89397, 25.43924).
- Temporal Scale
  - Extent: The simulation covers the time period starting in January of a chosen year (2002-2009) leading up to and including the spawning event.
  - Resolution: The resolution is set to "day" during the spawning preparation phase A and switches to "second" as soon the first coral spawns (discrete event) which starts phase B.

2.4.2.5 Additional calculations

Supplementary variables which provide insight into the system behaviour but are not required for the simulation functionality (see Table 4).

Table 4: Computed variables for simulation monitoring.

State Variable	Identifier	Data Type	Unit
Average spawning readiness of all agents.	`avgSpawnReady`	float	-
Minimum spawning readiness of all agents.	`minSpawnReady`	float	-
Maximum spawning readiness of all agents.	`maxSpawnReady`	float	-

2.4.2.6 Optional visualisations

These are designed to enhance understanding and presentation but do not affect the model's computational logic or outcomes (see Table 5).

Table 5: State variables for additional visualisations.

State Variable	Identifier	Data Type	Unit
Spatial file visualising reef depth.	`REEF_DEPTH_GRID`	file	.tif
Reef depth normalised value.	`normDepth`	float	-
RGB red value: for reef or coral color.	`red`	float	0-255
RGB green value for reef or coral color.	`green`	float	0-255
RGB blue value for reef or coral color.	`blue`	float	0-255
Pinkish hue for corals.	`PINK`	rgb	rgb(255, 192, 203)
Brownish hue for corals.	`BROWN`	rgb	rgb(139, 61, 33)
Randomiser for coral color.	`colorRandomiser`	float	0.1-1.2
3D object of a coral colony.	`CORAL_3D`	obj_file	.obj
Color of coral object.	`coralColor`	rgb	color code
Rotation angle of coral object.	`rotationAngle`	int	degrees

2.4.3 Process overview and scheduling

The process overview and scheduling for the model is separated into two phases to simulate coral spawning events (see Figure 6). Initially, the model operates in Phase A, where environmental conditions (water temperature, solar and lunar cycles) are updated daily. According to these factors, the coral agents' spawning readiness increases. The coral agent goes through three stages of readiness, the development stage, the maturation stage and the spawning stage, each focusing on a different set of environmental factors. When the first coral spawns, a discrete event is triggered. This discrete event causes the model to transitions to Phase B and the cycle duration switches from days to minutes.

In Phase B, the model introduces the communication of agents according to the selected scenario, where each agent assesses the readiness of its neighbours and adapts its own readiness accordingly. This phase continues until all corals have spawned.

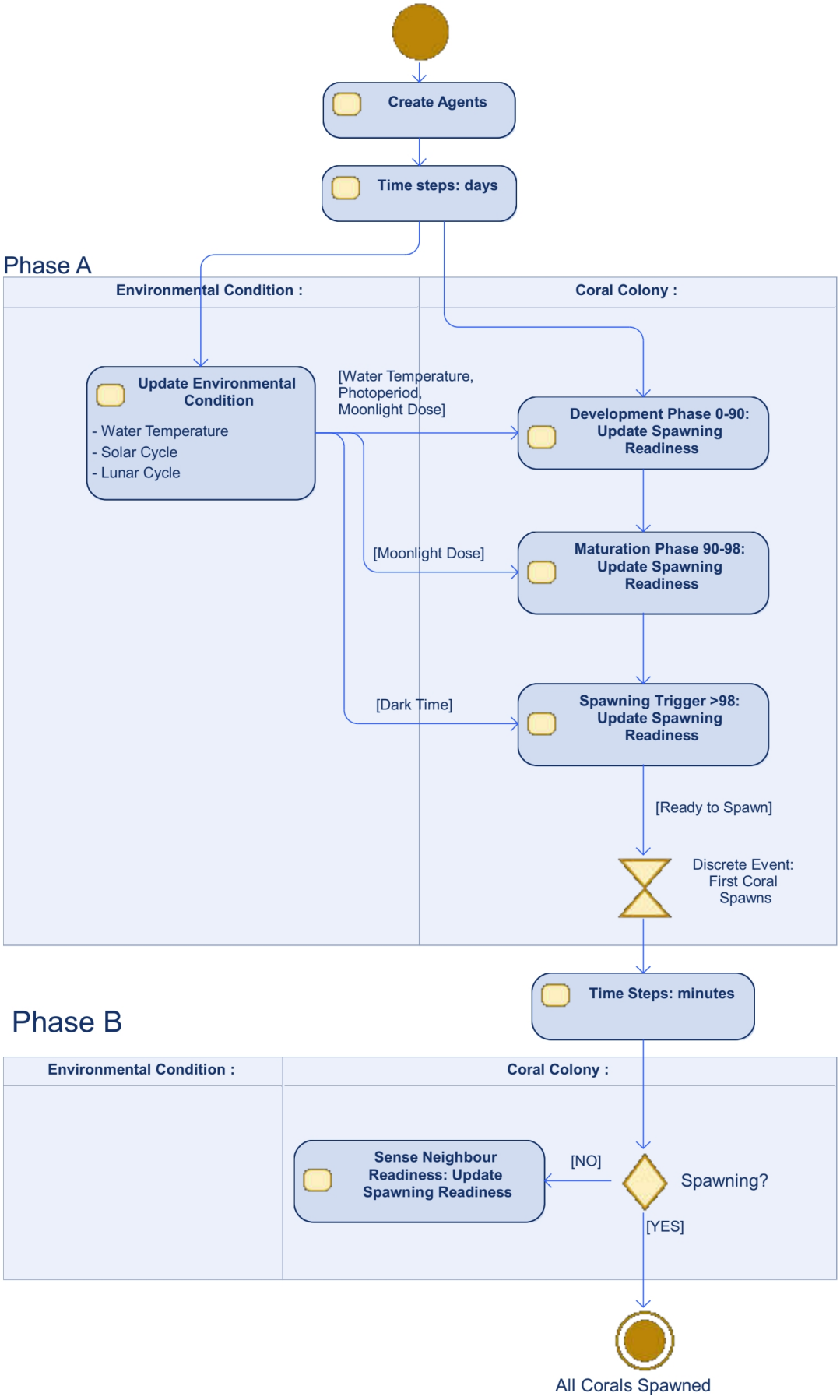

Figure 6: Process flow of model showing the two phases and scheduling of update events. Visualisation created with Modelio Version 5.4.01 (Modelio.org, 2023).

2.4.4 Design concepts

2.4.4.1 Basic principles

The design of this model is grounded in the principles of coral ecology, particularly focusing on the phenomenon of synchronised spawning, which is essential for successful fertilisation of released gametes. These principles are paired with the appropriate methods used in complex systems and modelling theories.

1. **Environmental cues influencing spawning.** Coral spawning is closely linked to environmental cycles, particularly the lunar cycle, solar cycle, and water temperature (Harrison, 2011). These large-scale environmental factors serve as primary triggers for the initiation of gametogenesis and the eventual synchronised release of gametes (Gouezo et al., 2020). The model incorporates these cycles to simulate the readiness of corals to spawn.
2. **Integration of Discrete-Event Simulation.** The integration of DES allows for the efficient simulation of events that vary in time scale (Law, 2014), such as the gradual development of gametes over months and the rapid release during spawning, which occurs within minutes. The event is defined by a trigger (the first coral spawning), the entities involved, and the resulting state changes. In this model, events such as coral spawning and environmental updates are scheduled and executed only in their corresponding phase (see Figure 6).
3. **Integration of Agent-Based Modelling and Individual-Based theory.** Each coral is modelled as an individual agent with specific traits, such as reproductive readiness and proximity to other corals (Gooding, 2019). These agents follow decision rules based on their internal states (e.g., gametogenesis progression) and external interactions (e.g., environmental cues, neighbour interactions). The model draws from individual-based theory, which emphasises how emergent behaviours, such as synchronised spawning, arise from the localised interactions of agents within a given environment (Grimm and Railsback, 2005).
4. **Emergent synchronisation through communication.** Beside the large-scale environmental factors, the fine-scale synchronous spawning of a coral reef remains a critical area of investigation (Sorek and Levy, 2014). In this model, fine-scale spawning synchrony arises from local communication interactions between corals, where the spawing readiness of coral agents is influenced by both the readiness of nearby individuals.
5. **Deterministic and stochastic processes.** The model incorporates both deterministic and stochastic elements. Deterministic processes are environmental factors which follow predictable patterns and are implemented as algorithms. The stochastic element is the variability in reproductive strength of each coral individual as a reflection of the internal biological variability. This stochasticity prevents unrealistic, simultaneous spawning of all corals.

2.4.4.2 Emergence

The key emergent output of the model is the fine-scale spatial pattern of coral spawning, which arises from the communication between coral agents. The model incorporates a feedback loop where a coral agent detects the higher spawning readiness state of neighbouring corals, which in turn increases its own readiness. On the other hand, corals exhibit individual reproductive strengths that influence their responses to environmental factors, these individual responses are defined by model rules rather than emergent properties. A coral agent can spawn based solely on environmental factors, however, these individual responses alone cannot reproduce the fine-scale timing and clustering of observed real-world spawning events.

While the focus of the model is on the fine-scale spatial patterns and clustering behaviour, the coral spawning synchrony is a collective outcome of the coral agents' adaptive responses to the changing environment and their emergent response to communication.

2.4.4.3 Adaptation

The model has no implemented adaptive traits of its individuals.

2.4.4.4 Objectives

The model has not implemented objectives for its individuals.

2.4.4.5 Learning

The model has not implemented learning abilities to its individuals.

2.4.4.6 Prediction

The model has not implemented predictive abilities to its individuals.

2.4.4.7 Sensing

Coral agents can sense the environmental factors in a way that they simply know the variables and don't need to obtain them. This reflects the condition on the reef where a coral, due to its immobility, is exposed to its environment. This exposition is emphasised by the coral's physiological processes being controlled by the environment (Brusca et al., 2016). For a simple example: while a mammal's body temperature is tightly controlled internally, the coral's body temperature is always equal to the surrounding sea water temperature. The output of all sensing procedures (four environmental factors and the inter-agent communication) is converged into the increase of the coral agent's spawning readiness. The spawning readiness used in this model represents the coral agent's internal physiological progression of gametogenesis. This variable summarises various biological factors that influence a coral's reproductive strength, including the maturation of reproductive tissues, energy reserves, and the overall health of the colony. As detailed in Figure 6, spawning readiness accumulates gradually over time within each agent, driven by large-scale environmental factors: sea water temperature, photoperiod and moonlight (Van Woesik et al., 2006; Nozawa, 2012; Gouezo et al., 2020). While the coral progresses through the gametogenesis, spawning readiness approaches 100%, signifying that the gametes are fully developed and the coral is physiologically prepared for spawning. After reaching 98%, the coral is getting ready to spawn and is triggered by the final clue, the dark-time period (time between sunset and moonrise). During spawning, the coral agents sense and adapt to their neighbours spawning readiness which influences the fine-scale spawning pattern.

2.4.4.8 Interaction

After the first coral spawns, the discrete event changes the model's time step from days to minutes. Following this, the remaining corals begin sensing the readiness state of their neighbours and adjust their own readiness accordingly. Although this process is implemented using a sensing-based approach, it serves as a computational simplification of a more complex communication process, where corals release signals that are received by neighbouring individuals.

2.4.4.9 Stochasticity

Variability is introduced with the reproductive strength of individual corals. By introducing stochasticity into the model, each coral's reproductive readiness is allowed to vary within a certain range, preventing all corals from spawning simultaneously under identical conditions. This introduces a level of unpredictability that mirrors real-world biological processes, where even under the same environmental conditions, individual corals may exhibit different timing and intensity in their spawning behaviours.

2.4.4.10 Collectives

The model has no implemented collectives or aggregations that affect, or are affected by individuals.

2.4.4.11 Observation

The simulated scenarios are directly compared with the equivalent real-world data. In the real world, the spawning times of each coral was recorded in minutes using SCUBA divers on the reef (Levitan et al., 2011). Accordingly, in the simulation when a coral agent starts spawning, it writes their attributes and spawning time into a CSV file. The simulation ends after the last coral has spawned and the file contains a complete list with all spawning times.

Saved coral attributes:
`coralID`: from real-world data.
`coralX`: from real-world data.
`coralY`: from real-world data.
`coralDepth`: from real-world data.
`coralSize`: from real-world data.
`reproductiveVar`: randomised value the agent received during initialisation.
`spawningStart`: minutes elapsed since reef spawning began.

The 3D visualisation of the reef and agents is not required to create the output for statistical analysis. However, it provides insight into the coral agent distribution and also over the environmental parameters progressing through time. Therefore, the optional visualisation variables are described in this ODD and a suitable graphical user interface (GUI) experiment can be set up. A screenshot showing the GUI setup is found in Appendix A.

Parameters:
- `spawningYear`: chose the spawning year between 2002 and 2009.
- `spawningDay`: select the spawning day between 1 or 2.
- `recordSpawning`: if enabled, spawning times of agents are recorded.
- `spawnFactor`: change the spawning factor, if required.
- `commFactor`: change the communication factor, if required.
- `distanceDecay`: change the distance decay factor, if required.
- `weightComm`: change the communication weight, if required.

Monitors (Textual Outputs):
- `current_date`: the simulation's current date.
- `maxSpawnReady`: the maximum value of spawning readiness, if it reaches 100, the reef starts spawning.
- `dayDifference`: how many days remain until the observed (real-world) spawning date.
- `isReefSpawning`: indicates whether spawning has begun (true/false).
- `spawningDuration`: displays the minutes elapsed since spawning began.

Reef Display:
Using the type "opengl", the reef grid and the coral species can be loaded.

Environmental Chart Display:
- Water temperature `waterTemp`.
- Photoperiod (day length) `photoperiod`.
- Moonlight dose `moonlightDose`.
- Dark time duration `darktime`.
- Min/Max spawning readiness values `minSpawnReady` & `maxSpawnReady`.

Spawning Chart (Pie Chart):
A pie chart that dynamically shows the proportion of corals that have spawned (`coralsNotSpawned`) versus those that have not yet spawned.

2.4.5 Initialisation

At the start of the simulation (time $t = 0$), the model is initialised with predefined conditions and settings.

The simulation is designed to run for a selected year, with `spawningYear` defined as a parameter (2002–2009), while `spawningDay` (set to 1 or 2) can be selected if this year showed two consecutive days of spawning in the real world. With `starting_date` defined during initialisation, the simulation always starts on the 1st of January of the selected year. This is because *O. franksi* gametogenesis begins around three months after the last spawning in September (see Figure 3).

The starting values of many global environmental parameters, as well as the submodels, are fundamental to the functioning of the model (see Table 6). Many astrological calculations require constants that are essential for determining daily changes.

Some values are optional visualisations. The action `load_reef` initialises the reef's depth data, which is used to visualise the reef in 2.5D and calculates the blue coloration based on depth. This data is imported from a raster file (`reef_depth.tif`).

Table 6: Initialisation values of global environmental variables and submodels.

Model Part	**Identifier**	**Init. value**
Global Variables	spawningYear	2009 (user defined)
	spawningDay	1 (user defined)
	recordSpawning	false (user defined)
	step	1 day
	shape	rectangle(37m, 80m)
	REEF_DEPTH_GRID	file containing depth values
	LunarEphemeris	file containing lunar ephemeris data for moon submodel
Solar Submodel	LATITUDE	9.3273
Moon Submodel	B0	1.0
	m1	0.308
	rho	4.862
	m2	0.877
	h	0.7
	d_average	384400.0
Temperature Submodel	T_MEAN	28.6 °C
	T_MIN	26.6 °C
	T_MAX	30.5 °C
	LOWEST_TEMP_DAY_SHIFT	182.0 days
Spawning	isReefSpawning	false
	count_not_spawning_corals	(not zero because of model stop condition)
	weightTemperature	0.209
	weightPhotoperiod	0.21
	weightMoonDose	0.175
	weightDarktime	0.2
Communication	spawnFactor	depends on scenario (see Table 17 & 19)
	distanceDecay	depends on scenario (see Table 19)
	weightComm	depends on scenario (see Table 19)
	CommFactor	depends on scenario (see Table 19)

During global initialisation, the `load_corals` action is triggered, which loads coral agents using values from the corresponding CSV file containing real-world data for a specific spawning day (see Table 7). Further variables are randomised during the species initialisation, from which only the reproductive variability (`reproductiveVar`) has a significant impact on the model. The remaining are used for optional 3D visualisation of coral agents.

Table 7: Initialisation values of the coral species.

Model Part	**Identifier**	**Init. value**
Coral Agent	`coralID`	Loaded from CSV file
	`coralSize`	Loaded from CSV file
	`coralX`	Loaded from CSV file
	`coralY`	Loaded from CSV file
	`coralDepth`	Loaded from CSV file
	`reproductiveVar`	Random (0.002 - 0.008)
	`coralColor`	Random (pink-brownish)
	`rotationAngle`	Random (0° to 360°)
	`colorRandomiser`	Random (0.1 - 1.2)

2.4.6 Input data

In-situ coral spawning time measurements. For the calibration and validation of the model, real in-situ measurements of coral spawning events are required. These datasets were kindly provided by Professor Don R. Levitan of the Florida State University. Levitan et al. (2011) observed and measured coral spawning on a reef at Bocas del Toro in Panama during the years between 2002 and 2009. These datasets contain following information: coral id, coral size, coral location (x and y from a starting point), time of spawning each year.

Lunar ephemeris data. To calculate the lunar cycle, lunar ephemeris data were downloaded from U.S. Naval Observatory (2024) which provides the daily results of the Moon's orbit and phases of a specific location on Earth. A sample of the original dataset structure can be seen in Appendix B.

Environmental conditions of each year's main spawning day, where most of the corals spawned, were extracted by running the simulation model in GAMA (see Table 8). In turn, these results are used for normalisation purposes in the submodels of some environmental factors.

Table 8: Environmental variables extracted from the simulation model on the main spawning days between 2002-2009 recorded by Levitan et al. (2011).

Date	Moonlight Dose (%)	Dark Time (h)	Water Temp. (°C)	Photoperiod (h)
27/09/2002	15.58	4.85	31.55	11.94
16/09/2003	15.28	4.76	31.46	12.04
04/09/2004	15.67	4.80	31.27	12.14
23/09/2005	14.57	5.11	31.53	11.98
13/09/2006	12.75	5.67	31.42	12.07
03/09/2007	11.85	5.91	31.23	12.15
20/09/2008	16.79	5.00	31.51	12.00
09/09/2009	20.23	4.15	31.35	12.10
Min	11.85	4.15	31.23	11.94
Max	20.23	5.91	31.55	12.15
Average	15.34	5.03	31.42	12.05

2.4.7 Submodels

Submodels may contain complex mathematical calculations. To maintain the clarity of these equations, the corresponding mathematical notation was used instead of the coding identifiers. At the beginning of each submodel a table states the mathematical notation and corresponding identifier of the state variables. Some state variables are repeated from the previous chapter 2.4.2 to help understand the equations, alongside the helper variables used only within the corresponding submodel.

2.4.7.1 Solar cycle

The solar cycle is driven by the Earth's rotation and its orbit around the Sun. The position of the Sun relative to a specific location on Earth determines the times of sunrise and sunset (Duffett-Smith and Zwart, 2011). The Earth's rotation on its axis over a 24-hour period generates the cycle of day and night. Its orbit around the Sun, completed in approximately 365 days, results in seasonal changes to the length of daylight throughout the year. The axial tilt of approximately 23.5 degrees is responsible for the seasonal changes in the solar cycle (Meeus, 1998).

Table 9: State variables (repetition marked with asterisk) and helper variables including their mathematical notation in equations to calculate the solar cycle.

State Variable	Math	Identifier	Data Type	Unit
**Sunrise time*	S_{rise}	`sunrise`	float	hours (decimal)
**Sunset time*	S_{set}	`sunset`	float	hours (decimal)
**Normalised photoperiod*	P_{norm}	`Normphotoperiod`	float	hours (decimal)
Latitude of reef location.	ϕ	`LATITUDE`	float	decimal degrees
Solar declination	δ	`solarDeclination`	float	degrees
Solar declination	H_{rise}	`sunriseHourAngle`	float	degrees
Solar declination	H_{set}	`sunsetHourAngle`	float	degrees
Photoperiod	-	`photoperiod`	float	hours (decimal)

1. Solar Declination

The solar declination (δ) is the angle between the rays of the Sun and the plane of the Earth's equator. It varies throughout the year as the Earth orbits the Sun. The declination can be approximated by the following formula (Meeus, 1998):

$$\delta_{(\mathrm{t})} = \varepsilon \times \sin\left(\frac{360}{365} \times (t - 81)\right) \tag{1}$$

where:
- δ is the solar declination,
- t is the day of the year, with January 1st as $t = 1$,
- ε is the Earth's tilt, 23.438 degrees, also called the obliquity of the ecliptic,
- $\frac{360}{365}$ converts the number of days in a year to an angular movement in a full circle,
- $(t - 81)$ shifts the day of the year such that $t = 81$ corresponds to the vernal equinox (March 21).

2. Solar Elevation at Sunrise and Sunset

Sunrise and sunset at a specific location occur when the solar elevation angle is zero (Meeus, 1998). Solving for the hour angle (H) at these times, results in:

$$\cos(H) = -\tan(\phi)\tan(\delta) \tag{2}$$

where:
- H is the solar hour angle,
- ϕ is the latitude of the location in degrees,
- δ is the solar declination from the previous equation (1).

Converting this equation, the hour angle at sunrise (H_{rise}) and sunset (H_{set}) results in:

$$H_{\mathrm{rise}} = -\cos^{-1}(-\tan(\phi)\tan(\delta)) \tag{3}$$

$$H_{\mathrm{set}} = \cos^{-1}(-\tan(\phi)\tan(\delta)) \tag{4}$$

3. Hour Angle at a Specific Time

The hour angle (H) is the measure of time since solar noon, expressed in degrees (Duffett-Smith and Zwart, 2011):

$$H = 15^\circ \times (S - 12) \tag{5}$$

where:
- 15° is the angular rotation of the Earth in one hour,
- S is the local solar time in hours.

4. Combining the equations

The hour angle equations (3) & (4) and the Specific Time equation (5) are set equal to each other and subsequently solved for the time (S) to find the exact times of sunrise and sunset:

$$S_{\mathrm{rise}} = 12 - \frac{H_{\mathrm{rise}}}{15} \tag{6}$$

$$S_{\mathrm{set}} = 12 + \frac{H_{\mathrm{set}}}{15} \tag{7}$$

5. Creating a Function Over Time

Expressing the above equations (6) & (7) as functions of the day of the year (t) requires to access t from the solar declination equation (1):

$$S_{\text{rise}}(t) = 12 - \frac{\cos^{-1}\left(-\tan(\phi)\tan\left(23.44° \times \sin\left(\frac{360}{365} \times (t-81)\right)\right)\right)}{15} \tag{8}$$

$$S_{\text{set}}(t) = 12 + \frac{\cos^{-1}\left(-\tan(\phi)\tan\left(23.44° \times \sin\left(\frac{360}{365} \times (t-81)\right)\right)\right)}{15} \tag{9}$$

where:

- ϕ is the latitude of the location in degrees,
- t is the day of the year, with January 1st as $t = 1$.

The resulting sunrise and sunset times will vary over time according to the relative position of the Earth to the Sun at a specific latitude (see Figure 7).

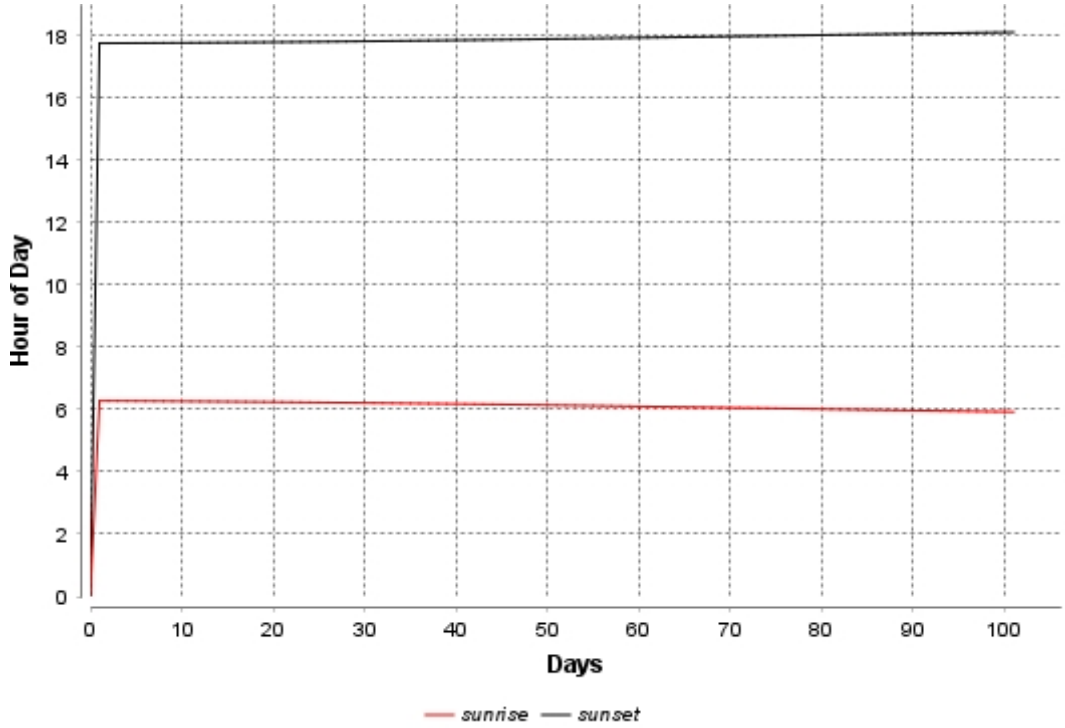

Figure 7: Example output of GAMA experiment for 100 cycles showing the variation of sunrise and sunset times.

6. Photoperiod & Normalisation

The photoperiod (P) of a given day is calculated by subtracting the sunrise time from the sunset time. Finally, the result is normalised with the optimal condition for spawning (see Table 8) which is 12.05 hours.

$$P_{\text{norm}}(t) = \frac{S_{\text{set}}(t) - S_{\text{rise}}(t)}{12.05} \tag{10}$$

Specific parameters to model solar cycle

The **latitude (ϕ)** for the coral reef at Bocas del Toro, Panama, is 9.3273°.

2.4.7.2 Lunar cycle

Calculating the lunar orbit is inherently complex due to several factors that affect the Moon's position. The Moon's elliptical orbit is inclined relative to the Earth's equator and is perturbed by the Sun and other gravitational influences (Meeus, 1998). Correspondingly, the positions of moonrise and moonset vary each day further complicating the exact calculation of lunar phases and illumination levels at specific times and locations (Duffett-Smith and Zwart, 2011).

To perform these calculations in the model would require simplifications of the astronomic equations. Consequently, this would induce systematic errors and high tolerances. To mitigate this error, historic lunar ephemeris data were downloaded from U.S. Naval Observatory (2024) which provides the daily results of the Moon's orbit and phases of a specific location on Earth. A subset of the original dataset structure can be seen in Appendix A.

Table 10: State variables (repetition marked with asterisk) and helper variables including their mathematical notation in equations to calculate the lunar cycle.

State Variable	Math	Identifier	Data Type	Unit
**Moonrise time*	-	`moonrise`	float	hours (decimal)
**Moonset time*	-	`moonset`	float	hours (decimal)
**Moonlight Dose*	-	`moonlightDose`	float	-
**Dark Time*	-	`darktime`	float	hours (decimal)
Ephemeris Matrix	-	`LunarEphemerisMatrix`	matrix	various
Ephemeris Map	-	`LunarEphemerisMap`	map	various
Indexer used to run through the map.	-	`indexer`	int	-
Moonshine (Midnight to Sunrise)	-	`moonshineMorning`	float	hours (decimal)
Moonshine (Sunset to Midnight)	-	`moonshineEvening`	float	hours (decimal)
Total Moonshine Duration	-	`moonshineDuration`	float	hours (decimal)
Yesterday's Sunset	-	`sunsetYesterday`	float	hours (decimal)
Fraction Illuminated from ephemeris data.	f	`f`	float	percent
Transit altitude from ephemeris data.	-	`altitude`	float	degrees
Moon-Earth Distance from ephemeris data.	d	`d1`	float	km
Phase Angle	α	`phaseAngle`	float	radians
Brightness of lunar disk.	B	`B`	float	-

** Table continued on next page*

State Variable	Math	Identifier	Data Type	Unit
Brightness normalisation factor	B_0	`B0`	float	-
Coefficient (m1) (Korokhin et al., 2007)	m_1	`m1`	float	-
Coefficient (rho) (Korokhin et al., 2007)	ρ	`rho`	float	-
Coefficient (m2) (Korokhin et al., 2007)	m_2	`m2`	float	-
Surface Roughness (h) (Korokhin et al., 2007)	h	`h`	float	-
Distance correction factor	D	`D`	float	-
Average Distance between Earth and Moon	-	`dAverage`	float	km
Atmospheric Correction	A	`A`	float	-
Zenith Angle	z	`zenithAngle`	float	degrees
Angle of Incidence	I	`I`	float	-
Relative Intensity	M	`M`	float	-

1. Moonrise and moonset times

The moonrise and moonset times (see Figure 8) are directly extracted from the ephemeris dataset.

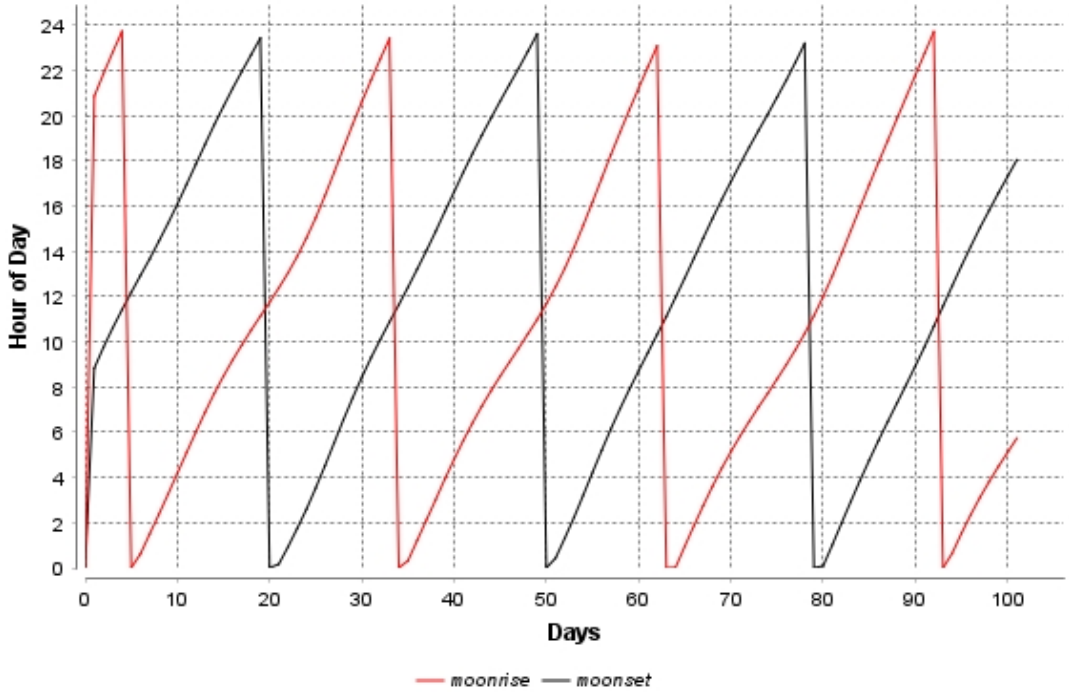

Figure 8: Example output of GAMA experiment for 100 cycles showing the variation of moonrise and moonset times during lunar phases.

2. Moonlight intensity

Traditional measures using the moon phase (or fraction of the moon illuminated) as a proxy for moonlight intensity are insufficient because they fail to account for the nonlinear relationship between the illuminated fraction and actual intensity on the ground (Śmielak, 2023). For instance, a full moon is not only double but six times brighter than a half-moon, emphasising the clear distinction of full moon days (see Figure 9).

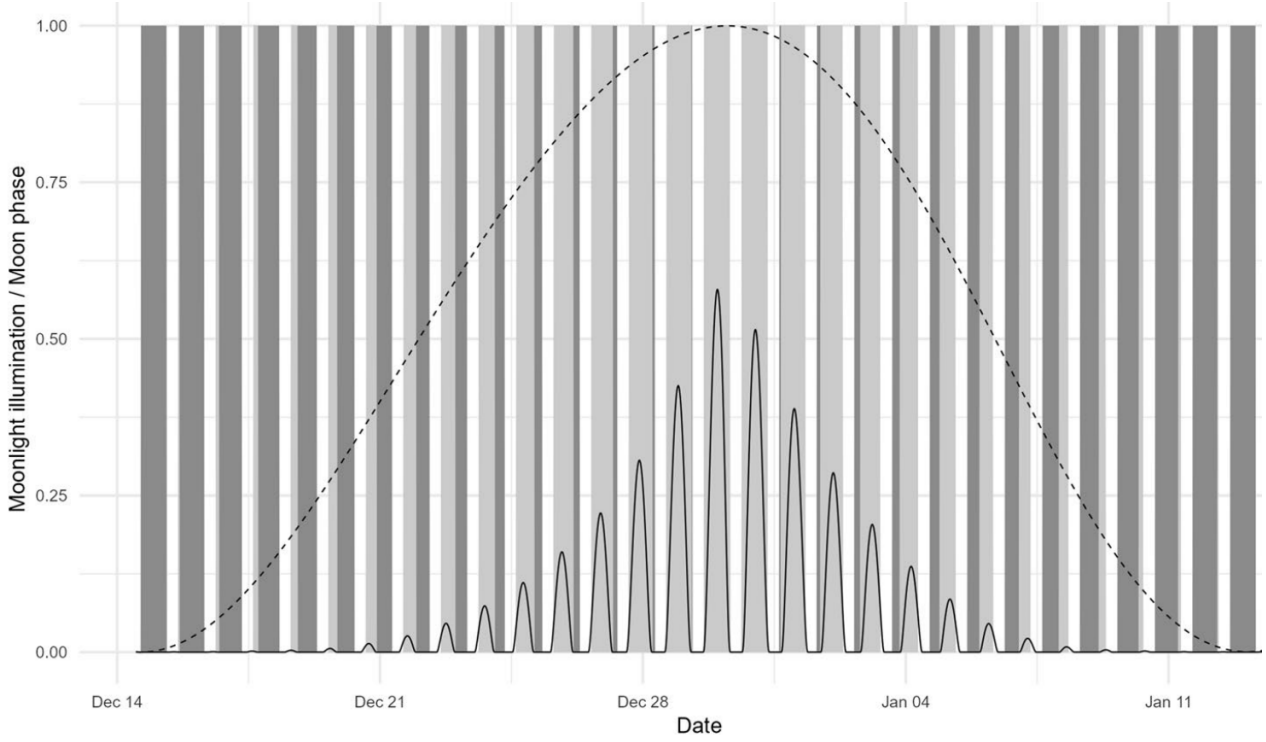

Figure 9: Reprinted from Śmielak (2023), p. 3, under the terms of the Creative Commons Attribution 4.0 International License. The original caption reads: "Lunar phase (dashed line) and moonlight intensity on the ground (solid line). Grey bars in the background represent night, with light grey representing parts of the night when the moon is visible and dark grey representing parts of the night when there is no moonlight."

According to Austin et al. (1976), two main factors influence the intensity of moonlight reaching the Earth's surface at any given time. The first is the Moon's intrinsic brightness and its distance from Earth, which determine the amount of light entering the Earth's atmosphere. The second factor is the Moon's altitude in the sky, as atmospheric refraction and absorption reduce the moonlight reaching the ground. Additionally, the angle of incidence at which moonlight strikes the ground further affects illumination levels (Meeus, 1998). Following is the proposal by Śmielak (2023) to include these influences into a final equation for relative moonlight intensity (M).

$$M = B \times D \times A \times I \tag{11}$$

where:
- B is the lunar disk brightness,
- D is the correction for the distance to the moon,
- A is the correction for atmospheric extinction,
- I is the correction for the angle of incidence.

B - Lunar Disk Brightness

As mentioned before, the brightness of the lunar disk does not vary proportionally with the Moon's phases due to the complexity of its reflection properties, such as opposition surge, surface roughness, wavelength-dependency, etc. (Korokhin et al., 2007; Buratti et al., 1996). The crucial variable is the amount of reflected sunlight, i.e. the Moon's albedo.

Further astronomic calculations require the the lunar phase angle (α) which is acquired by the conversion of an equation by Meeus (1998) to calculate the fraction of the moon illuminated (f) :

$$f = \frac{1 + \cos(\alpha)}{2} \times \frac{\pi}{180} \quad \Longrightarrow \quad \alpha = \arccos(2f - 1) \times \frac{\pi}{180} \tag{12}$$

where:
- f is the fraction of the moon illuminated from the lunar ephemeris data,
- α is the phase angle,
- $\frac{\pi}{180}$ converts the angle from degrees to radians for the calculation of the Moon's equigonal albedo.

The Moon's albedo is calculated as equigonal albedo $A_{eq}(\alpha)$ and has been standardised in a study by Korokhin et al. (2007):

$$A_{eq}(\alpha) = m_1 e^{-\rho\alpha} + m_2 e^{-h\alpha} \tag{13}$$

where:
- α is the phase angle calculated in equation (12),
- m_1 and m_2 are coefficients,
- ρ is the coefficient of an additional phase slope appearing at relatively small phase angles,
- $h = 0.7$ mean roughness factor of the Moon's landscape.

The three coefficients (m_1, m_2 and ρ) are dependent on wavelength of the reflected light (Korokhin et al., 2007). Coral research showed that moonlight in the blue spectrum (around 480 nm) is effective in regulating coral spawning cycles, making it the most accurate wavelength for studying the impact of lunar light on corals (Levy et al., 2007; Gorbunov and Falkowski, 2002). Therefore, the closest wavelength from Korokhin et al. (2007) is 501.2 nm, resulting in the following coefficients:
- $m_1 = 0.308$,
- $m_2 = 0.877$,
- $\rho = 4.862$.

The lunar disk brightness (B) changes over time, as the fraction of the moon illuminated (f) and thus the phase angle (α) varies:

$$B(\alpha) = B_0 \times A_{eq}(\alpha) \tag{14}$$

where:
- B_0 is a normalisation constant (set to 1) representing the brightness of an average full moon.

D - Distance to the Moon

The average distance between the Earth and the Moon (D) is 384 400 km, ranging from 357 000 km to 407 000 km (Meeus, 1998). This variation causes a difference of up to 30 % in moonlight bright-

ness between perigee (the closest point) and apogee (the farthest point), due to the inverse square relationship of the light propagation with distance.

$$D(t) = \left(\frac{d(t)}{384400}\right)^{-2} \tag{15}$$

where:
- d is the distance between the moon and the Earth at time t (in days) from the lunar ephemeris dataset.

A - Atmospheric Extinction

Moonlight travelling through the atmosphere will be scattered, refracted, and absorbed (Meeus, 1998). The lower the Moon's altitude in the sky, the longer the distance where moonlight travels through the atmosphere, reducing the intensity of light reaching the surface. This atmospheric extinction (A) is calculated as follows (Duffett-Smith and Zwart, 2011).

$$A = 10^{-0.4\left(\frac{0.2}{\cos z}\right)} \tag{16}$$

where:
- $10^{-0.4x}$ converts a stellar magnitude to a proportion (Meeus, 1998),
- z is the zenith angle, defined as $z = 90° - altitude$ (the altitude is from the lunar ephemeris dataset),
- 0.2 is the assumption of an average extinction coefficient per air mass (Duffett-Smith and Zwart, 2011).

I - Angle of Incidence

When the Moon is in the zenith (a 90° altitude), the angle of incidence is 0°, meaning that the light is scattered over the smallest surface area. As the angle of incidence increases, the surface area illuminated increases, and the moonlight intensity decreases (Śmielak, 2023).

$$I = \sin(z) \tag{17}$$

where:
- z is the zenith angle, defined as $z = 90° - altitude$ (the altitude in in the lunar ephemeris dataset).

3. Moonlight Dose

The moonlight dose (see Figure 10) is defined here as a normalisation of the moonlight intensity (B) from equation (11) using the amount of time the Moon is visible at night (see Figure 10). All calculations are made for a day lasting from midnight to midnight. Therefore, the visibility in the morning and in the evening have to be summed up. Following scenarios define the calculations.

1. Midnight to Sunrise:
   - If the moon is visible at midnight and moonset occurs after sunrise:
     Calculate the time from midnight to sunrise.
   - If the moon is visible at midnight, and moonset occurs before sunrise:
     Calculate the time from midnight to moonset.
   - If moonrise occurs before sunrise:
     Calculate the time from moonrise to sunrise.

2. Sunset to Midnight:
   - If moonrise occurs after sunset:
     Calculate the time from moonrise to midnight.
   - If moonrise occurs before sunset and moonset is the next day:
     Calculate the time from sunset to midnight.
   - If moonrise occurs before sunset and moonset is between sunset and midnight:
     Calculate the time from sunset to moonset.

Finally, the daily moonshine hours is the sum of the moonshine time from midnight to sunrise and sunset to midnight.

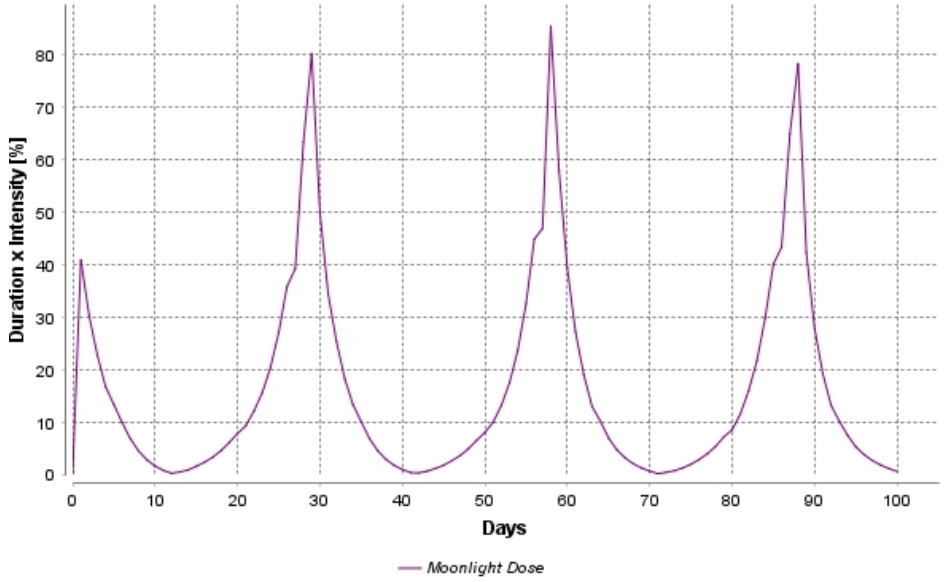

Figure 10: Example output of GAMA experiment for 100 cycles showing the moonlight dose.

4. Dark Time

Dark Time defines the duration between sunset and moonrise. It further includes the duration between midnight and sunrise in the morning (see Figure 11).

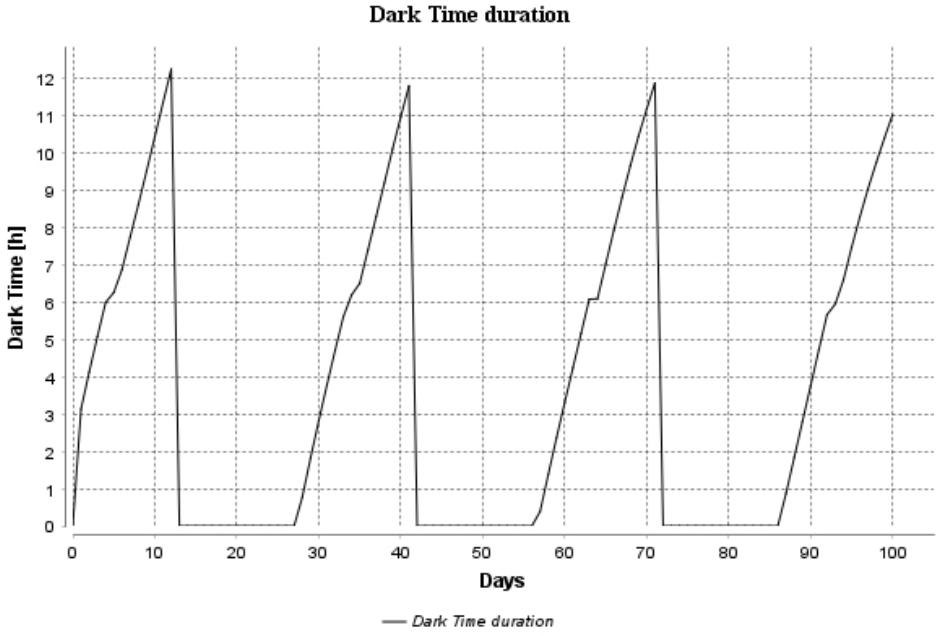

Figure 11: Example output of GAMA experiment for 100 cycles showing the dark time.

2.4.7.3 Sea water temperature

Sea water temperature at Bocas del Toro varies due to seasonal changes, ocean currents, and atmospheric conditions (Kaufmann and Thompson, 2005). A sinusoidal function provides a useful first-order approximation for the seasonal cycle of solar radiation (see Figure 12). This approach is commonly used in climate modelling to represent periodic phenomena like seasonal temperature changes (Thomson, 1995).

Table 11: State variables (repetition marked with asterisk) and helper variables including their mathematical notation in equations to calculate the sea water temperature cycle.

State Variable	Math	Identifier	Data Type	Unit
**Mean annual water temperature*	T_{mean}	`TEMP_MEAN`	float	°C
**Min annual water temperature*	-	`TEMP_MIN`	float	°C
**Max annual water temperature*	-	`TEMP_MAX`	float	°C
**Summer amplitude*	A_summer	`amplitudeSummer`	float	°C
**Winter amplitude*	A_winter	`amplitudeWinter`	float	°C
**Normalised water temperature*	T_{norm}	`waterTemp`	float	-
Phase shift to day of lowest annual sea water temperature (Kaufmann and Thompson, 2005).	ϕ	`LOWEST_TEMP_DAY_SHIFT`	float	days
Sinus Angle inside sea water temperature function.	-	`sinAngle`	float	degrees
Sea Water Temperature	T	`waterTemp`	float	°C

For the summer season, when the sine value is positive:

$$T(t) = T_{\text{mean}} + A_{\text{summer}} \cdot \sin\left(\left(\frac{2\pi(t-\phi)}{T_{\text{year}}}\right) \times \left(\frac{180}{\pi}\right)\right) \tag{18}$$

For the winter season, when the sine value is negative:

$$T(t) = T_{\text{mean}} + A_{\text{winter}} \cdot \sin\left(\left(\frac{2\pi(t-\phi)}{T_{\text{year}}}\right) \times \left(\frac{180}{\pi}\right)\right) \tag{19}$$

Final normalisation with the optimal condition for spawning (see Table 8) which is 31.42 °C:

$$T_{\text{norm}}(t) = \frac{T(t)}{31.42} \tag{20}$$

where:
- $T(t)$ is the water temperature at time t (in days),
- T_{mean} is the mean annual temperature,
- A_{summer}: amplitude of the temperature variation during summer,

- A_{winter}: amplitude of the temperature variation during winter,
- t is the day of the year, with January 1st as $t = 1$,
- T_{year} is the period of the function, here 365 days,
- ϕ is the phase shift, aligning the sine function to the measured temperature changes,
- $\frac{180}{\pi}$ converts the angle from radians to degrees as expected by the GAML trigonometric functions.

Specific parameters to model water temperature

These values are derived from long-term data by Kaufmann and Thompson (2005) who between 1999 and 2004 monitored physical conditions around Bocas del Toro, Panama. The designated location is labelled as "Isla Colón Coral Reef". The values are taken from the mean of the 4m depth because the mean depth of the observed corals by Levitan et al. (2011) is 5.3m.

1. **sea water temperature values:** $T_{\text{mean}} = 28.6°\text{C}$, $T_{\text{min}} = 26.6°\text{C}$, $T_{\text{max}} = 30.5°\text{C}$.
2. The **Amplitude (A)** is calculated as the difference between the mean and the minimum or maximum temperature.
3. **Phase Shift (ϕ)** The phase shift adjusts the timing of the maximum and minimum temperatures to match the observed seasonal pattern. The mean temperatures peak in May or June and reach lows in December or January (Kaufmann and Thompson, 2005). Assuming a simple sinusoidal model, the mean temperature would be reached roughly halfway between these extremes and results in a ϕ of 182 days.

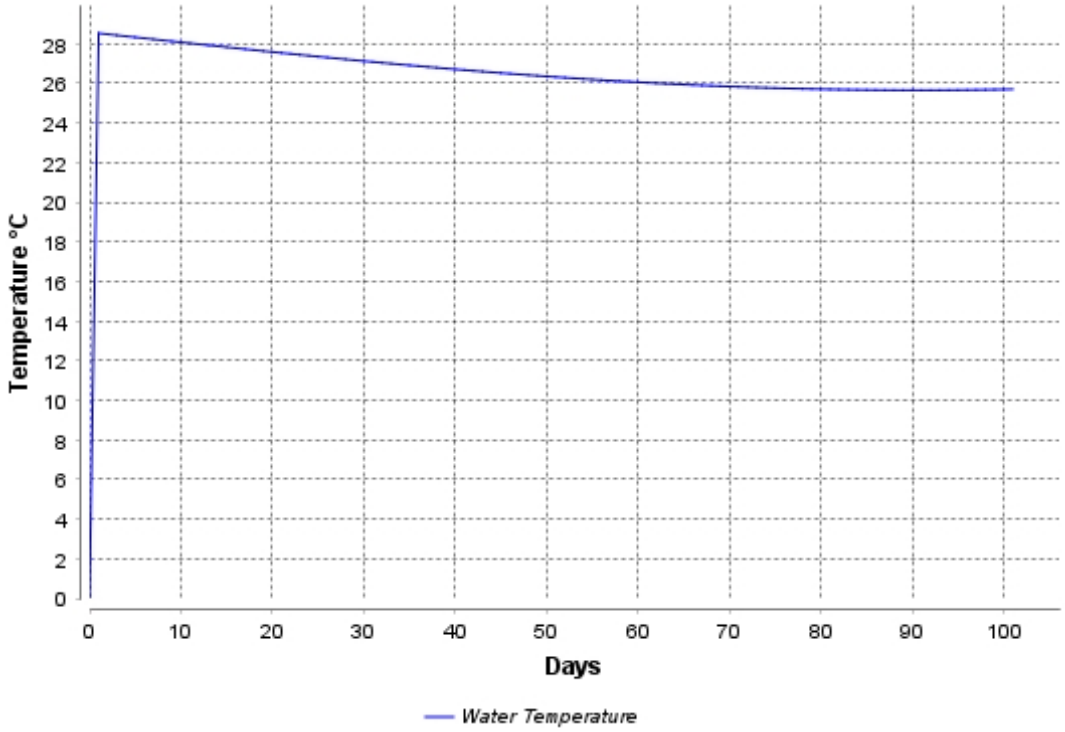

Figure 12: Example output of GAMA experiment for 100 cycles showing the water temperature.

2.4.7.4 Spawning

The spawning submodel defines how the spawning readiness (R) of the coral agent is influenced by large-scale environmental factors and fine-scale inter-agent communication (see Figure 13). A detailed description was given in chapter 2.4.4.7 *Sensing*.

Table 12: State variables (repetition marked with asterisk) and helper variables including their mathematical notation in equations to calculate the spawning readiness of a coral.

State Variable	Math	Identifier	Data Type	Unit
**Spawning event has started.*	-	`isReefSpawning`	bool	true/false
**Spawning readiness of coral agent.*	R	`spawnReadiness`	float	-
**Reproductive variability.*	V	`reproductiveVar`	float	-
Hard-coded list of observed spawning dates for each year.	-	`OBSERVED_SPAWNING_DATES`	map	dates
Number of corals that have not spawned yet.	-	`coralsNotSpawned`	int	count
Weight of temperature influence on corals.	w_T	`weightTemperature`	float	-
Weight of photoperiod influence on corals.	w_P	`weightPhotoperiod`	float	-
Weight of moon dose influence on corals.	w_M	`weightMoonDose`	float	-
Weight of darktime influence on corals.	w_D	`weightDarktime`	float	-
Factor to calculate dynamic weights.	$\bar{R}$	`unreadyFactor`	float	-
Dynamic temperature weight.	w'_T	`dynamicWeightTemperature`	float	-
Dynamic photoperiod weight.	w'_P	`dynamicWeightPhotoperiod`	float	-
Dynamic moon dose weight.	w'_M	`dynamicWeightMoonDose`	float	-
Counts the minutes after spawning start	-	`spawningDuration`	int	minutes
Day difference of simulated spawning to OBSERVED_SPAWNING_DATES	-	`dayDifference`	int	days

1. Gametogenesis Initiation

For many coral species, gametogenesis is initiated (start of stage II in Figure 3) as water temperatures decline during the winter months (Sorek and Levy, 2014).

Model implementation. Accordingly, the modelled initiation of gametogenesis begins on the first day of the year, together with the start of the simulation.

2. Development Phase

The development phase of coral gametogenesis (stage II - IV in Figure 3) encompasses several months of gamete growth within the coral polyps (Mendes, 2002). The accumulation of spawning readiness (R) increases as the environment approaches optimal spawning conditions (see Table 8).

Model implementation. Sea water temperature and photoperiod are the main drivers when the gametogenesis starts (Nozawa, 2012). To implement an increasing influence of the moonlight, the triggers are modelled using dynamic weights. This approach allows moonlight dose to have an increasing influence as spawning readiness nears completion, reflecting its role to specify the spawning day (Levy et al., 2007; Gorbunov and Falkowski, 2002).

For every timestep t (in days), the dynamic weights are calculated as:

$$w'_T(t) = \bar{R}(t) \cdot w_T, \quad w'_P(t) = \bar{R}(t) \cdot w_P, \quad w'_M(t) = (1 - \bar{R}(t)) \cdot w_M \tag{21}$$

where:
- w'_T, w'_P, and w'_M are the dynamic weights for temperature, photoperiod, and moonlight dose,
- $\bar{R}$ is the unready factor (opposite of spawning readiness), calculated as $\bar{R} = \frac{100-R}{100}$,
- w_T, w_P, and w_M are the calibrated weights for temperature, photoperiod, and moonlight dose.

Accordingly, the spawning readiness (R) is updated as:

$$R(t) = R(t-1) + w'_T(t) \cdot T(t) + w'_P(t) \cdot P(t) + w'_M(t) \cdot M(t) + V \tag{22}$$

where:
- $T(t)$ is the temperature at time t,
- $P(t)$ is the photoperiod (daylight hours) at time t,
- $M(t)$ is the moonlight dose at time t,
- V is the reproductive variability, randomly assigned to a coral agent.

3. Maturation Phase

The maturation phase is the final stage of gametogenesis (stage V in Figure 3), during which the coral's gametes reach full maturity and the coral becomes ready to spawn. During this phase, the egg volume increases in a relatively short time. This phase is heavily influenced by the lunar cycle (Levy et al., 2007; Gorbunov and Falkowski, 2002).

Model implementation. The gametogenesis enters the maturation phase as soon as the spawning readiness reaches 90%. Now the spawning readiness (R) increases based only on moonlight dose.

$$R(t) = R(t-1) + w_M \cdot M(t) + V \tag{23}$$

where:
- $M(t)$ is the moonlight dose at time t,
- w_M is the calibrated weight for moonlight dose,
- V is the reproductive variability, randomly assigned to a coral agent.

4. Spawning Trigger

Stage VI is the day of spawning where the gametes are released and the spawning cycle ends (Figure 3). Darktime has a strong influence on the exact moment of spawning (Lin et al., 2021). The spawning of *O. franksi* observed by Levitan et al. (2011) happened approximately two hours after sundown, i.e. when the darktime duration was 1.97 hours (decimal). This value is calculated from the average of individual spawning times over all observed years. However, it is important to notice that the total darktime duration for these spawning days range between 4.15 and 5.91h (see Table 8).

Model implementation. The coral agent is ready to spawn as spawning readiness crosses 98%. Now the spawning readiness (R) increases only based on the darktime duration.

$$R(t) = R(t-1) + w_D \cdot D(t) \tag{24}$$

where:
- w_D is the calibrated weight for moonlight dose,
- $D(t)$ is the darktime duration at time t.

5. Spawning Event

When the first coral agent reaches a readiness level of 100%, the discrete event of spawning happens. The simulation switches from phase A to phase B (see Figure 6). The cycle duration switches from days to minutes. Accordingly, the update of environmental factors stops. It is important to note that this is the calibration and validation point of the model (see Figure 16). Subsequently, coral agents with a readiness level equal or above 90% will increase their spawning readiness according to the communication scenarios described in the following submodels.

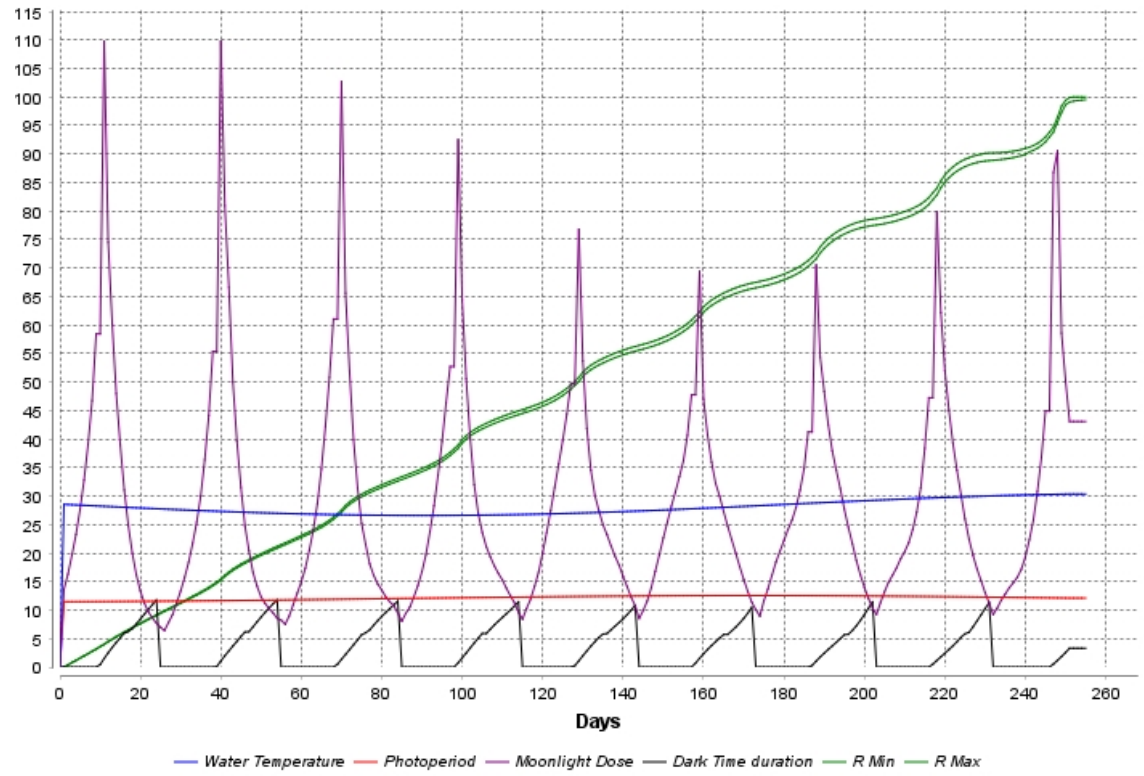

Figure 13: Example output of a GAMA experiment for the year 2002 showing the changes of all environmental factors over time and, in green, the spawning readiness (min and max) increasing due to the influence of the factors.

2.4.7.5 No-communication model

The no-communication model simulates a spawning coral reef with no inter-agent communication.

Table 13: State variables (repetition marked with asterisk) and helper variables including their mathematical notation in equations to simulate the no-communication scenario.

State Variable	Math	Identifier	Data Type	Unit
**Spawning readiness of coral agent.*	R	`spawnReadiness`	float	-
**Reproductive variability.*	V	`reproductiveVar`	float	-
Spawning factor for phase B.	-	`spawnFactor`	float	-

Model implementation. The simulated reef must achieve an identical total spawning duration as the real-world coral reef. To achieve this, the `spawnFactor` is implemented controlling the increase of spawning readiness during the spawning event. Note that for each spawning day, the `spawnFactor` must be calibrated separately (see Table 17).

The spawning readiness (R) increases linearly according to the coral's individual reproductive variability (V).

$$R(t) = R(t-1) + \texttt{spawnFactor} \cdot V \tag{25}$$

where:
- R is the spawning readiness,
- `spawnFactor` is calibrated to simulate the real-world spawning duration,
- V is the reproductive variability, randomly assigned to a coral agent.

2.4.7.6 Communication model

The communication model simulates how neighbouring coral agents influence the spawning readiness. The proximity to neighbours and the difference in spawning readiness both define how a coral agent evaluates this influence. Thus, the fine-scale spawning pattern emerges from this spatially distributed communication.

Table 14: State variables (repetition marked with asterisk) and helper variables including their mathematical notation in equations to calculate to simulate the communication scenario.

State Variable	Math	Identifier	Data Type	Unit
**Spawning readiness of coral agent.*	R	`spawnReadiness`	float	-
Communication signal decay.	k	`distanceDecay`	float	-
Communication factor for Scenario 2.	-	`commFactor`	float	-
Weight of communication influence on corals.	-	`weightComm`	float	-

** Table continued on next page*

State Variable	Math	Identifier	Data Type	Unit
Distance to the neighbouring coral.	$d_{\text{neighbour}}$	`distanceNeighbour`	float	m
Difference between readiness levels.	-	`differenceReady`	float	-
Influence of neighbour.	F	`influence`	float	-

Model implementation. The exponential decay function simulates the decreasing influence of a neighbour with increasing spatial distance. The neighbourhood distance decay factor, k, determines the spatial extent of influence corals have on each other (influence attenuation). Higher k values (closer to 1) indicate that only very close neighbours affect each other, whereas lower k values (closer to 0) extend the communication range, allowing corals to influence others at greater distances (see Figure 14).

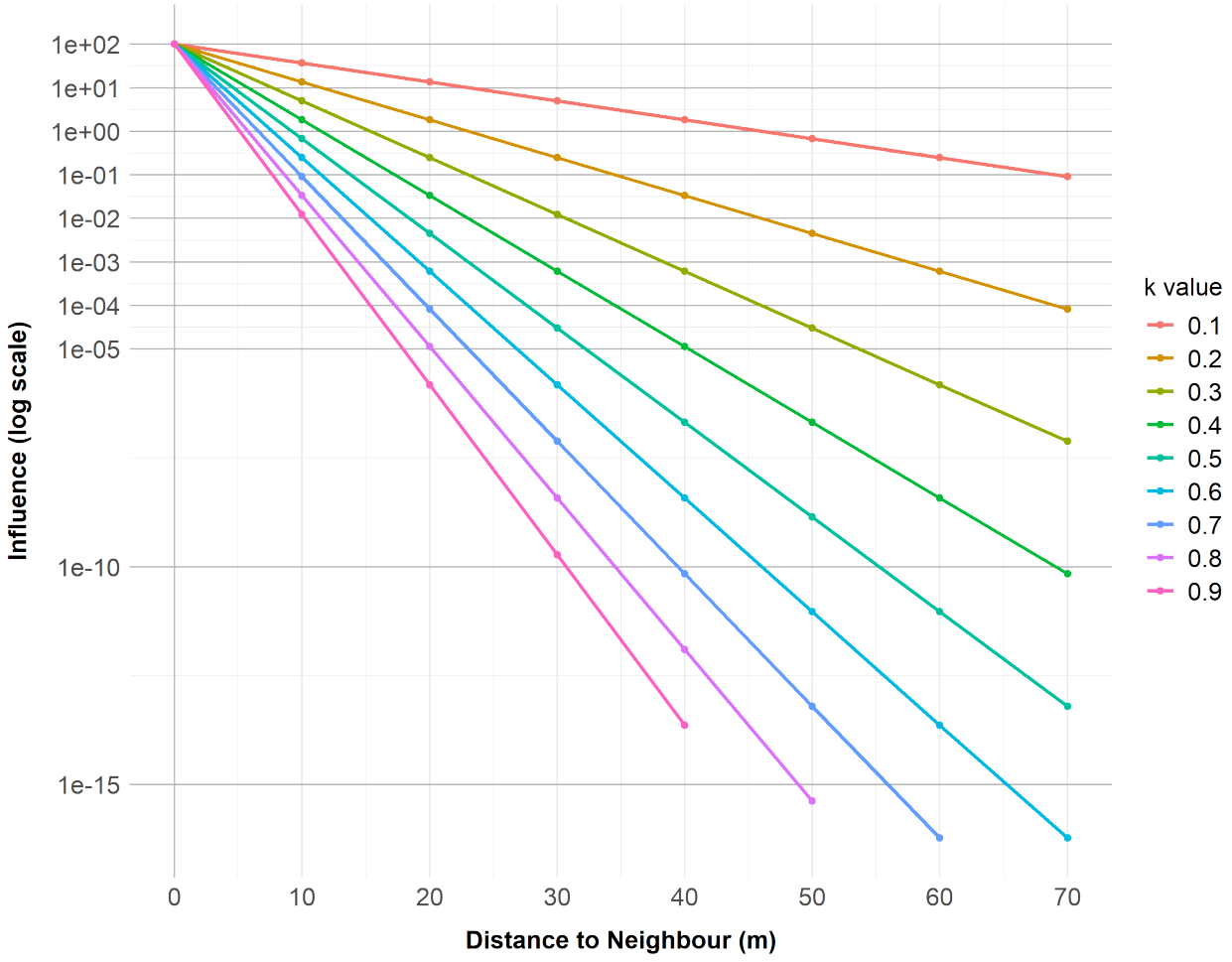

Figure 14: Influence decay over distance for different values of k from a test setup in GAMA. Influence values were derived from a fixed readiness difference of 100 between a tested coral (readiness = 0) and neighboring corals (readiness = 100), spaced at 10 m intervals. The y-axis is plotted on a log scale to common for exponential functions.

The influence (F) is the sum of all neighbours' influence on a coral's spawning readiness.

$$F = \sum_{i=1}^{N} \Delta R_i \cdot \exp\left(-k \cdot d_{\text{neighbour},i}\right) \tag{26}$$

where:
- i is the index of each neighbour,
- N is the total number of neighbours,
- $\Delta R_{\text{i}} = R_{\text{neighbour}} - R_{\text{self}}$ is the difference in spawning readiness,
- k is the exponential decay constant,
- $d_{\text{neighbour,i}}$ is the distance between the corals.

The no-communication equation (25) acts as a base maintaining the `spawnFactor` as a calibrated value for each spawning day. For this communication scenario, the equation is expanded where the communication influence (F) is multiplied with a communication factor (`commFactor`). This communication factor will be the new variable to calibrate the total spawning duration, similar to the `spawnFactor` in the no-communication scenario. The balance between the two parts is regulated with the communication weight wC, valued between 0 and 1, and its antagonist $(1 - wC)$. The introduction of this balance is necessary to gain control over how strong the communication influence acts on the coral agent compared to the no-communication influence (see Figure 15).

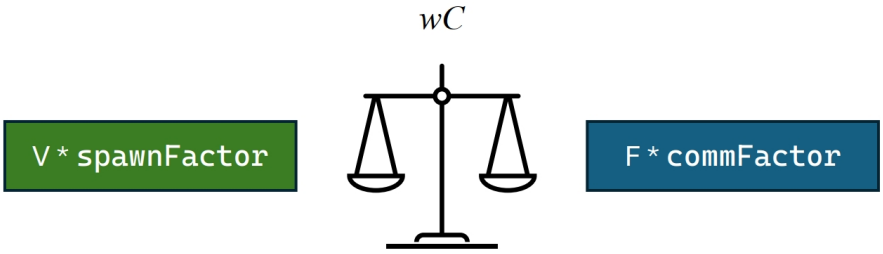

Figure 15: Infographic to visualise the use of wC as balancing weight between the linear increase of no-communication (green) and the influence of coral communication (blue).

$$R(t) = R(t-1) + V \cdot (\texttt{spawnFactor} \cdot (1 - wC)) + F \cdot \texttt{commFactor} \cdot wC \tag{27}$$

where:
- R is the spawning readiness,
- V is the reproductive variability, randomly assigned to a coral agent,
- `spawnFactor` as it was calibrated during the no-communication scenario,
- wC and $(1 - wC)$ are the balancing weights between communication and no-communication,
- `commFactor` is calibrated to simulate the real-world spawning duration.

3 Calibration and validation

The calibration and validation of the model is partitioned into phase A, the large-scale spawning synchronisation according to the environmental factors, and phase B, the fine-scale synchronisation of spawning times by individual corals (see Figure 16). The environmental model has been calibrated and validated to the real-world spawning days. Subsequently, phase B is based on this validated framework. To create output with comparable clustering results, the (no)-communication scenarios are calibrated to achieve similar spawning durations like the real-world reef.

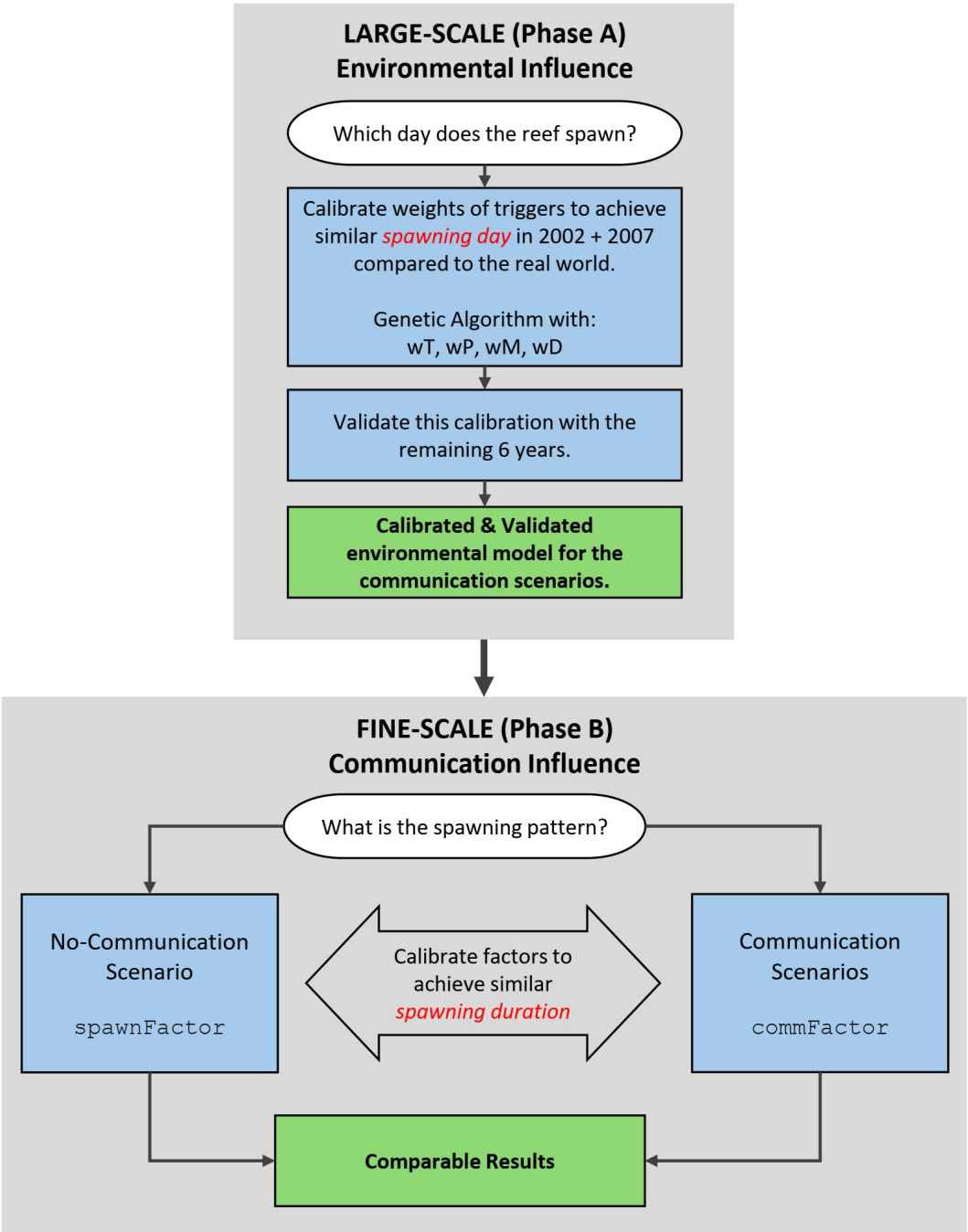

Figure 16: Calibration and validation plan showing how the validated environment is created and the how the communication scenarios are calibrated to achieve comparable results. Visualisation created with Modelio Version 5.4.01 (Modelio.org, 2023).

3.1 Baseline: the real world

The baseline scenario presents real-world measurements of *O. franksi* spawning days from 2002 to 2009 by Levitan et al. (2011). The resulting value of spawning duration (see Table 15) will aid to calibrate the scenarios ensuring comparable spawning times for the final spatiotemporal pattern analysis.

Table 15: Real-world spawning durations. The three marked spawning days are chosen for further investigation in the communication scenarios.

Real-world Spawning Date	**Spawning Day**	**Spawning Duration (min)**
2002, 27. Sept	1	67
2003, 15. Sept	1	62
2003, 16. Sept	2	71
2004, 04. Sept	1	72
2004, 05. Sept*	2	157
2005, 23. Sept	1	83
2005, 24. Sept	2	104
2006, 12. Sept	1	15
2006, 13. Sept	2	161
2007, 2. Sept	1	43
2007, 3. Sept	2	61
2008, 20. Sept	1	61
2008, 21. Sept*	2	53
2009, 09. Sept*	1	73
2009, 10. Sept	2	99

The Global Moran's I analysis of the baseline scenario revealed Moran's I global values ranging from -0.12 to 0.36, indicating varying degrees of spatial autocorrelation (see Figure 17). The highest positive correlation was observed on 21 September 2008 (Moran's I = 0.36, Z-score = 5.15), suggesting significant clustering, while the lowest value appeared on 12 September 2006 (Moran's I = -0.12, Z-score = -0.39), indicating spatial dispersion.

Three Z-scores indicated significant positive spatial clustering on 21 September 2008 (Z-score = 5.15), 9 September 2009 (Z-score = 4.83), and 5 September 2004 (Z-score = 3.26). These Z-scores exceed the ±1.96 threshold for a 95% confidence level, confirming that clustering on these dates is unlikely to be random. These dates were selected for further analysis of coral spawning patterns.

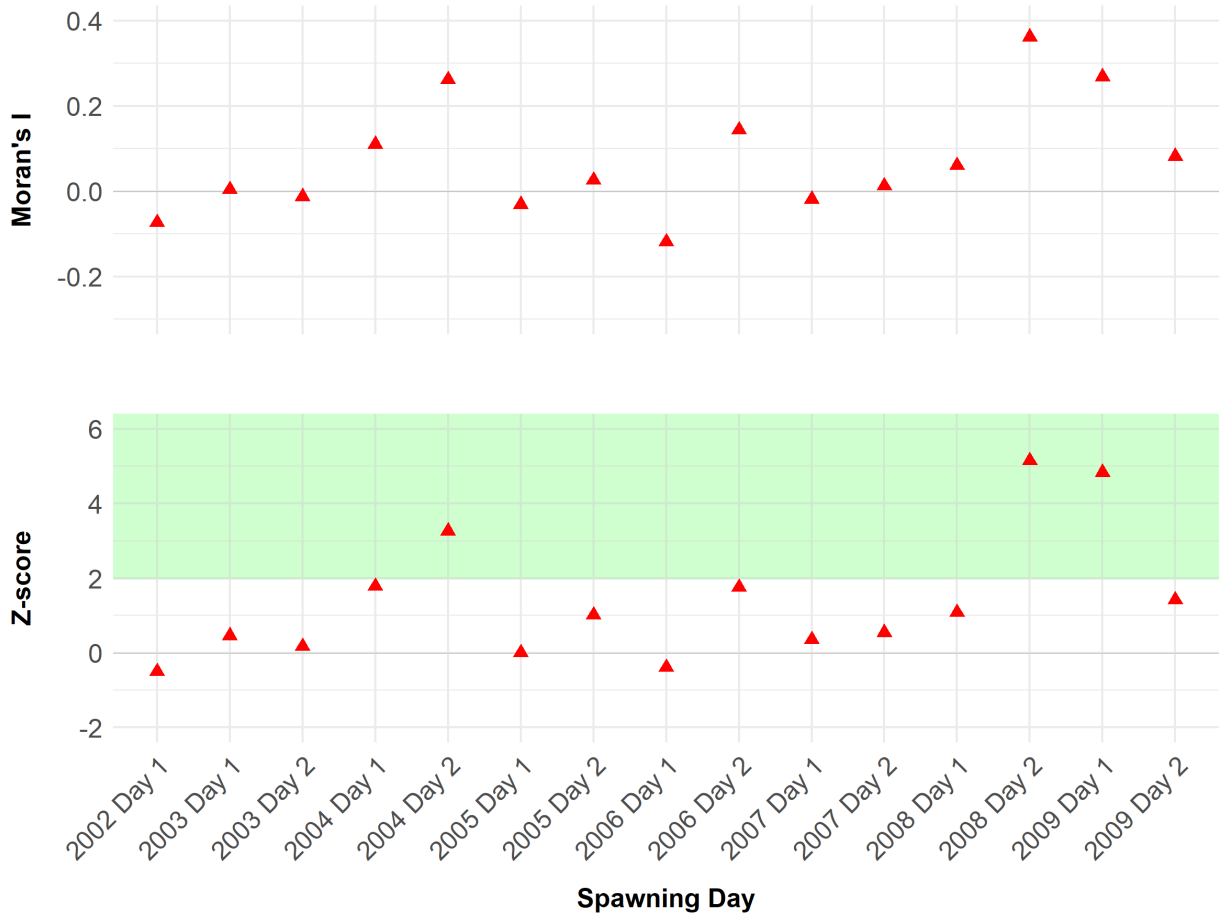

Figure 17: Spatial analysis results for the real-world data by Levitan et al. (2011). The figure displays the mean Moran's I values and Z-scores (red triangles) of all spawning days. The green area indicates the ±1.96 threshold for a 95% confidence level.

3.2 Large-scale calibration

To ensure the spawning readiness model accurately reflects real-world timing, the environmental weights wT (temperature), wP (photoperiod), wM (moonlight dose), and wD (dark time) were calibrated.

Calibration Data Selection. The years 2002 and 2007 were selected as calibration benchmarks due to their differences in spawning day, where the 3rd of September 2007 represents the earliest observed spawning date and the 27th of September 2002 the latest (see Table 8). Calibrating the model for these years presents a challenge: without precise weight values, the model can trigger spawning one full moon too early or too late.

Genetic Algorithm Calibration. The genetic algorithm (GA) implemented in GAMA was chosen for its ability to test the range of multiple parameters at the same time and locating optimal solutions that fit the target spawning dates (GAMA Platform, 2024). By iteratively adjusting the four weight variables, the GA searched for weight combinations that minimise the difference between the simulated spawning date and the observed spawning date in both calibration years.

Firstly, a broad range of weights with large steps was chosen to evaluate an approximate average value. Afterwards, the finer GA setup was as follows:

```
experiment GeneticAlgorithm type: batch repeat: 5 keep_seed: false until: (
    isReefSpawning = true) {
   parameter "wT" var: wT min: 0.20 max: 0.22 step:0.005;
   parameter "wP" var: wP min: 0.20 max: 0.22 step:0.005;
   parameter "wM" var: wM min: 0.17 max: 0.18 step:0.005;
   parameter "wD" var: wD min: 0.19 max: 0.21 step:0.005;

   method genetic maximise: -abs(day_of_year(current_date) - day_of_year(
       OBSERVED_SPAWNING_DATES[spawningYear]))
   pop_dim: 50 crossover_prob: 0.8 mutation_prob: 0.1    max_gen: 100;
   reflex save_output{
      save [spawningYear, spawningDay, dayDifference,wT, wP, wM, wD]
      to: "file.csv" format:"csv" rewrite:false;}}
```

The value combinations which led to the closest fitting spawning day compared to the real world dates were filtered and analysed (see Figure 18). The averages of these results serve as the calibrated weight values for the model:

- wT (temperature) = 0.209
- wP (photoperiod) = 0.21
- wM (moonlight dose) = 0.175
- wD (dark time) = 0.2

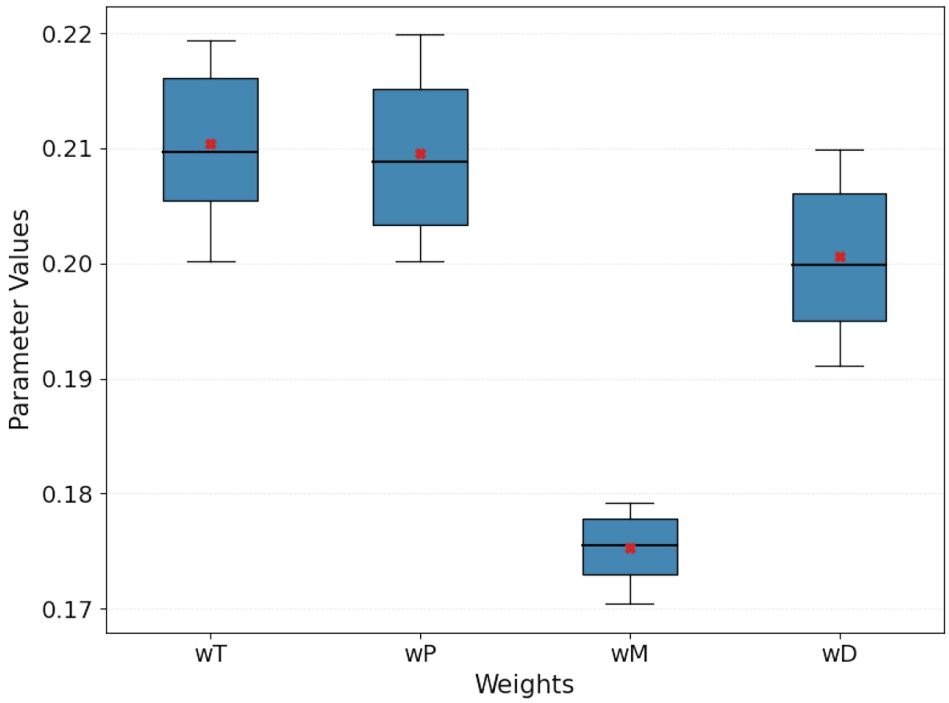

Figure 18: Weight values of wT, wP, wM and wD which result in the similar spawning date as the calibration dataset of 2004 and 2007. n = 230. The boxplot shows the median (horizontal line), the mean (red cross), the 1st and the 3rd quartile (box start/end) and 1.5 times the interquartile range (whiskers).

3.3 Large-scale validation

The validation of the model compared the simulated spawning dates against real-world spawning dates for the years 2002-2009. The two calibration years 2002 and 2007 have been included for additional verification. A batch of 100 simulations for each year were performed in GAMA and the mean difference between simulated and observed spawning dates (`dayDifference`) extracted.

```
experiment ValidationBatch type: batch repeat: 100 keep_seed: false until: (
    isReefSpawning = true) {
   parameter "spawningYear" var: spawningYear among: [2002, 2003, 2004, 2005, 2006,
       2007, 2008, 2009];
   parameter "spawningDay" var: spawningDay among: [1, 2];

   reflex save_output {
      save [spawningYear, spawningDay, simulations mean_of each.dayDifference]
      to: "file.csv" format: "csv" rewrite: false;}}
```

A `dayDifference` of zero indicates perfect alignment with the real-world spawning date, while negative values signify that spawning occurred either earlier or later than observed. Table 16 shows the average `dayDifference` across the years.

Table 16: Validation results for the spawning date. The years in blue (2002 and 2007) were used for calibration.

Real-world Spawning Date	Spawning Day	Mean Difference (days)
2002, 27. Sept	1	-2
2003, 15. Sept	1	-3
2003, 16. Sept	2	-4
2004, 04. Sept	1	0
2004, 05. Sept	2	-1
2005, 23. Sept	1	-3
2005, 24. Sept	2	-3.9
2006, 12. Sept	1	-1
2006, 13. Sept	2	-2
2007, 2. Sept	1	+0.7
2007, 3. Sept	2	0
2008, 20. Sept	1	-2
2008, 21. Sept	2	-3
2009, 09. Sept	1	-1
2009, 10. Sept	2	-2

The model predicts spawning dates with an average deviation of 1.8 days ranging from -4 to +0.7 day across the six validated years. Known coral spawning calendars by several research institutes publish with a prediction accuracy of 2-4 days (ORE, 2024). Compared to these calendars the model captures the temporal dynamics of coral spawning with a reasonable degree of accuracy.

3.4 Fine-scale calibration: communication scenarios

3.4.1 Scenario 1: no-communication (null hypothesis)

This scenario assumed that corals do not communicate, and the only factor contributing to differences in spawning time was the stochastic variability in reproduction strength (`reproductiveVar`). The spawning factor (`spawnFactor`) was calibrated for each spawning day to replicate the duration of spawning observed on the real reef (see Table 17).

Table 17: Calibrated Spawning factor values for the no-communication scenario.

Real-world Spawning Date	**Spawning Day**	`spawnFactor`
2002, 27. Sept	1	3.025
2003, 15. Sept	1	10.250
2003, 16. Sept	2	9.700
2004, 04. Sept	1	18.000
2004, 05. Sept	2	7.166
2005, 23. Sept	1	5.200
2005, 24. Sept	2	3.000
2006, 12. Sept	1	22.200
2006, 13. Sept	2	2.230
2007, 2. Sept	1	22.300
2007, 3. Sept	2	17.400
2008, 20. Sept	1	5.375
2008, 21. Sept	2	6.090
2009, 09. Sept	1	6.517
2009, 10. Sept	2	4.835

3.4.2 Scenario 2: communication with varying distance decay factor

This scenario examined the impact of communication among corals using the distance decay factor k to simulate varying influence over distance of neighbouring corals.

Required Calibrations:

- A sensitivity analysis was conducted on one specific spawning day (2008, 21. Sept) to investigate the relationship between the balancing weight of the communication wC and the distance decay factor k (see Table 18). Resulting from this analysis, the wC-value of 0.5 was chosen for the rest of the simulations. Because wC and k are important discussion points in this thesis, the results and discussion are in the corresponding chapters.
- Three spawning days with significant clustering were selected: 21 September 2008, 9 September 2009 and 5 September 2004 (see Figure 17). The distance decay factor k was adjusted across a range of values, where the `commFactor` required recalibration for each setting (see Table 19).

Table 18: Calibrated `commFactor` for the sensitivity analysis of the relationship between the weight of the communication wC and the distance decay factor k (weightComm x distanceDecay).

Spawning Date	**Spawning Day**	`spawnFactor`	wC	k	`commFactor`
2008, 21. Sept	2	6.090	0.8	0.1	0.018
2008, 21. Sept	2	6.090	0.9	0.1	0.028
2008, 21. Sept	2	6.090	0.5	0.3	0.044
2008, 21. Sept	2	6.090	0.6	0.3	0.055
2008, 21. Sept	2	6.090	0.7	0.3	0.075
2008, 21. Sept	2	6.090	0.5	0.5	0.13
2008, 21. Sept	2	6.090	0.6	0.5	0.22
2008, 21. Sept	2	6.090	0.4	0.7	0.28
2008, 21. Sept	2	6.090	0.5	0.7	0.285
2008, 21. Sept	2	6.090	0.6	0.7	0.56
2008, 21. Sept	2	6.090	0.5	0.8	0.415
2008, 21. Sept	2	6.090	0.6	0.8	1.00
2008, 21. Sept	2	6.090	0.4	0.9	0.65
2008, 21. Sept	2	6.090	0.5	0.9	1.25

Table 19: Calibrated `commFactor` for Communication Scenarios with varying distance decay factor k.

Spawning Date	**Spawning Day**	`spawnFactor`	wC	k	`commFactor`
2008, 21. Sept	2	6.090	0.5	0.1	0.0085
2008, 21. Sept	2	6.090	0.5	0.3	0.044
2008, 21. Sept	2	6.090	0.5	0.5	0.13
2008, 21. Sept	2	6.090	0.5	0.7	0.285
2008, 21. Sept	2	6.090	0.5	0.8	0.415
2008, 21. Sept	2	6.090	0.5	0.9	1.25
2009, 09. Sept	1	6.517	0.5	0.1	0.003
2009, 09. Sept	1	6.517	0.5	0.3	0.014
2009, 09. Sept	1	6.517	0.5	0.5	0.04
2009, 09. Sept	1	6.517	0.5	0.7	0.085
2009, 09. Sept	1	6.517	0.5	0.9	0.39
2004, 05. Sept	2	7.166	0.5	0.1	0.0039
2004, 05. Sept	2	7.166	0.5	0.3	0.025
2004, 05. Sept	2	7.166	0.5	0.5	0.1
2004, 05. Sept	2	7.166	0.5	0.7	0.48
2004, 05. Sept	2	7.166	0.5	0.9	1

4 Results

4.1 Scenario 1: no-communication (null hypothesis)

The results of Scenario 1 showed that the mean Moran's I values across 30 simulation runs for each spawning day ranged from -0.17 to 0.02 (see Table 19). The majority of the Z-scores were near zero or negative, reflecting no significant spatial clustering across the simulated spawning days. Whith this scenario, no clustering can be simulated across all spawning days.

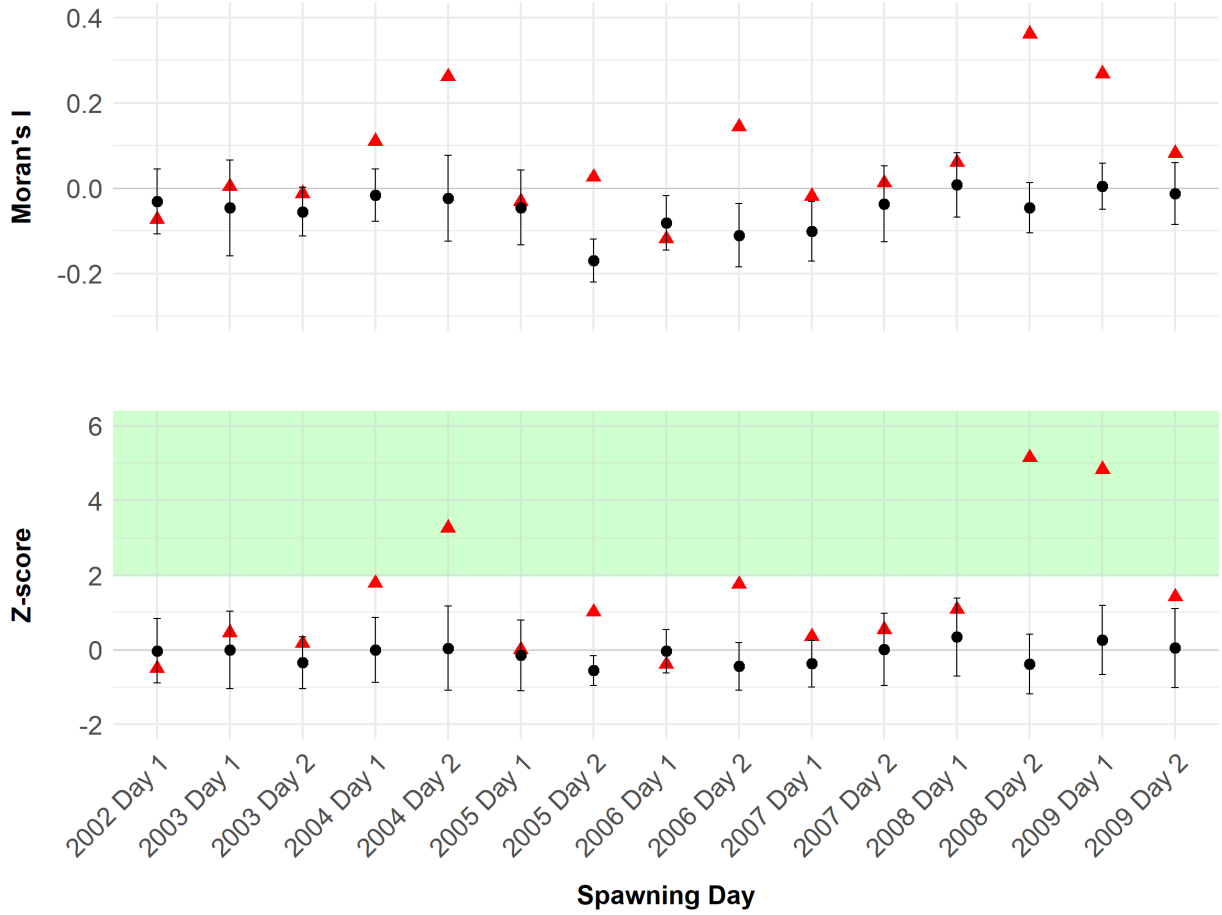

Figure 19: Spatioal analysis result of scenario 1: no-communication. Black points show the mean Moran's I values and Z-scores with corresponding standard deviations (error bars) across 30 simulation runs for each spawning day. Red triangles represent the Z-scores from the real-world baseline scenario as a reference.

4.2 Scenario 2: communication between agents

4.2.1 Sensitivity analysis of wC and k

Results showed an inverse exponential relationship between wC and k, visualised by the fitted curve (see Figure 20). The real-world clustering patterns can be reproduced using suitable variable pairs within a range of wC values 1 to 0.45 and k values 0.2 to 0.9.

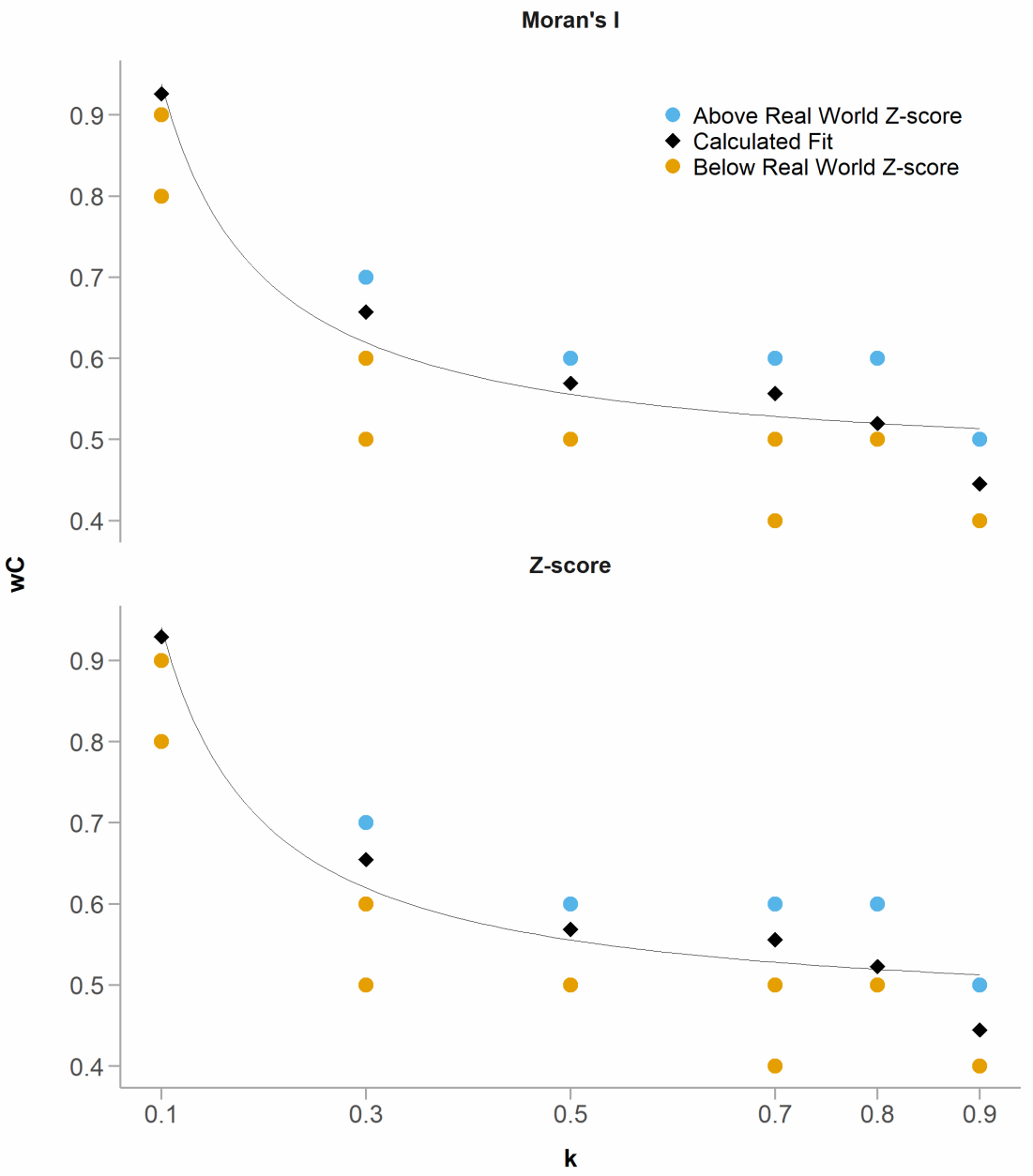

Figure 20: Sensitivity analysis of wC and k. This figure displays the mean Moran's I and Z-score values for specific wC and k combinations for the spawning day 2 in 2008. Blue points indicate a mean value above the baseline real-world result and orange points indicate a mean value below the baseline. Each mean value is based on 20–30 simulation runs per combination. The black diamond marker represents the calculated wC that aligns with the real-world values and its corresponding fitted black line depicts the inverse exponential relationship observed in this sensitivity analysis.

4.2.2 Sensitivity Analysis of k

For the specified spawning days (2004 Day 2, 2008 Day 2, and 2009 Day 1), the sensitivity analysis showed that a similar clustering strength to the baseline real-world results was achievable (see Figure 21). The specific k values where clustering matched the baseline were found at $k = 7.3$ for 2004 Day 2, $k = 8.3$ for 2008 Day 2, and $k = 8.6$ for 2009 Day 1.

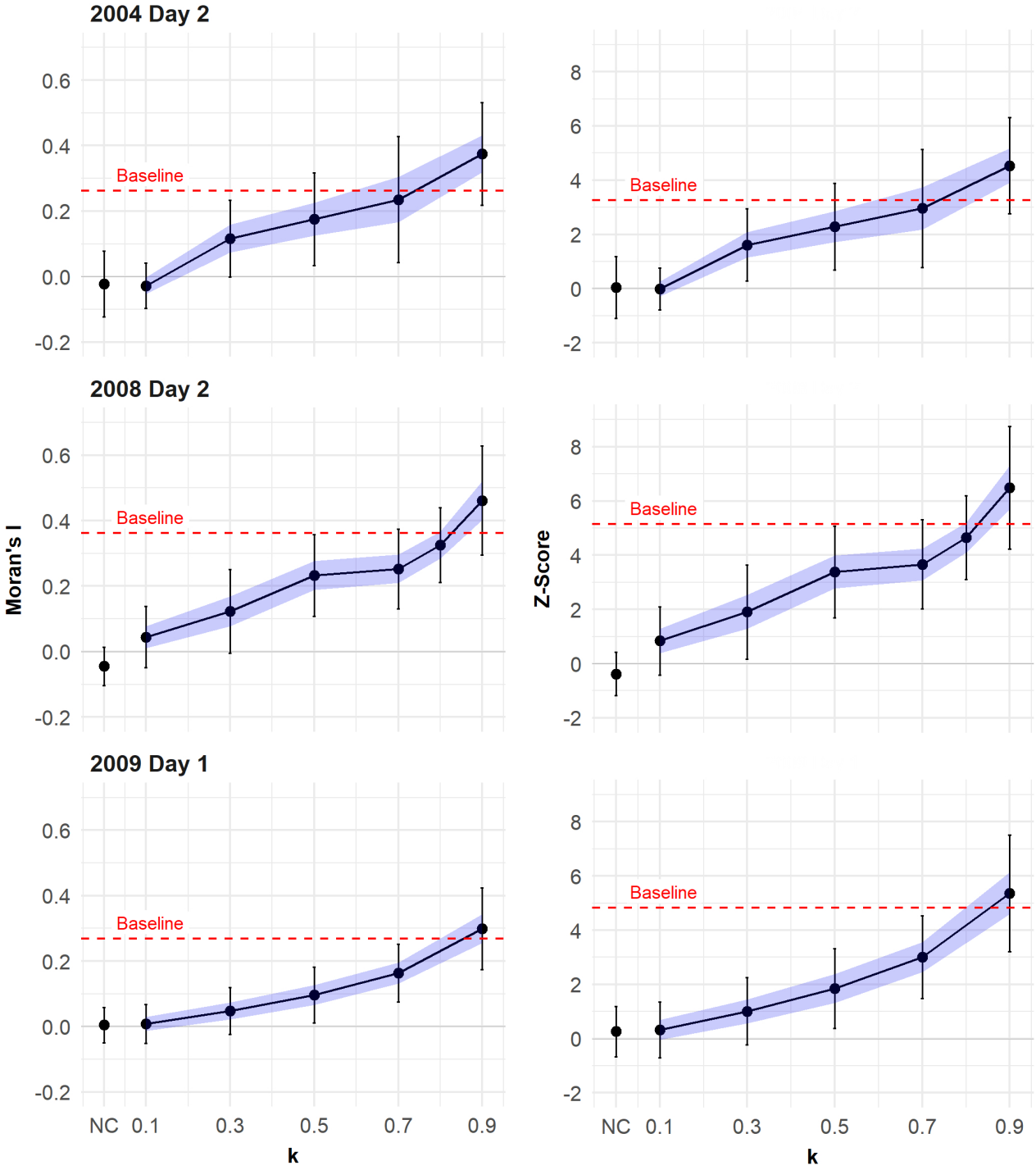

Figure 21: Spatial analysis results of scenario 2: communication. The mean Moran's I values and Z-scores are shown as black points, along with their standard deviation (error bars), based on 30 simulation runs for each spawning day (2004 Day 2, 2008 Day 2, and 2009 Day 1) under varying k values. The blue shaded area represents the 95% confidence interval. For comparison, results from scenario 1 (no-communication) are shown as first value on the left, as well as the real-world baseline results (Moran's I and Z-score) as a red dashed line.

Figures 22, 23, and 24 on following three pages show the fine-scale spatial spawning pattern across various simulation scenarios for three specific spawning events: 2004 Day 2, 2008 Day 2, and 2009 Day 1. The histograms of spawning time distribution in each figure show the spatio-temporal clustering difference between the baseline distribution (real-world data) and simulated outcomes under both the no-communication and communication scenarios.

For all three spawning days, it is evident that the baseline (real-world data) showed natural clustering, while the no-communication scenario displayed no apparent clustering. Increasing distance decay factors (k) corresponded with progressively stronger clustering trends. A distance decay factor of 0.7 or 0.9 resulted in a similar spawning time histogram as the real-world especially for the years 2008 and 2009.

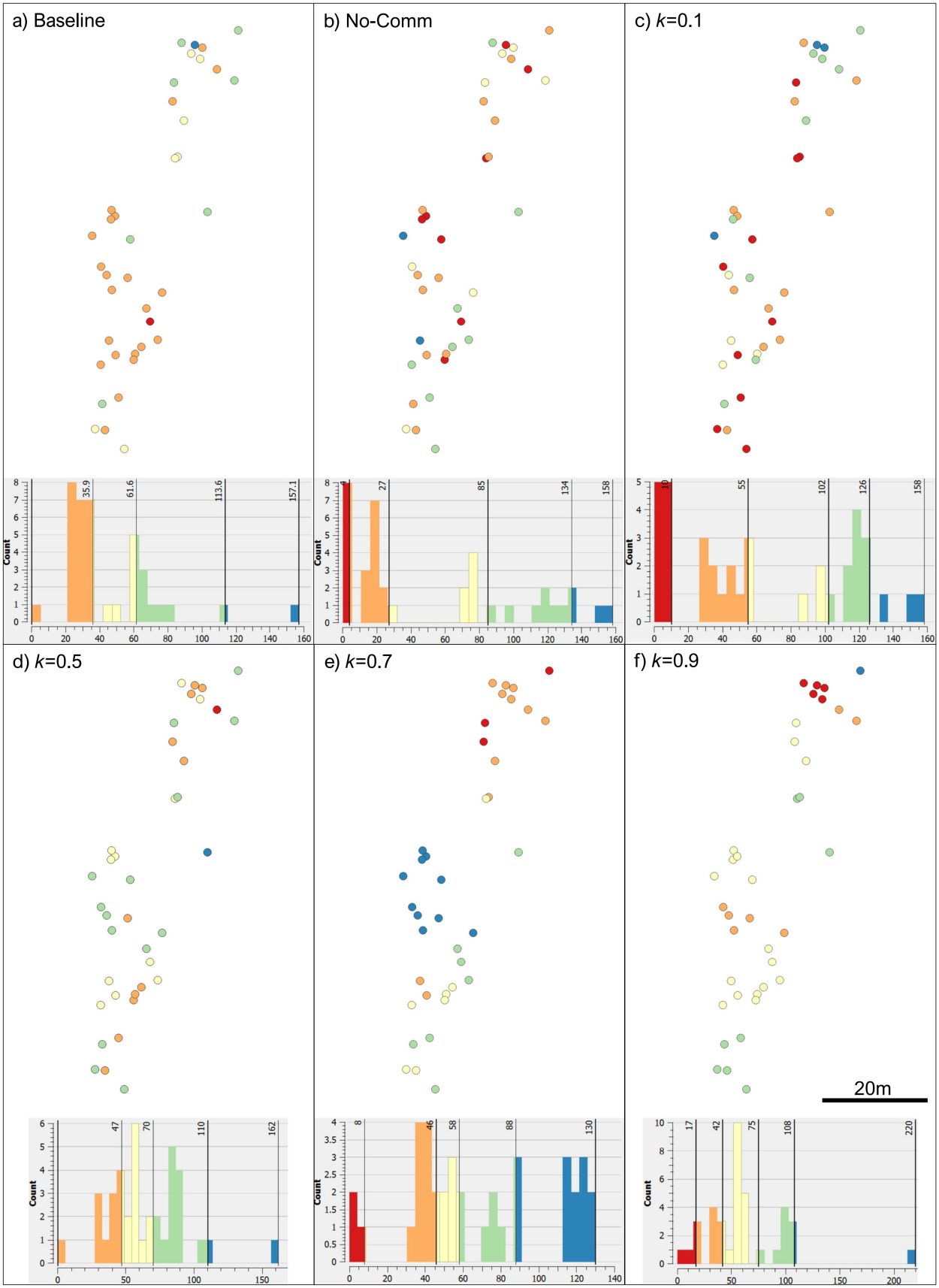

Figure 22: Spatio-temporal distribution of spawning corals on 2004 Day 2. Except the baseline, each result is from one randomly chosen simulation sample of the corresponding scenario. Colour classification of spawning time (in min) into five bins using natural jenks, with 30-bin histograms for each scenario: (a) baseline - real-world data, (b) no-communication, and (c-f) communication scenarios with varying k values: 0.1, 0.5, 0.7, and 0.9.

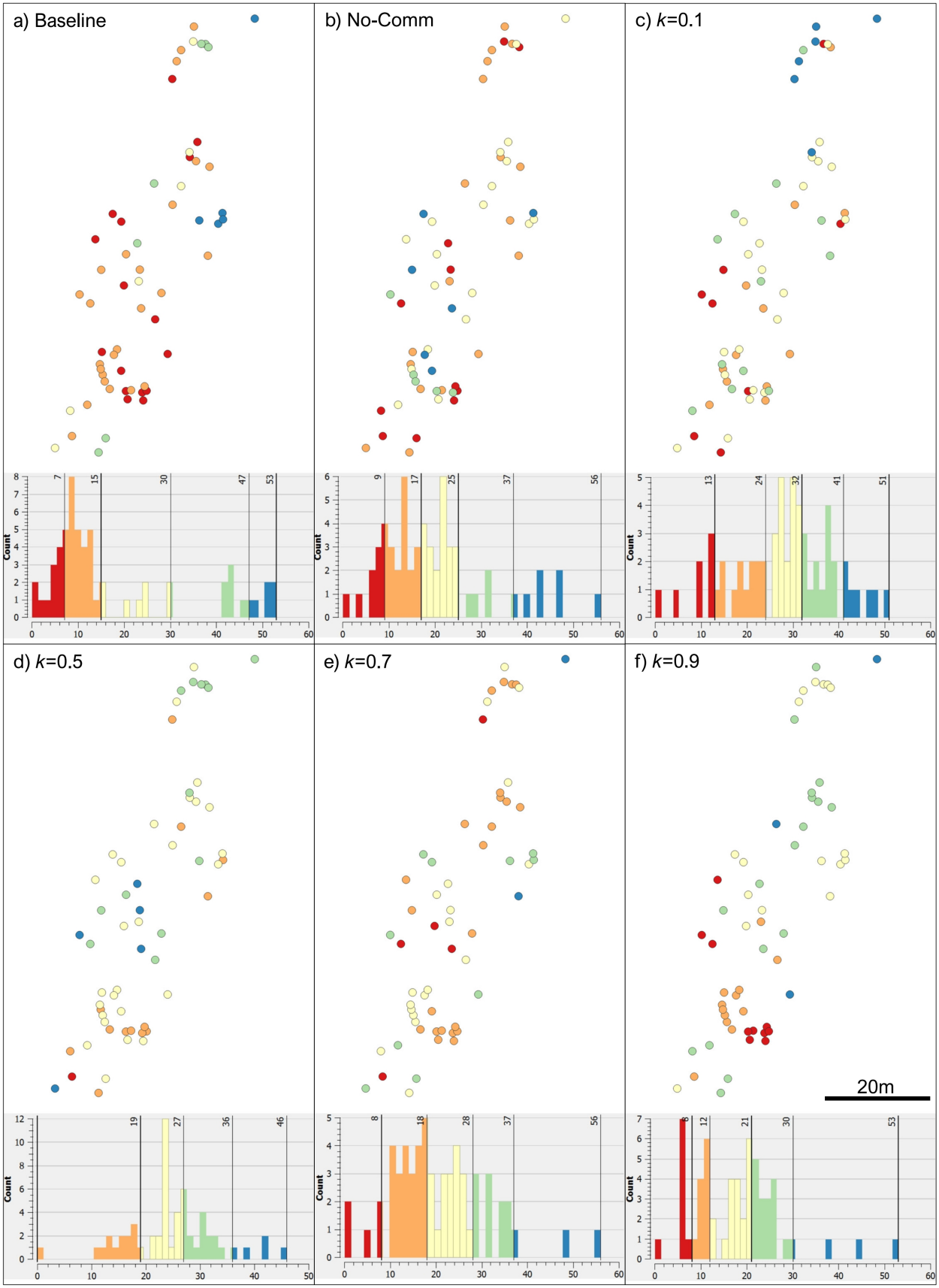

Figure 23: Spatio-temporal distribution of spawning corals on 2008 Day 2. Except the baseline, each result is from one randomly chosen simulation sample of the corresponding scenario. Colour classification of spawning time (in min) into five bins using natural jenks, with 40-bin histograms for each scenario: (a) baseline - real-world data, (b) no-communication, and (c-f) communication scenarios with varying k values: 0.1, 0.5, 0.7, and 0.9.

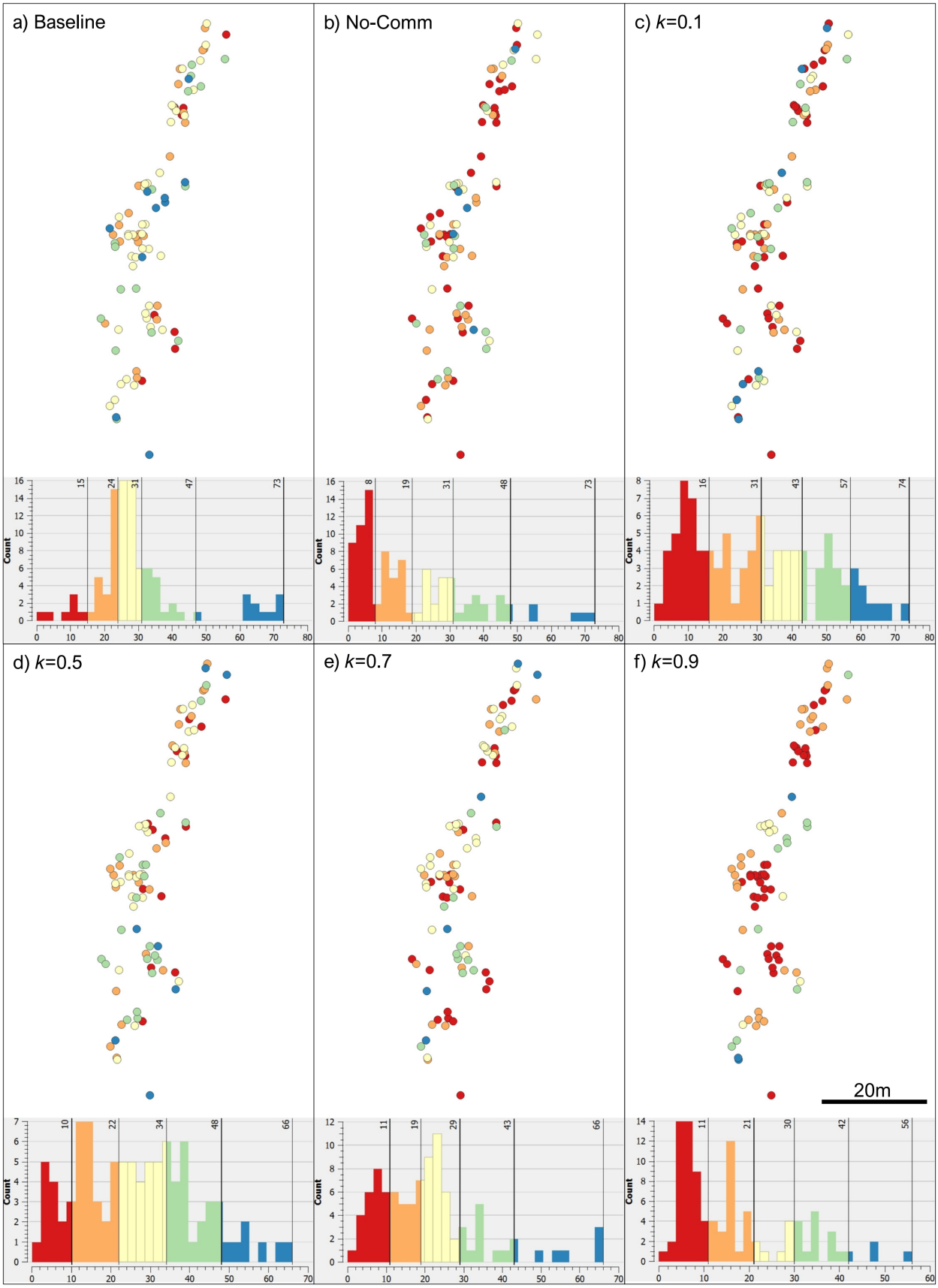

Figure 24: Spatio-temporal distribution of spawning corals on 2009 Day 1. Except the baseline, each result is from one randomly chosen simulation sample of the corresponding scenario. Colour classification of spawning time (in min) into five bins using natural jenks, with 30-bin histograms for each scenario: (a) baseline - real-world data, (b) no-communication, and (c-f) communication scenarios with varying k values: 0.1, 0.5, 0.7, and 0.9.

5 Discussion

5.1 Ancillary finding: predictive accuracy

The validation of environmental factors selected to simulating *O. franksi* spawning events revealed a relatively high degree of accuracy in predicting real-world spawning dates even though forecasting was not the primary focus of this model (see Table 16). Despite the randomisation of individual reproductive strength to reflect biological variability, the model reproduced known spawning events with a deviation mean of 1.8 days and a range of -4 to +0.7 days. This accuracy underscores the validity of the chosen environmental factors as foundational to the model's performance.

Before implementing agent-based sensitivity of reproductive readiness to each environmental variable, initial model development involved hardcoded ranges for spawning start, defined by the real-world data (see Table 8). This preliminary approach produced an even closer approximation to real-world spawning dates, suggesting that strict environmental thresholds can enhance predictive precision of the model. However, to sustain biological authenticity and agent sensing behaviour, the hardcoded ranges were removed.

Nevertheless, there is indisputable potential to adapt the model for coral spawning day predictions. Including prediction parameters to include more coral species would be a valuable enhancement.

5.2 Scenario 1: no-communication (null hypothesis)

The no-communication scenario tests whether clustering patterns randomly appear in the absence of inter-agent communication. Its results showed that the simulated fine-scale coral spawning patterns exhibited no detectable clustering and were distributed randomly (see Figure 19). This supports the expectations of the null hypothesis, stating that clustering does not emerge without communication mechanisms.

Compared to the real-world, where several spawning days showed various degrees of clustering (see Figure 17), the no-communication scenario invariably produces random spawning patterns, with means Moran's I and Z-scores close to zero (see Figure 19). Some real-world spawning days, specifically 2002 Day 1, both 2003 days, 2005 Day 1, 2006 Day 1, both 2007 days, and 2008 Day 1, fall within the standard deviation range (error bars) of the no-communication scenario, suggesting that also the no-communication scenario may be true for theses days.

Certain real-world days like 2004 Day 1, 2005 Day 2, and 2006 Day 2 demonstrated clustering that exceeded the no-communication scenario's standard deviation range, however, their Z-scores did not reach statistical significance.

These results imply that the null hypothesis holds in years with no clustering. On the other hand, it cannot explain the increased clustering of certain years and definitely not the significant clustering of the three chosen communication years. Therefore, the no-communication scenario is both supported and refuted, depending on the specific year and spawning day.

5.3 Scenario 2: communication between agents

The results from the communication scenarios reveal that interactions between coral agents enhance spawning synchronisation which results in spatio-temporal clustering patterns more closely aligned with real-world observations than the no-communication scenario (see Figures 22, 23, 24).

The sensitivity analysis of the interplay between the communication weight (wC) and the distance decay factor (k) shows their variability in creating similar synchronisation patterns. Meaning that different combination of these values result in similar clustering (see Figure 20). Accordingly, if the calibrated value of wC would have been chosen higher than 0.5, the real-world clustering intensity would haven been crossed at lower k values than the current results (see Figure 21). Given this influence of wC, it is difficult to assign either a quantitative distance or a communication speed to k. However, it can be said that a lower k indicates that communication lasts over a longer distance and effectively broadens the spatial range over which corals influence one another's spawning readiness. Which can be inferred to a "higher communication speed". In this model, a high k was required to approximate real-world spawning patterns which correlates to a slow communication between coral agents.

These results suggest that chemical signalling is the more appropriate communication method compared to the theory of acoustic signalling. The transmission speed of sound underwater is approximately $1500\,\mathrm{m\,s^{-1}}$, more than four times faster than the transmission speed of sound in air. Such acoustic signals underwater would be modelled with a very low k (see Figure 20) where the observed spatial spawning patterns could not be achieved.

Furthermore, research of other marine invertebrates found that chemical signals promoted reproductive synchrony (Watts and Wasson, 2020). However, recent studies present conflicting evidence about the biological pathways within corals to detect and respond to chemical signals. On the one hand, although steroid hormones are found in corals and sea anemones, Morgan et al. (2022) emphasises the lack of traditional estrogen receptors and steroidogenic pathways. On the other hand, Khalturin et al. (2018) identified a family of steroid receptor-like proteins (NR3E) in certain cnidarians which suggests they may have receptors capable of binding aromatic steroids in unconventional ways. These contradictions underpin the need for targeted studies clarifying whether corals possess pathways to perceive and respond to chemical signals.

Concluding, the communication scenarios suggest that observed fine-scale spawning patterns may be due to early-spawning corals releasing chemical signals that form localised gradients around them. Subsequently, these gradients may induce the observed synchronisation of spawning time of nearby colonies. The model's simulation results can be regarded as circumstantial support for the concept of chemical communication during coral spawning.

5.4 Model limitations and uncertainties

The environmental factors modelled in this study are not directly validated against local measurements for the observed years 2002-2009. While the submodels rely on well-established datasets and methods, this lack of validation against ground-truthed measurements introduces uncertainties.

5.4.1 Calculation of environmental factors

The model's large-scale synchrony which lead to a spawning event align closely with real-world timing data over multiple years (see Table 8). This emphasises the importance of the chosen environmental factors, the lunar and solar cycles, water temperature, and dark time, as main drivers of spawning events. Nevertheless, coral research proposes further possible environmental factors. For example van Woesik (2009) pointed out a positive relationship between calm weather periods and the onset of spawning. However, because of limited sources and the complexity of implementing weather data into the model, this environmental factor was not considered. Furthermore, some studies investigated the influence of tides, particularly neap tides, as spawning factor (Mendes, 2002; Babcock et al., 1986). As the tide is dependent on the moon phase, it remains unclear how these two factors can be distinguished. For this model it is assumed that accounting for the influence of the lunar cycle, indirectly considers the tidal influence.

Furthermore, it should be noted that the influence of each environmental factor is modelled linearly and it is not certain whether this approach is biologically accurate. The regulation of a coral's metabolism may not respond linearly to changes, as demonstrated by Sawall et al. (2022), who observed non-linear metabolic variation to temperature changes. Additionally, coral species differ in their sensitivity to environmental factors depending on their locations' environmental characteristics (Gouezo et al., 2020). This model is specifically tailored to simulate the spawning behaviour of *O. franksi* and thus, improvements would require research on this particular species.

Solar Cycle. While the solar cycle calculations presented here yield reliable approximations for sunrise and sunset times, there are potential uncertainties. For instance, the formulas by Meeus (1998) assume a perfectly spherical Earth and consistent orbital parameters. Furthermore, they neglect atmospheric refraction, cloud cover, and the coral reef bathymetry that can slightly change observed daylight hours as well as the light attenuation due to water depth.

Another model limitation is the choice of photoperiod as solar influence compared to solar insolation. The findings by Penland et al. (2004) suggested that solar insolation, particularly its maxima during the vernal and autumnal equinoxes, provide a more reliable environmental influence to coral spawning in tropical regions. They explain this observation that at higher latitudes the photoperiod changes strongly throughout the year but remains relatively constant near the equator where solar insolation peaks may be more influential. Furthermore, Mendes (2002) found no correlation between photoperiod and spawning for *Montastraea annularis* in Jamaica, suggesting that photoperiod may not universally drive spawning timing, particularly at lower latitudes. They concluded that temperature and light intensity were correlated with gonad size. This further supports the role of light availability (via solar insolation) influencing coral spawning times. Improvement of this model could exchange the photoperiod with solar insolation.

Lunar Cycle. The calculations of the lunar cycle depend on the accuracy of the lunar ephemeris dataset by the U.S. Naval Observatory (2024). Some irregularities in the dataset must be assumed because the moonlight curves exhibit a recurring anomaly at each monthly change of the dataset tables (see Figure 10). Furthermore, the accuracy of lunar cycle calculations can be improved through more precise methods (Duffett-Smith and Zwart, 2011), however, beyond a certain level of complexity,

the involvement of an astronomy expert is required. The moonlight dose calculations define the moonlight reaching the ground but the model does not account for light attenuation and scattering by sea water (Jerlov, 1976). This would theoretically introduce an additional gradient depending on the depth at which the coral agents are located.

Dark Time. The darktime is inferred from the solar cycle submodel and the lunar ephemeris dataset (U.S. Naval Observatory, 2024) and its accuracy is defined by the uncertainties in these data sources.

Water Temperature. The sinusoidal model provides a convenient mathematical approximation for the seasonal pattern of sea water temperatures. However, the real-world observations at Bocas del Toro deviate clearly (Kaufmann and Thompson, 2005). Interactions between local oceanographic conditions, atmospheric processes, and large-scale climate patterns lead to non-sinusoidal temperature cycles exhibiting asymmetry, abrupt shifts, or multiple peaks (Yang and Wu, 2024; Proietti and Maddanu, 2022).

Suggestions for Model Improvement. Improving the modelling accuracy of physical processes over time is a constantly iterating process. At the beginning of creating this model, there was the vision to create a simulated world that is independent from a fixed location, i.e. to have the choice to change the geographic location and the environmental calculations would adapt accordingly. While implementing the lunar cycle, this vision was suspended due to the extent of such a calculation (Duffett-Smith and Zwart, 2011).

Therefore, before implementing improvements, it must be decided which way the model has to evolve. One way is to improve the model accuracy of a specific location with the goal to assess the spawning of a specific set of corals. The other way is to evolve the model to be independent of location where spatial fine-scale fluctuations of the environment are probably not included. The creation of a hybrid version implementing both features is theoretically feasible but would require greater effort.

5.4.2 Modelling of a coral agent

Which coral spawns first? Some studies hypothesised that larger and more mature colonies reach readiness earlier due to their greater energy reserves and enhanced capacity for gamete production (Szmant, 1991; Kai and Sakai, 2008). However, when analysing the raw data provided by Levitan et al. (2011), there was no correlation between coral size and spawning time. Therefore, the size factor was not introduced into this model. Their finding is supported by the gametogenesis development of fragmented corals which reach maturity at the same time as their parent colony (Rapuano et al., 2023). Accordingly, the analysis for correlation between genotype and spawning time by Levitan et al. (2011) also resulted in a more synchronous spawning time of cloning-mates. Thus, genetic factors are suspected to answer the question of which coral spawns first.

The random reproductive variability `reproductiveVar` was introduced as placeholder for this unknown cause of variability. However, this randomness further induces another variability across multiple simulations in regard of the distribution of the first-spawning corals. The location of these corals influences spawning patterns by affecting their respective distances to neighbours.

No sensitivity analysis was performed for the variable `reproductiveVar` because the variation is balanced out by the model's calibration. Increasing the variability would only delay the spawning

of certain corals, requiring an adjustment of the factors `spawnFactor & commFactor` to ensure the resulting spawning simulation matches the real-world spawning duration. Reducing variability would require lower calibration factors respectively.

Gametogenesis. The model assumes that the initiation of gametogenesis starts on the first day of the year across all coral colonies. During the development phase, the assumption is that gamete growth is influences by temperature and photoperiod. Similarly, the maturation phase assumes the influence of solely the moonlight dose where the dark time duration is the final trigger to spawning. Even though these decisions were based on coral biology research, as described in the corresponding submodel in Chapter 2.4.7.4, the equation implementation of the factors, weights, and reproductive variability remains open to scrutiny.

Suggestions for model improvement. Further coral research is required to provide transferable results quantifying the mechanisms behind early and late spawners. Given the strong influence of this stochastic variability on the resulting fine-scale spawning patterns, it represents a critical limitation of the model.

5.4.3 Communication implementation versus null hypothesis

In the model, the influence of communication begins after the spawning starts. The environment was calibrated and validated without communication. This approach uses the real-world spawning day as a calibration and validation point. Consequently, the environment and the influence of the four environmental factors must cause the coral reef to spawn at a specific time without communication. Otherwise, this validated environment could not be used for the no-communication null hypothesis. Introducing communication earlier would have required a different validation of the environment or the exclusion of the no-communication scenario, which would prevent the formulation of a null hypothesis. To scientifically justify a result comparison between differently validated environments was considered difficult.

This approach prohibited the testing of the concept that coral spawning emerges as self-organised criticality through coral communication. This is a drawback because self-organised criticality would provide a compelling explanation for the emergent spawning phenomenon (Tadić and Melnik, 2021). However, out of the before mentioned reason the decision was made to retain a hypothesis-driven focus and pursue the null hypothesis and its comparison to the communication scenario and the real-world dataset.

However, it is acknowledged that this method may have introduced an inherent systemic error in how the corals become ready to spawn and how communication influences this process.

Suggestions for model improvement. Developing a validation method for the environment that does not rely on distinguishing between communication and no-communication scenarios would provide more freedom to implement and test emergent behaviours such as self-criticality.

5.4.4 Missing communication definition

Because no unified and validated explanation of the communication mechanism exists in the literature, the model uses a generic distance-based communication approach. The exponential decay

function is often used to model influence spread in spatial ecological systems (Costa and Schulte, 2023). Exponential decay is preferred over linear decay when modelling rapid decline in influence over distance which is assumed in a 3D environment (de Smith et al., 2024).

Suggestions for model improvement. Spatially modelling the dispersal of sexual hormones, which is the most widely researched theory of coral communication, would give the model more validity. However, implementing such a detailed process may subsequently lead to incorporating hydrological dynamics using a 3D reef model and water flow simulations. Including hydrodynamics is inevitable for this approach because dispersion of chemical signals through water flow would be stronger compared to simple diffusion. This enhancement would increase model complexity and require additional data and expertise in physical oceanography.

6 Conclusion

In this study, coral communication explains the clustering observed in fine-scale spawning patterns of some years through a simulated coral reef. These findings demonstrate that inter-agent communication is likely necessary to achieve certain observed spatial patterns. While the model required strong simplification of biological processes, such as a simplified distance-based influence mechanism, it effectively connects large-scale environmental factors with fine-scale synchronisation.

The model, in its present form, functions as a baseline highlighting knowledge gaps through the difficulty of assigning precise values or parameters to certain biological processes. It indicates where targeted empirical research and quantification efforts are needed. In this sense, the model does not merely simulate current understanding, it serves as a "playground," where new hypotheses can be tested and refined, guiding future investigations into the mechanisms underlying coral communication and synchronised spawning.

As coral reefs face increasing environmental pressures, scientific observations already report the negative influence of climate change on coral spawning (Levitan et al., 2014; Paxton et al., 2016; Bouwmeester et al., 2023; Shlesinger and Loya, 2019). Improving our knowledge about the underlying mechanisms of coral spawning, including the role of coral communication, may prove essential to predict how spawning synchrony might shift under future conditions. This information will further inform conservation strategies and management decisions aimed at preserving the reproductive resilience and biodiversity of coral reef ecosystems.

6.1 Implications for future research

As repeatedly stated within the possible model improvements discussed in the previous chapter, targeted research on coral biology is foundational. The specific spawning mechanisms have to be quantified in a transferable way to enhance the model's accuracy. Two key areas have been evaluated as most important for further exploration.

Mechanisms of coral communication. The primary focus is on understanding the mechanisms of coral communication. The current model assumes a generic distance-based influence of inter-agent communication, without knowing the biological basis for this interaction. Investigating these mechanisms in a controlled in-vitro settings would excludes external factors. Subsequently, the distribution speed of these signals must be quantified. The final results may require the implementation of reef hydrology modelling to simulate distribution and diffusion.

Reproductive variability in spawning readiness. The model uses stochastic variability in reproductive strength to account for differences in spawning timing among corals, leading to randomisation of the first corals to spawn. Identifying the specific biological or environmental factors that influence this spawning initiation would refine the model's parameters, reducing the reliance on randomisation. Controlled experiments or detailed field surveys could help correlate spawning readiness with biological traits of this individual. The results must clarify whether the observed reproductive variability is truly random or due to clearly identifiable differences between individuals.

7 AI statement

The UNIGIS guidline "Leitfaden zum Umgang mit generativer KI" provided by UNIGIS (2024) released in September 2024 was considered during the creation of this document. Acknowledging the release of an updated version on 2 December 2024, when the draft of this thesis had already been created. Therefore, the AI statement is still included to comply to the previous version of the guideline.

7.0.1 Text review

For grammar review, ChatGPT (version 4, November 2024) was used. I, the author, reviewed and corrected the output, as needed, and takes full responsibility for the content of this document.

Example prompt for text review: *"Please, review the following chapter for grammatical errors. Follow these guidelines: Mark your changes, keep your changes minimal, do not change the content and meaning of sentences, be concise, do not change or move citations, do not add repetitive or redundant words."*

7.0.2 GAML coding

I, the author, confirm that NO AI support was used for the creation of the simulation code in the software GAMA.

7.0.3 Graphs

I, the author, confirm that NO graphs were created with AI. The graphs are the result of loading the raw data into the statistical software R (R Core Team, 2024) to create the accurate graphical output.

7.0.4 QGIS and spatial analysis

I, the author, confirm that NO AI support or AI-plugins were used for GIS analysis, the creation of maps or visual outputs.

References

Andreatta, G. and Tessmar-Raible, K. (2020) 'The Still Dark Side of the Moon: Molecular Mechanisms of Lunar-Controlled Rhythms and Clocks'. *Journal of Molecular Biology*, 432(12):3525–3546.

Anselin, L. (1995) 'Local Indicators of Spatial Association—LISA'. *Geographical Analysis*, 27(2):93–115.

Aoki, N., Weiss, B., Jézéquel, Y., Zhang, W. G., Apprill, A., and Mooney, T. A. (2024) 'Soundscape enrichment increases larval settlement rates for the brooding coral *Porites astreoides*'. *Royal Society Open Science*, 11(3):231514.

Atkinson, S. and Atkinson, M. J. (1992) 'Detection of estradiol-17β during a mass coral spawn'. *Coral Reefs*, 11(1):33–35.

Austin, R. H., Phillips, B. F., and Webb, D. J. (1976) 'A Method for Calculating Moonlight Illuminance at the Earth's Surface'. *Journal of Applied Ecology*, 13:741.

Babcock, R. C., Bull, G. D., Harrison, P. L., Heyward, A. J., Oliver, J. K., Wallace, C. C., and Willis, B. L. (1986) 'Synchronous spawnings of 105 scleractinian coral species on the Great Barrier Reef'. *Marine Biology*, 90(3):379–394.

Baird, A. H., Guest, J. R., and Willis, B. L. (2009) 'Systematic and Biogeographical Patterns in the Reproductive Biology of Scleractinian Corals'. *Annual Review of Ecology, Evolution, and Systematics*, 40(1): 551–571.

Bouwmeester, J., Daly, J., Zuchowicz, N., Lager, C., Henley, E. M., Quinn, M., and Hagedorn, M. (2023) 'Solar radiation, temperature and the reproductive biology of the coral Lobactis scutaria in a changing climate'. *Scientific Reports*, 13(1):246.

Brady, A. K., Hilton, J. D., and Vize, P. D. (2009) 'Coral spawn timing is a direct response to solar light cycles and is not an entrained circadian response'. *Coral Reefs*, 28(3):677–680.

Brady, A. K., Snyder, K. A., and Vize, P. D. (2011) 'Circadian Cycles of Gene Expression in the Coral, *Acropora millepora*'. *PLOS ONE*, 6(9):e25072.

Brusca, R. C., Moore, W., and Shuster, S. M. (2016) *Invertebrates*. 3^{rd} edition, Sinauer Associates, Sunderland, USA, 1104pp.

Budd, A. F., Fukami, H., Smith, N. D., and Knowlton, N. (2012) 'Taxonomic classification of the reef coral family Mussidae (Cnidaria: Anthozoa: Scleractinia)'. *Zoological Journal of the Linnean Society*, 166(3): 465–529.

Buratti, B. J., Hillier, J. K., and Wang, M. (1996) 'The Lunar Opposition Surge: Observations by Clementine'. *Icarus*, 124(2):490–499.

Camazine, S., Deneubourg, J.-L., Franks, N. R., Sneyd, J., Theraulaz, G., and Bonabeau, E. (2001) *Self-Organization in Biological Systems*. 1^{st} edition, Princeton University Press, Princeton, 562pp.

Chui, A. P. Y., Wong, M. C., Liu, S. H., Lee, G. W., Chan, S. W., Lau, P. L., Leung, S. M., and Ang Jr., P. (2014) 'Gametogenesis, Embryogenesis, and Fertilization Ecology of *Platygyra acuta* in Marginal Nonreefal Coral Communities in Hong Kong'. *Journal of Marine Sciences*, 2014(1):953587.

Costa, D. G. and Schulte, P. J. (2023) *An Invitation to Mathematical Biology*. 1^{st} edition, Springer, Cham, 124pp.

D'Angelo, C. and Wiedenmann, J. (2014) 'Impacts of nutrient enrichment on coral reefs: new perspectives and implications for coastal management and reef survival'. *Current Opinion in Environmental Sustainability*, 7:82–93.

Darwin, C. (1842) *The Structure and Distribution of Coral Reefs, Being the First Part of the Geology of the Voyage of the Beagle, Under the Command of Capt. Fitzroy, R.N. During the Years 1832 to 1836.* 1^{st} edition, Smith Elder and Co., London, 214pp.

Davies, T. W., Levy, O., Tidau, S., de Barros Marangoni, L. F., Wiedenmann, J., D'Angelo, C., and Smyth, T. (2023) 'Global disruption of coral broadcast spawning associated with artificial light at night'. *Nature Communications*, 14(1):2511.

de Smith, M. J., Goodchild, M., and Longley, P. A. (2024) *Geospatial Analysis.* 7^{th} edition, Winchelsea Press, 602pp.

Duane, D., Freeman, S., and Freeman, L. (2024) 'Moonlight-driven biological choruses in Hawaiian coral reefs'. *PLOS ONE*, 19(3):e0299916.

Duffett-Smith, P. and Zwart, J. (2011) *Practical Astronomy with your Calculator or Spreadsheet.* 4^{th} edition, Cambridge University Press, Cambridge, 216pp.

Encyclopædia Britannica Inc. (2024) *Cross section of a generalized coral polyp.* Available at: `https://www.britannica.com/animal/coral#/media/1/137037/19644` (Accessed: 2024-08-15).

Fogarty, N. D. and Marhaver, K. L. (2019) 'Coral spawning, unsynchronized'. *Science*, 365(6457):987–988.

GAMA Platform (2024) *Genetic Algorithm.* Available at: `https://gama-platform.org/wiki/ExplorationMethods#genetic-algorithm-genetic` (Accessed: 2024-10-20).

Gooding, T. (2019) 'Agent-Based Model History and Development'. In: Gooding, T., (ed.), *Economics for a Fairer Society: Going Back to Basics using Agent-Based Models.* Springer International Publishing, Cham, pp. 25–36.

Gorbunov, M. Y. and Falkowski, P. G. (2002) 'Photoreceptors in the cnidarian hosts allow symbiotic corals to sense blue moonlight'. *Limnology and Oceanography*, 47(1):309–315.

Gornik, S. G., Bergheim, B. G., Morel, B., Stamatakis, A., Foulkes, N. S., and Guse, A. (2021) 'Photoreceptor Diversification Accompanies the Evolution of Anthozoa'. *Molecular Biology and Evolution*, 38(5):1744–1760.

Gouezo, M., Doropoulos, C., Fabricius, K., Olsudong, D., Nestor, V., Kurihara, H., Golbuu, Y., and Harrison, P. (2020) 'Multispecific coral spawning events and extended breeding periods on an equatorial reef'. *Coral Reefs*, 39(4):1107–1123.

Grimm, V. and Railsback, S. F. (2005) *Individual-based Modeling and Ecology.* 1^{st} edition, Princeton University Press, Princeton, 448pp.

Grimm, V., Berger, U., DeAngelis, D. L., Polhill, J. G., Giske, J., and Railsback, S. F. (2010) 'The ODD protocol: A review and first update'. *Ecological Modelling*, 221(23):2760–2768.

Harrison, P. L. (2011) 'Sexual Reproduction of Scleractinian Corals'. In: Dubinsky, Z. and Stambler, N., (ed.), *Coral reefs: An ecosystem in transition.* Springer Netherlands, Dordrecht, pp. 59–85.

Harrison, P. L., Babcock, R. C., Bull, G. D., Oliver, J. K., Wallace, C. C., and Willis, B. L. (1984) 'Mass spawning in tropical reef corals'. *Science*, 223(4641):1186–1189.

Hein, M. Y., Vardi, T., Shaver, E. C., Pioch, S., Boström-Einarsson, L., Ahmed, M., Grimsditch, G., and McLeod, I. M. (2021) 'Perspectives on the Use of Coral Reef Restoration as a Strategy to Support and Improve Reef Ecosystem Services'. *Frontiers in Marine Science*, 8.

Hoegh-Guldberg, O., Poloczanska, E. S., Skirving, W. J., and Dove, S. G. (2017) 'Coral reef ecosystems under climate change and ocean acidification'. *Frontiers in Marine Science*, 4:158.

Houlbrèque, F. and Ferrier-Pagès, C. (2009) 'Heterotrophy in tropical scleractinian corals'. *Biological Reviews*, 84(1):1–17.

Hughes, T. P., Barnes, M. L., Bellwood, D. R., Cinner, J. E., Cumming, G. S., Jackson, J. B. C., Kleypas, J., van de Leemput, I. A., Lough, J. M., Morrison, T. H., Palumbi, S. R., van Nes, E. H., and Scheffer, M. (2017) 'Coral reefs in the Anthropocene'. *Nature*, 546:82–90.

Hughes, T. P., Kerry, J. T., Álvarez-Noriega, M., Álvarez-Romero, J. G., Anderson, K. D., Baird, A. H., Babcock, R. C., Beger, M., Bellwood, D. R., Berkelmans, R., Bridge, T. C., Butler, I. R., Byrne, M., Cantin, N. E., Comeau, S., Connolly, S. R., Cumming, G. S., Dalton, S. J., Diaz-Pulido, G., Eakin, C. M., Figueira, W. F., Gilmour, J. P., Harrison, H. B., Heron, S. F., Hoey, A. S., Hobbs, J.-P. A., Hoogenboom, M. O., Kennedy, E. V., Kuo, C.-y., Lough, J. M., Lowe, R. J., Liu, G., McCulloch, M. T., Malcolm, H. A., McWilliam, M. J., Pandolfi, J. M., Pears, R. J., Pratchett, M. S., Schoepf, V., Simpson, T., Skirving, W. J., Sommer, B., Torda, G., Wachenfeld, D. R., Willis, B. L., and Wilson, S. K. (2017) 'Global warming and recurrent mass bleaching of corals'. *Nature*, 543(7645):373–377.

Ibanez, C. and Hawker, J. (2021) 'Ultrasonic Planimals! Identifying Genes Associated with Coral Bioacoustics'. *The FASEB Journal*, 35.

Jerlov, N. G. (1976) 'Chapter 3 Beam Attenuation'. In: *Marine Optics*, volume 14. Elsevier, chapter 3, pp. 47–66.

Kai, S. and Sakai, K. (2008) 'Effect of colony size and age on resource allocation between growth and reproduction in the corals *Goniastrea aspera* and *Favites chinensis*'. *Marine Ecology Progress Series*, 354: 133–139.

Kaniewska, P., Alon, S., Karako-Lampert, S., Hoegh-Guldberg, O., and Levy, O. (2015) 'Signaling cascades and the importance of moonlight in coral broadcast mass spawning'. *eLife*, 4:e09991.

Kaufmann, K. and Thompson, R. (2005) 'Water Temperature Variation and the Meteorological and Hydrographic Environment of Bocas del Toro, Panama'. *Caribbean Journal of Science*, 41.

Khalturin, K., Billas, I. M. L., Chebaro, Y., Reitzel, A. M., Tarrant, A. M., Laudet, V., and Markov, G. V. (2018) 'NR3E receptors in cnidarians: A new family of steroid receptor relatives extends the possible mechanisms for ligand binding'. *The Journal of Steroid Biochemistry and Molecular Biology*, 184:11–19.

Kojis, B. L. and Quinn, N. J. (1981) 'Aspects of Sexual Reproduction and Larval Development in the Shallow Water Hermatypic Coral, *Goniastrea Australensis* (Edwards and Haime, 1857)'. *Bulletin of Marine Science*, 31(3):558–573.

Komoto, H., Lin, C.-H., Nozawa, Y., and Satake, A. (2023) 'An External Coincidence Model for the Lunar Cycle Reveals Circadian Phase-Dependent Moonlight Effects on Coral Spawning'. *Journal of Biological Rhythms*, 38(2):148–158.

Korokhin, V. V., Velikodsky, Y. I., Shkuratov, Y. G., and Mall, U. (2007) 'The phase dependence of brightness and color of the lunar surface: a study based on integral photometric data'. *Solar System Research*, 41(1): 19–27.

LaJeunesse, T. C., Parkinson, J. E., Gabrielson, P. W., Jeong, H. J., Reimer, J. D., Voolstra, C. R., and Santos, S. R. (2018) 'Systematic Revision of Symbiodiniaceae Highlights the Antiquity and Diversity of Coral Endosymbionts'. *Current Biology*, 28(16):2570–2580.e6.

Law, A. M. (2014) *Simulation Modeling and Analysis*. 5^{th} edition, McGraw-Hill Education, New York, 776pp.

Levitan, D., Fukami, H., Jara, J., Kline, D., Mcgovern, T., McGhee, K., Swanson, C., and Knowlton, N. (2004) 'Mechanisms of reproductive isolation among sympatric broadcast-spawning corals of the *Montastraea annularis* species complex'. *Evolution; international journal of organic evolution*, 58:308–323.

Levitan, D. R., Fogarty, N. D., Jara, J., Lotterhos, K. E., and Knowlton, N. (2011) 'GENETIC, SPATIAL, AND TEMPORAL COMPONENTS OF PRECISE SPAWNING SYNCHRONY IN REEF BUILDING CORALS OF THE MONTASTRAEA ANNULARIS SPECIES COMPLEX'. *Evolution*, 65(5):1254–1270.

Levitan, D. R., Boudreau, W., Jara, J., and Knowlton, N. (2014) 'Long-term reduced spawning in Orbicella coral species due to temperature stress'. *Marine Ecology Progress Series*, 515:1–10.

Levy, O., Appelbaum, L., Leggat, W., Gothlif, Y., Hayward, D. C., Miller, D. J., and Hoegh-Guldberg, O. (2007) 'Light-Responsive Cryptochromes from a Simple Multicellular Animal, the Coral *Acropora millepora*'. *Science*, 318(5849):467–470.

Lin, C.-H., Takahashi, S., Mulla, A. J., and Nozawa, Y. (2021) 'Moonrise timing is key for synchronized spawning in coral *Dipsastraea speciosa*'. *Proceedings of the National Academy of Sciences*, 118(34): e2101985118.

Meeus, J. (1998) *Astronomical Algorithms*. 2^{nd} edition, Willmann-Bell Inc., Richmond, 477pp.

Mendes, J. M. (2002) 'Timing of reproduction in *Montastraea annularis*: relationship to environmental variables'. *Marine Ecology Progress Series*, 227:241–251.

Moberg, F. and Folke, C. (1999) 'Ecological goods and services of coral reef ecosystems'. *Ecological Economics*, 29(2):215–233.

Modelio.org (2023) *Modelio*. Available at: `https://www.modelio.org/index.htm` .

Moran, P. A. P. (1950) 'NOTES ON CONTINUOUS STOCHASTIC PHENOMENA'. *Biometrika*, 37(1-2): 17–23.

Morgan, M. B., Ross, J., Ellwanger, J., Phrommala, R. M., Youngblood, H., Qualley, D., and Williams, J. (2022) 'Sea Anemones Responding to Sex Hormones, Oxybenzone, and Benzyl Butyl Phthalate: Transcriptional Profiling and in Silico Modelling Provide Clues to Decipher Endocrine Disruption in Cnidarians'. *Frontiers in Genetics*, 12.

Moulding, A. and Ladd, M. (2022) *Staghorn coral (Acropora cervicornis), elkhorn coral (Acropora palmata), lobed star coral (Orbicella annularis), mountainous star coral (Orbicella faveolata), boulder star coral (Orbicella franksi), rough cactus coral (Mycetophyllia fero*. Available at: `https://repository.library.noaa.gov/view/noaa/45015` .

Muscatine, L. (1990) 'The role of symbiotic algae in carbon and energy flux in reef corals'. In: Dubinsky, Z., (ed.), *Ecosystems of the world*. Elsevier, Amsterdam, pp. 75–87.

Naylor, E. (2010) *Chronobiology of marine organisms*. 1^{st} edition, Cambridge University Press, New York, 252pp.

Nozawa, Y. (2012) 'Annual Variation in the Timing of Coral Spawning in a High-Latitude Environment: Influence of Temperature'. *The Biological Bulletin*, 222(3):192–202.

ORE, I. . A. (2024) *Caribbean Coral Spawning Database - Spawning Prediction Calendars*. Available at: https://www.agrra.org/coral-spawning/ (Accessed: 2024-11-01).

Oxoli, D. and Prestifilippo, G. (2017) *Hotspot Analysis*. Available at: https://github.com/danioxoli/HotSpotAnalysis_Plugin .

Pandolfi, J. M. and Budd, A. F. (2008) 'Morphology and ecological zonation of Caribbean reef corals: the *Montastraea 'annularis'* species complex'. *Marine Ecology Progress Series*, 369:89–102.

Paxton, C. W., Baria, M. V. B., Weis, V. M., and Harii, S. (2016) 'Effect of elevated temperature on fecundity and reproductive timing in the coral *Acropora digitifera*'. *Zygote*, 24(4):511–516.

Pedersen, T. L. (2024) *patchwork: The Composer of Plots*. Available at: https://cran.r-project.org/package=patchwork .

Penland, L., Kloulechad, J., Idip, D., and van Woesik, R. (2004) 'Coral spawning in the western Pacific Ocean is related to solar insolation: evidence of multiple spawning events in Palau'. *Coral Reefs*, 23(1):133–140.

Posit-team (2024) *RStudio: Integrated Development Environment for R*. Available at: http://www.posit.co/ .

Proietti, T. and Maddanu, F. (2022) 'Modelling cycles in climate series: The fractional sinusoidal waveform process'. *Journal of Econometrics*, 239.

QGIS Development Team (2024) *QGIS Geographic Information System*. Available at: http://qgis.org .

R Core Team (2024) *R: A Language and Environment for Statistical Computing*. Available at: https://www.r-project.org/ .

Rädecker, N., Pogoreutz, C., Voolstra, C. R., Wiedenmann, J., and Wild, C. (2015) 'Nitrogen cycling in corals: the key to understanding holobiont functioning?'. *Trends in Microbiology*, 23(8):490–497.

Railsback, S. F. and Grimm, V. (2019) *Agent-Based and Individual-Based Modeling*. 2^{nd} edition, Princeton University Press, Princeton and Oxford, 340pp.

Rapuano, H., Shlesinger, T., Roth, L., Bronstein, O., and Loya, Y. (2023) 'Coming of age: Annual onset of coral reproduction is determined by age rather than size'. *iScience*, 26(5).

Reuter, K. E. and Levitan, D. R. (2010) 'Influence of sperm and phytoplankton on spawning in the echinoid *Lytechinus variegatus*'. *Biological Bulletin*, 219(3):198–206.

Rougée, L. R. A., Richmond, R. H., and Collier, A. C. (2015) 'Molecular reproductive characteristics of the reef coral *Pocillopora damicornis*'. *Comparative Biochemistry and Physiology Part A: Molecular & Integrative Physiology*, 189:38–44.

Sawall, Y., Nicosia, A. M., McLaughlin, K., and Ito, M. (2022) 'Physiological responses and adjustments of corals to strong seasonal temperature variations (20–28°C)'. *Journal of Experimental Biology*, 225(13): jeb244196.

Shlesinger, T. and Loya, Y. (2019) 'Breakdown in spawning synchrony: A silent threat to coral persistence'. *Science*, 365(6457):1002–1007.

Slattery, M., Hines, G. A., Starmer, J., and Paul, V. J. (1999) 'Chemical signals in gametogenesis, spawning, and larval settlement and defense of the soft coral *Sinularia polydactyla*'. *Coral Reefs*, 18(1):75–84.

Śmielak, M. K. (2023) 'Biologically meaningful moonlight measures and their application in ecological research'. *Behavioral Ecology and Sociobiology*, 77(2):21.

Sorek, M. and Levy, O. (2014) 'Coral Spawning Behavior and Timing'. In: Numata, H. and Helm, B., (ed.), *Annual, Lunar, and Tidal Clocks*. Springer Japan, Tokyo, pp. 81–97.

Spalding, M. D. and Grenfell, A. M. (1997) 'New estimates of global and regional coral reef areas'. *Coral Reefs*, 16(4):225–230.

Spalding, M. D., Burke, L., Wood, S. A., Ashpole, J., Hutchison, J., and zu Ermgassen, P. (2017) 'Mapping the global value and distribution of coral reef tourism'. *Marine Policy*, 82:104–113.

Stimson, J. S. (1978) 'Mode and timing of reproduction in some common hermatypic corals of Hawaii and Enewetak'. *Marine Biology*, 48(2):173–184.

Szmant, A. M. (1991) 'Sexual reproduction by the Caribbean reef corals *Montastrea annularis* and *M. cavernosa*'. *Marine Ecology Progress Series*, 74(1):13–25.

Tadić, B. and Melnik, R. (2021) *Self-Organised Critical Dynamics as a Key to Fundamental Features of Complexity in Physical, Biological, and Social Networks* .

Taillandier, P., Gaudou, B., Grignard, A., Huynh, Q.-N., Marilleau, N., Caillou, P., Philippon, D., and Drogoul, A. (2019) 'Building, composing and experimenting complex spatial models with the GAMA platform'. *GeoInformatica*, 23(2):299–322.

Tan, E. S., Izumi, R., Takeuchi, Y., Isomura, N., and Takemura, A. (2020) 'Molecular approaches underlying the oogenic cycle of the scleractinian coral, *Acropora tenuis*'. *Scientific Reports*, 10(1):9914.

Tan, E. S., Hamazato, H., Ishii, T., Taira, K., Takeuchi, Y., Takekata, H., Isomura, N., and Takemura, A. (2021) 'Does estrogen regulate vitellogenin synthesis in corals?'. *Comparative Biochemistry and Physiology Part A: Molecular & Integrative Physiology*, 255:110910.

Tarrant, A. M. (2015) 'Endocrine-Like Signaling in Corals'. In: Woodley, C. M., Downs, C. A., Bruckner, A. W., Porter, J. W., and Galloway, S. B., (ed.), *Diseases of Coral*. 1^{st} edition, John Wiley & Sons Inc., pp. 138–149.

Tarrant, A. M., Atkinson, S., and Atkinson, M. J. (1999) 'Estrone and estradiol-17 beta concentration in tissue of the scleractinian coral, *Montipora verrucosa*'. *Comparative Biochemistry and Physiology Part A: Molecular & Integrative Physiology*, 122(1):85–92.

The Modern Language Association of America (2022) *MLA Handbook*. 9^{th} edition, The Modern Language Association of America, New York.

Thomson, D. J. (1995) 'The Seasons, Global Temperature, and Precession'. *Science*, 268(5207):59–68.

Twan, W.-H., Hwang, J.-S., and Chang, C.-F. (2003) 'Sex Steroids in Scleractinian Coral, *Euphyllia ancora*: Implication in Mass Spawning1'. *Biology of Reproduction*, 68(6):2255–2260.

Twan, W.-H., Hwang, J.-S., Lee, Y.-H., Jeng, S.-R., Yueh, W.-S., Tung, Y.-H., Wu, H.-F., Dufour, S., and Chang, C.-F. (2006) 'The Presence and Ancestral Role of Gonadotropin-Releasing Hormone in the Reproduction of Scleractinian Coral, *Euphyllia ancora*'. *Endocrinology*, 147(1):397–406.

Twan, W.-H., Hwang, J.-S., Lee, Y.-H., Wu, H.-F., Tung, Y.-H., and Chang, C.-F. (2006) 'Hormones and reproduction in scleractinian corals'. *Comparative Biochemistry and Physiology Part A: Molecular & Integrative Physiology*, 144(3):247–253.

UNIGIS (2024) *Leitfaden zum Umgang mit generativer KI*. University of Salzburg, Salzburg, Austria. Available at: `https://unigis.at/files/UNIGIS_Leitfaden_generative_KI.pdf`, 4pp.

U.S. Naval Observatory (2024) *Astronomical Applications Department*. Available at: `https://aa.usno.navy.mil/data/index` (Accessed: 2024-07-22).

Van Veghel, M. L. J. (1994) 'Reproductive characteristics of the polymorphic Caribbean reef building coral *Montastrea annularis*. I. Gametogenesis and spawning behavior'. *Marine Ecology Progress Series*, 109 (2/3):209–219.

van Woesik, R. (2009) 'Calm before the spawn: global coral spawning patterns are explained by regional wind fields'. *Proceedings of the Royal Society B: Biological Sciences*, 277(1682):715–722.

Van Woesik, R., Lacharmoise, F., and Köksal, S. (2006) 'Annual cycles of solar insolation predict spawning times of Caribbean corals'. *Ecology Letters*, 9(4):390–398.

von Bertalanffy, L. (2003) *General system theory : foundations, development, applications*. Revised edition, George Braziller, New York, 289.

Waldrop, M. (1992) *Complexity: The Emerging Science at the Edge of Order and Chaos*. Simon & Schuster, New York, 376pp.

Watts, S. A. and Wasson, K. M. (2020) 'Chapter 5 - Endocrine regulation of regular echinoid reproduction'. In: Lawrence, J. M. B. T. D. i. A. and Science, F., (ed.), *Sea Urchins: Biology and Ecology*, volume 43. Elsevier, pp. 65–75.

Wickham, H. (2016) *ggplot2: Elegant Graphics for Data Analysis*. 2^{nd} edition, Springer New York.

Wickham, H., François, R., Henry, L., Müller, K., and Vaughan, D. (2023) *dplyr: A Grammar of Data Manipulation*. Available at: `https://cran.r-project.org/package=dplyr` .

Witzany, G. (2010) 'Biocommunication of Corals'. In: Witzany, G., (ed.), *Biocommunication and Natural Genome Editing*. Springer Netherlands, Dordrecht, pp. 67–87.

Woodhead, A. J., Hicks, C. C., Norström, A. V., Williams, G. J., and Graham, N. A. J. (2019) 'Coral reef ecosystem services in the Anthropocene'. *Functional Ecology*, 33(6):1023–1034.

Yang, F. and Wu, Z. (2024) 'The phase change in the annual cycle of sea surface temperature'. *npj Climate and Atmospheric Science*, 7(1):48.

Yeemin, T., Tuan, V. S., and Suharsono (2022) 'Advances in Coral Biology'. In: Zhang, J., Yeemin, T., Morrison, R. J., and Hong, G. H., (ed.), *Coral Reefs of the Western Pacific Ocean in a Changing Anthropocene*. Springer International Publishing, Cham, pp. 25–53.

Appendix A: GUI setup of GAMA experiment

Following screenshots provide an example in how to setup the experimental GUI in GAMA to perform the simulations of coral reef spawning. It is repeated here that the GUI is not mandatory to create the model output which could be achieved solely by coding.

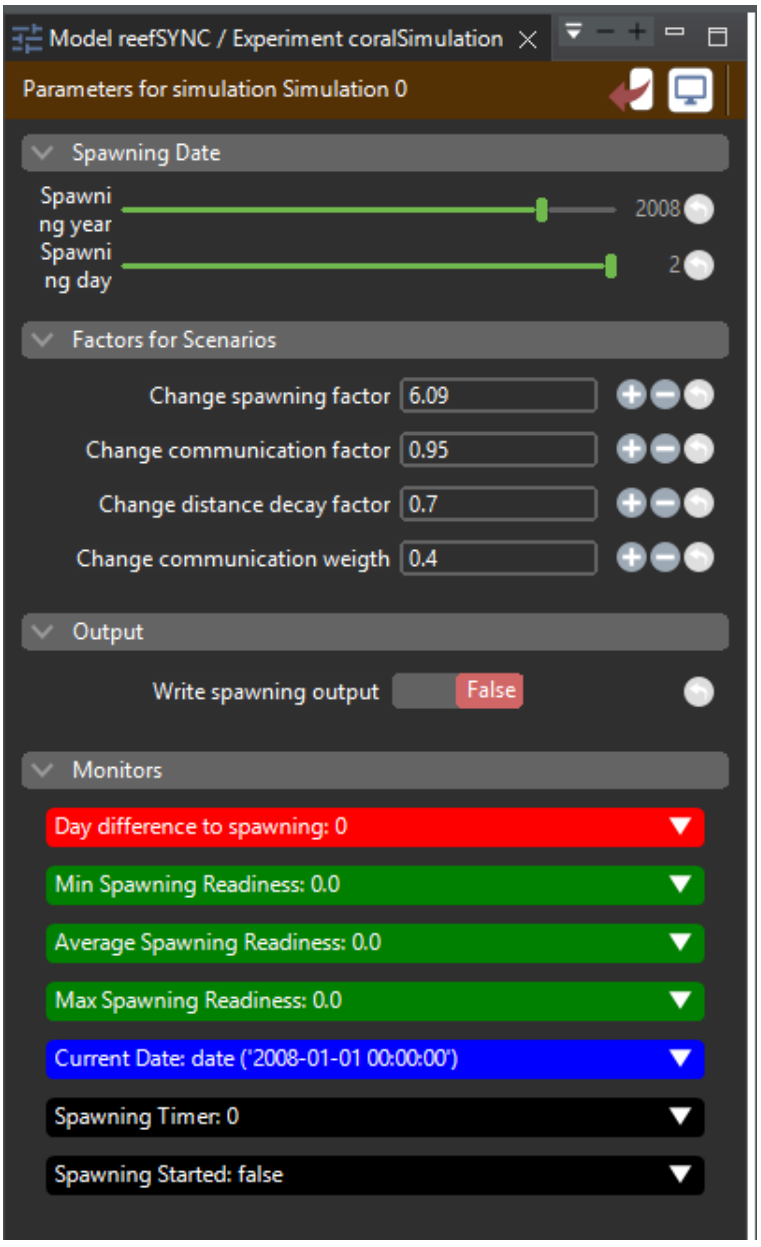

Figure 25: GUI Setup of parameters and monitors in GAMA.

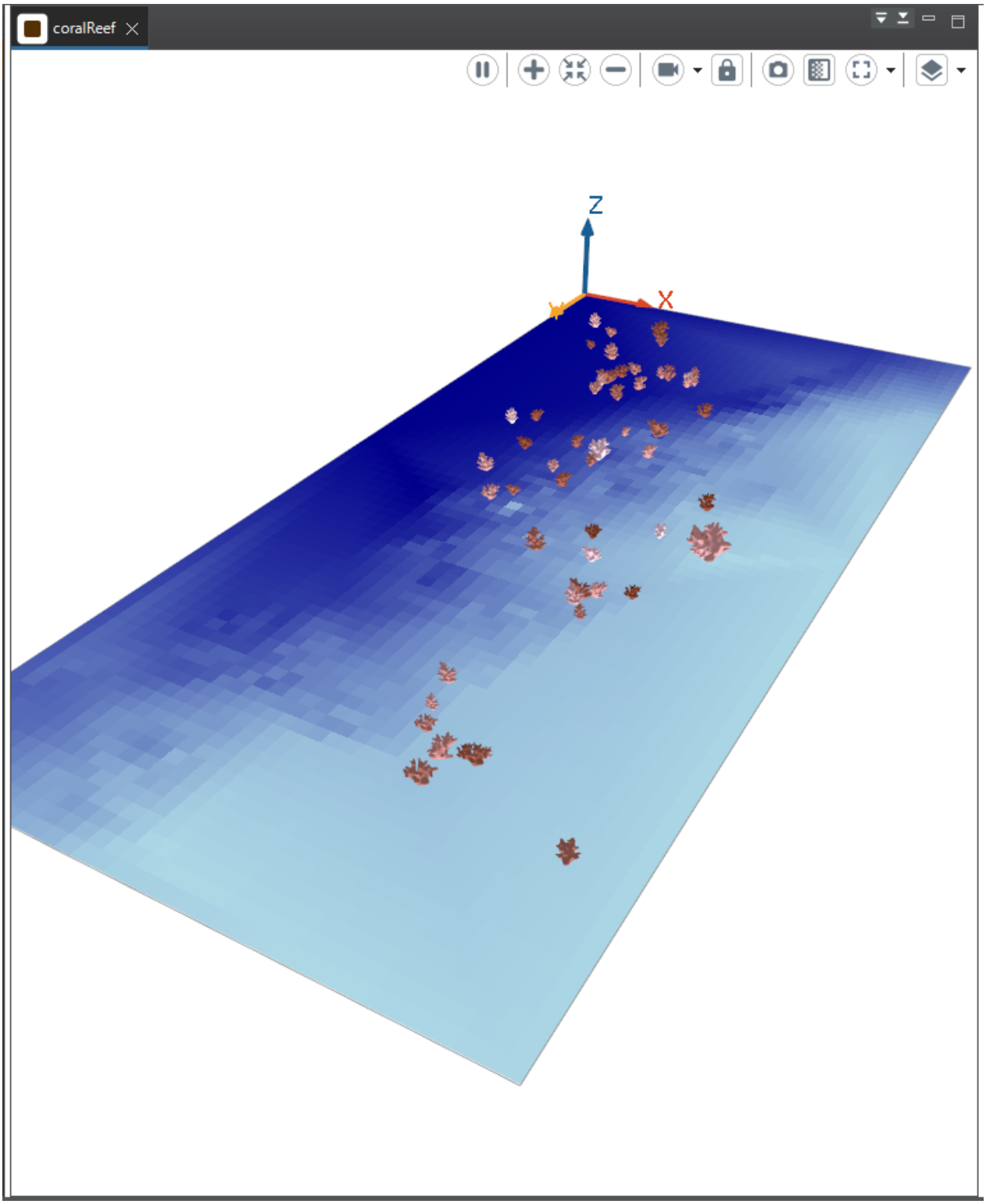

Figure 26: GUI Setup of 3D coral reef visualisation in GAMA.

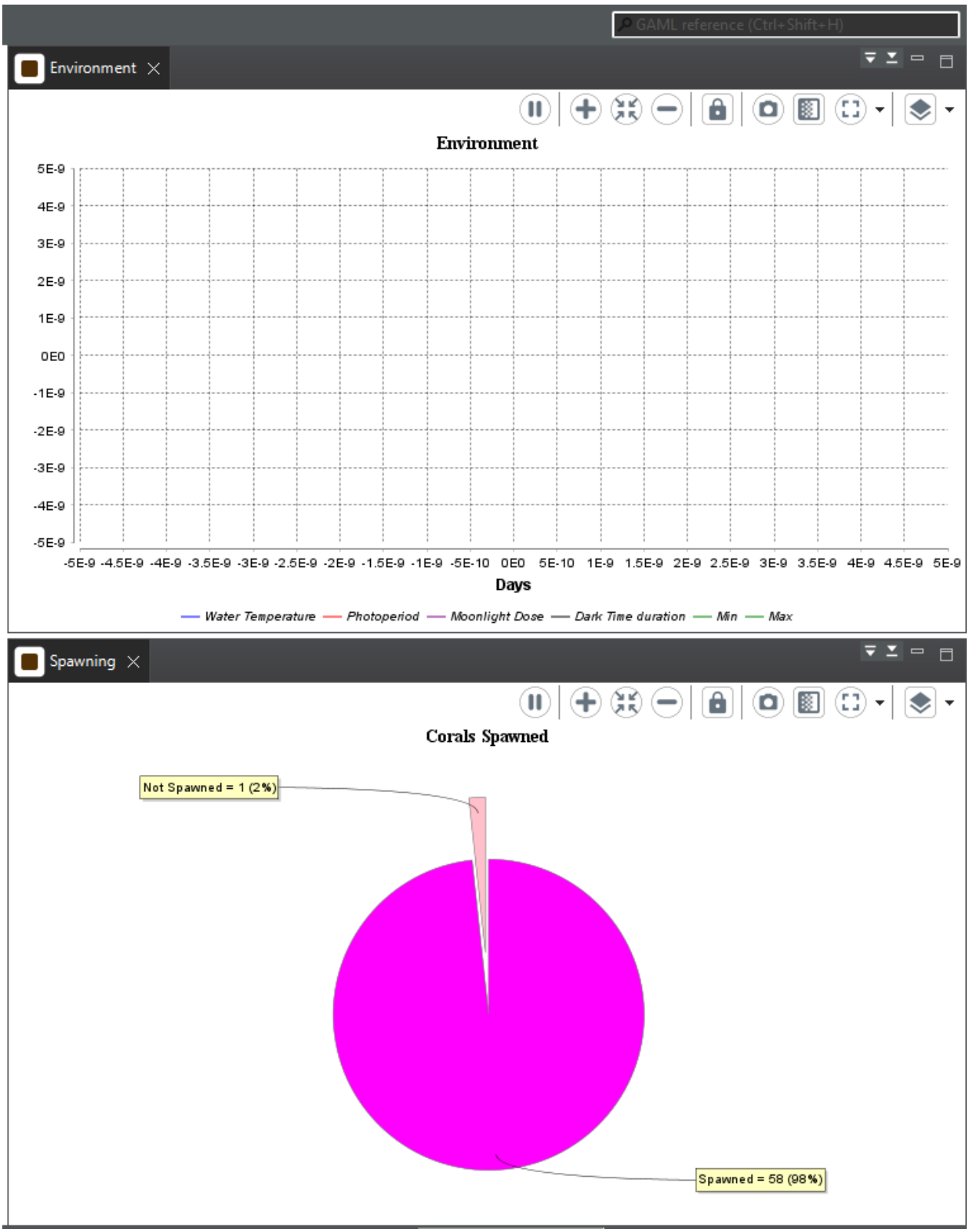

Figure 27: GUI Setup of charts showing changes in environmental factors, spawning readiness and number of corals spawned / not-spawned.

Appendix B: lunar ephemeris data

The lunar ephemeris data by U.S. Naval Observatory (2024) has been downloaded for a timespan from 2002-01-01 to 2029-05-17. Because of the extend of the data, only an excerpt is shown here. The complete dataset is attached to the thesis as supplementary file.

```
Rise/Set/Transit Times for Major Solar System Bodies and Bright Stars

Astronomical Applications Department
U. S. Naval Observatory
Washington, DC 20392-5420

Moon
Location:  W 82°12’14.0", N 9°19’38.3",     0m
(Longitude referred to Greenwich meridian)
Time Zone:  5h 00m west of Greenwich

Date and Time        Rise     Transit  Transit Altitude  Set   Fraction Illuminated
2002-01-01 00:00:00  20.867   2.350    77                8.833    0.96
2002-01-02 00:00:00  21.867   3.333    81                9.767    0.9
2002-01-03 00:00:00  22.817   4.267    85                10.617   0.82
2002-01-04 00:00:00  23.733   5.133    89                11.417   0.72
2002-01-05 00:00:00  none     5.967    83                12.183   0.61
2002-01-06 00:00:00  0.617    6.783    77                12.933   0.5
2002-01-07 00:00:00  1.500    7.600    71                13.667   0.39
2002-01-08 00:00:00  2.367    8.417    66                14.450   0.28
2002-01-09 00:00:00  3.267    9.267    62                15.250   0.19
2002-01-10 00:00:00  4.183    10.133   59                16.083   0.11
2002-01-11 00:00:00  5.100    11.033   57                16.967   0.06
2002-01-12 00:00:00  6.000    11.933   56                17.850   0.02
2002-01-13 00:00:00  6.883    12.800   57                18.733   0
2002-01-14 00:00:00  7.717    13.650   59                19.600   0
2002-01-15 00:00:00  8.483    14.450   62                20.417   0.03
2002-01-16 00:00:00  9.200    15.200   65                21.217   0.07
2002-01-17 00:00:00  9.867    15.900   70                21.967   0.12
2002-01-18 00:00:00  10.517   16.600   75                22.700   0.19
2002-01-19 00:00:00  11.133   17.267   80                23.433   0.27
2002-01-20 00:00:00  11.750   17.950   85                none     0.36
2002-01-21 00:00:00  12.383   18.650   90                0.167    0.45
2002-01-22 00:00:00  13.050   19.383   85                0.933    0.55
2002-01-23 00:00:00  13.783   20.183   81                1.750    0.64
2002-01-24 00:00:00  14.600   21.050   78                2.600    0.74
2002-01-25 00:00:00  15.483   22.000   76                3.533    0.83
2002-01-26 00:00:00  16.467   23.000   75                4.517    0.9
2002-01-27 00:00:00  17.500   none     none              5.533    0.96
2002-01-28 00:00:00  18.567   0.033    76                6.550    0.99
2002-01-29 00:00:00  19.617   1.050    79                7.517    1
2002-01-30 00:00:00  20.617   2.050    83                8.433    0.98
2002-01-31 00:00:00  21.583   2.983    89                9.300    0.92
```